University of New Orleans

ScholarWorks@UNO

University of New Orleans Theses and Dissertations

Dissertations and Theses

5-21-2004

Determination of Noncovalent Intermolecular Interaction Energy from Electron Densities

Yuguang Ma
University of New Orleans

Follow this and additional works at: https://scholarworks.uno.edu/td

Recommended Citation

DETERMINATION OF NONCOVALENT INTERMOLECULAR INTERACTION ENERGY FROM ELECTRON DENSITIES

A Dissertation

Submitted to the Graduate Faculty of the
University of New Orleans
in the partial fulfillment of the
requirements for the degree of

Doctor of Philosophy
in
The Department of Chemistry

by

Yuguang Ma

B.S., Fudan University, China, 1996
M.S., Shanghai Institute of Organic Chemistry, 1999

May 2004

ACKNOWLEDGEMENTS

The author wishes to express the greatest gratitude to his advisor, Dr. Peter Politzer for his friendly guidance and assistance throughout the course of this research. Also, the author deeply appreciates Dr. Jane S. Murray for her valuable suggestions and helpful discussions.

The author would like to thank his group members: Dr. Sylke Boyd, Mrs. Monica Concha, Dr. Ed Grice, Mr. Abraham Jalbout, Mrs. Ping Jin, Mrs. Pat Lane and Dr. Zenaida Peralta-Inga for their full support and help in preparing this dissertation.

In addition, the author expresses his appreciation to the committee members: Dr. Edwin Stevens, Dr. Steven Rick, Dr. Paul Hansen and Dr. Branko Jurisc for their helpful suggestions.

Finally, the author thanks his family and parents for their encouragement, understanding and support.

TABLE OF CONTENTS

LIST OF TABLES

LIST OF FIGURES

ABSTRACT

Noncovalent intermolecular interactions, widely found in molecular clusters and bio-molecules, play a key role in many important processes, such as phase changes, folding of proteins and molecular recognition. However, accurate calculation of interaction energies is a very difficult task because the interactions are normally very weak. Rigorous expressions for the electrostatic and polarization interaction energies between two molecules A and B, in term of the electronic densities, have been programmed:

$$E_{es} = \sum_A \sum_B \frac{Z_A Z_B}{|\vec{R}_A - \vec{R}_B|} - \sum_A \int \frac{Z_A \rho_B^0(\vec{r}_B)}{|\vec{R}_A - \vec{r}_B|} d\vec{r}_B - \sum_B \int \frac{Z_B \rho_A^0(\vec{r}_A)}{|\vec{R}_B - \vec{r}_A|} d\vec{r}_A + \iint \frac{\rho_A^0(\vec{r}_A)\rho_B^0(\vec{r}_B)}{|\vec{r}_A - \vec{r}_B|} d\vec{r}_A d\vec{r}_B \qquad \textbf{(1)}$$

$$E_{pol} = -\sum_A \int \frac{Z_A \Delta\rho_B^{pol}(\vec{r}_B)}{|\vec{R}_A - \vec{r}_B|} d\vec{r}_B - \sum_B \int \frac{Z_B \Delta\rho_A^{pol}(\vec{r}_A)}{|\vec{R}_B - \vec{r}_A|} d\vec{r}_A + \iint \frac{\rho_A^0(\vec{r}_A)\Delta\rho_B^{pol}(\vec{r}_B)}{|\vec{r}_A - \vec{r}_B|} d\vec{r}_A d\vec{r}_B$$
$$+ \iint \frac{\rho_B^0(\vec{r}_B)\Delta\rho_A^{pol}(\vec{r}_A)}{|\vec{r}_A - \vec{r}_B|} d\vec{r}_A d\vec{r}_B + \iint \frac{\Delta\rho_A^{pol}(\vec{r}_A)\Delta\rho_B^{pol}(\vec{r}_B)}{|\vec{r}_A - \vec{r}_B|} d\vec{r}_A d\vec{r}_B \qquad \textbf{(2)}$$

Z is atomic charge, ρ^0 is the electron density of the isolated molecule and $\Delta\rho^{ind}$ is the electron density change of the molecule caused by polarization. With some approximations, procedures for electrostatic and polarization energy calculations were developed that involve numerical integration. Electrostatic and polarization energies for several bimolecular systems, some of which are hydrogen bonded, were calculated and the results were compared to other theoretical and experimental data.

A second method for the computing of intermolecular interaction energies has also been developed. It involves a "supermolecule" calculation for the entire system, followed by a partitioning of the overall electric density into the two interacting components and then application of eq. (1) to find the interaction energy. In this approach, according to Feynman's explanation to intermolecular interactions, all contributions are treated in a unified manner. The advantages of this method are that it avoids treating the supersystem and subsystems separately and no basis set superposition error (BSSE) correction is needed. Interaction energies for several hydrogen-bonded systems are calculated by this method. Compared with the result from experiment and high level *ab initio* calculation, the results are quite reliable.

CHAPTER 1. INTRODUCTION

1.1.   Covalent and Noncovalent Interactions

It is found that there are four types of interactions in nature. They are strong, weak, electromagnetic and gravitational forces. The strong and weak interactions are short-range forces and only act between protons, neutrons and other elementary particles.   Gravitational interactions are associated with all mass systems. According to the generalized theory of relativity, this interaction originates from the distortion of space. The electromagnetic interactions, mainly acting between atomic and sub-atomic systems, directly lead to the formation of atoms and molecules.

Among the four interactions, only electromagnetic forces are fundamentally important to molecular systems, in that the interaction range of strong and weak forces is too short (less than 10^{-5} nm) and gravitational forces are too weak. Electromagnetic forces are responsible for the formation of covalent bonds and noncovalent bonds in chemistry. According to molecular quantum mechanics, a covalent bond usually originates from the overlap of the partially occupied orbitals. Covalent interactions were first described by Lewis in 1916 [1]. With the development of the quantum theory of the chemical bond, the properties of covalent bonds are well understood and their theoretical treatment is now routine work with quantum chemical software packages. Many physical properties, such as energy,

bond lengths and bond angles *etc.*, can be accurately evaluated at various theoretical levels.

There is another kind of interaction of atoms and molecules, which is to form molecular complexes. Since there is no breaking or formation of covalent bonds in this process, these are called noncovalent interactions or van der Waals (vdW) interactions. In this dissertation, we recommend the term "noncovalent interactions", because some of them, such as the electrostatic and polarization interactions, are normally not included in "vdW interactions".

Noncovalent interactions, widely found in molecular clusters and bio-molecular systems, play a key role in many important processes such as phase changes, folding of proteins and molecular recognition. Compared to covalent interactions, noncovalent interactions are much weaker (normally 1 to 2 orders of magnitude less than covalent interactions).

The noncovalent interactions may be intramolecular or intermolecular. However, compared to covalent interactions, the noncovalent intramolecular interactions are too weak to affect the properties of molecules in most cases. Therefore, we only focus on noncovalent intermolecular interactions, which are very important in many fields of chemistry and physics.

1.2. Noncovalent Intermolecular Interactions

According to their different origins, noncovalent intermolecular interactions are grossly classified into four categories: repulsion-exchange, electrostatic, polarization and dispersion interactions. The first one is connected with the overlap

of occupied orbitals and the rest of them originate, respectively, from the interaction between two permanent multipoles, between a permanent multipole and an induced multipole, and between an induced multipole and an instantaneous multipole. Hence the total intermolecular interaction energy is the sum of these four different intermolecular energies:

$$E_{int} = E_{es} + E_{pol} + E_{dis} + E_{ex} \qquad (1.1)$$

where E_{es}, E_{ind}, E_{dis} and E_{ex} represent electrostatic, polarization, dispersion and exchange energy separately.

The basic equation for describing electrostatic interactions is Coulomb's law, which gives the relationship between the Coulomb force F and two point charges q_1 and q_2 with a certain separation r:

$$F = \frac{q_1 q_2}{4\pi\varepsilon_0 \varepsilon r^2} \qquad (1.2)$$

where ε_0 is the dielectric constant of a vacuum and ε is the dielectric constant of the medium. The Coulomb force is a long-range interaction, vanishing as r^{-2}.

As we know, most molecules do not carry any net charge; however, many of them, called polar molecules, have permanent electric dipoles. By Coulomb's law, the electrostatic interaction energies between charges and dipoles can be expressed as shown in Table 1.1 [2].

The permanent dipole moments of polar molecules bring into being an electric field around them. When any atom or molecule is placed in an electric field, its charge is redistributed and thus an induced dipole moment is generated (Figure 1.1). This process is called polarization. The induced dipole moment $\bar{\mu}$ is given by

$$\vec{\mu} = \alpha \vec{E} \qquad\qquad (1.3)$$
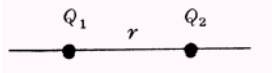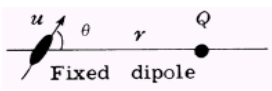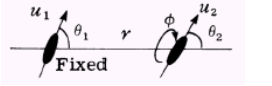
Type of interaction		Interaction Energy
Charge-charge		$Q_1Q_2/4\pi\varepsilon_0 r$
Charge-dipole		$Qu\cos\theta/4\pi\varepsilon_0 r^2$
Dipole-dipole		$-u_1u_2[2\cos\theta_1\cos\theta_2 - \sin\theta_1\sin\theta_2\cos\phi]/4\pi\varepsilon_0 r^3$

Table 1.1 Some types of electrostatic interactions. Q, electric charge; μ, electric dipole moment.

where α is the static polarizability and $\vec{E}$ the electric field. The energy due to the interaction between an electric field $\vec{E}$ and an induced dipole moment $\vec{\mu}$ is:

$$E_{pol} = -\int_o^E \vec{\mu} \cdot d\vec{E} = -\frac{1}{2}\alpha E^2 \qquad\qquad (1.4)$$

Electric field **E**

δ^- δ^+

μ_{ind}
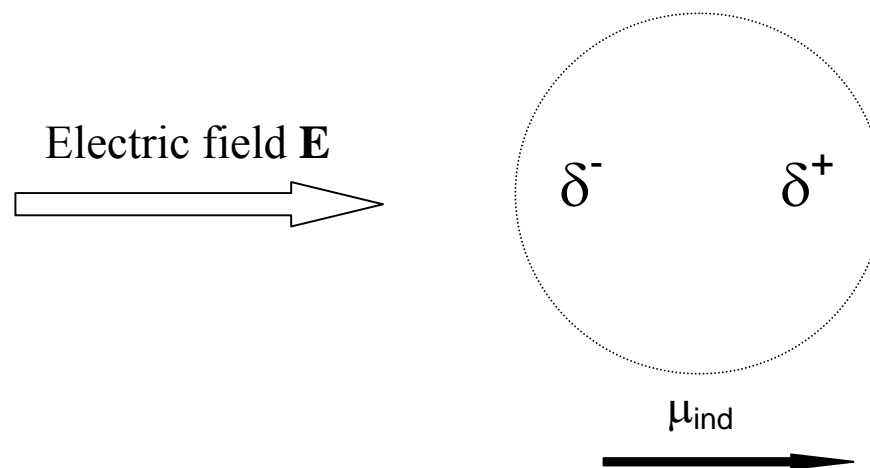
Fig. 1.1 The process of polarization.

Dispersion interactions have also long-range character. They are present in all kinds of intermolecular systems. In the view of modern quantum mechanics, dispersion interactions arise from the mutual correlation of electrons which belong to different molecules.

The theory of dispersion interactions is less well understood than that of electrostatic and polarization interactions. In 1930s, London made an interpretation with the oscillator model [3-4]. He found that the dispersion energy is proportional to the sixth power of the reciprocal distance. The dispersion interaction energy between two identical atoms or molecules is

$$E_{dis} = -\frac{C_6}{r^6} = -\frac{3}{4}\frac{\alpha_0^2 I}{(4\pi\varepsilon_0)^2 r^6}$$
(1.5)

where I is the ionization potential and α_0 is the polarizability. The oscillator model was extended to higher multipole moment interactions by Margenau [5], and Hornig and Hirschfelder [6]. The dispersion interaction energy can be written in the form

$$E_{dis} = -\frac{C_6}{r^6} - \frac{C_8}{r^8} - \frac{C_{10}}{r^{10}} - \cdots,$$
(1.6)

where C_n (n=6, 8, 10,…) are all dispersion coefficients. They can be obtained in several different ways, such as dipole oscillator strength distributions (DOSDs) [7-9] and *ab initio* calculations.

Exchange interactions originate from charge overlap and exchange effects. When two molecules come together, according to the Pauli exclusion principle, two electrons cannot have the same spatial and spin wave functions. Therefore, the

electron density between the molecules falls when their orbitals begin to overlap. The process brings a kind of repulsion force between molecules, which is called exchange-repulsion.

Exchange-repulsion is characterized by its short interaction distance. Unfortunately, there is no strictly defined equation for describing the distance dependence. Hence some empirical potential functions have been employed. Among them, the three most common are the hard sphere potential, the inverse power-law potential and the exponential potential. Each of them can fit experimental data well with proper parameters. For instance, as a valid approximation, the exchange potential is proportional to the square of an overlap integral between orbitals of two molecules [10]. Since the wave functions decay exponentially with distance, it is reasonable that the exchange repulsion energy is represented exponentially with intermolecular distance R:

$$E_{ex} = Ae^{-BR} \tag{1.7}$$

where A and B are coefficients. As all these three potentials have simple mathematical forms, they are widely used in many fields.

1.3.   Methods for Intermolecular Interaction Energy Calculation

Mainly, there are three different methods for intermolecular interaction energy calculation: empirical force-field methods, semi-empirical methods and *ab initio* methods. Each of them has advantages and drawbacks.

In the molecular simulations of bioorganic and polymeric systems, empirical force field methods are very popular. Generally, the total interaction energy is the sum of the electrostatic energy, polarization energy and vdW interaction energy:

$$E_{int} = E_{es} + E_{pol} + E_{vdw} \qquad (1.8)$$

Normally, the electrostatic energy is described by the point charge model and the vdW interaction energy is given by Lennard-Jones or Buckingham types of potentials. As a simple example, the interaction energy can be expressed as:

$$E_{int} = \sum_{ij} (\frac{q_i q_j}{R_{ij}} + \frac{a_{ij}}{R_{ij}^{12}} - \frac{b_{ij}}{R_{ij}^6}) \qquad (1.9)$$

where the first term gives the electrostatic interactions, the second term describes the short-range repulsion energy, and the third term the dispersion energy. The point charges and vdW parameters are from experimental data and theoretical calculations.

There are many different force-field models such as AMBER [11-15], CHARMM [16-22], MM2 [23-25] *etc*. Some of these force-fields are much more complicated than the above examples: polarization effect and angle factors are included and also the effect of hydrogen bonds is considered.

The force-field models are computationally efficient and thus can be carried out for big molecular systems. Some typical applications of force field methods are solution phase simulations and conformation searches for proteins and DNAs. Using the correct force-field parameters, the method may obtain good results.

Nevertheless, it cannot describe the interaction energy of electrons and also the accuracy is obviously less than that of quantum chemical calculations.

Traditionally, the concept of semiempirical methods is from semi-empirical quantum methods, such as INDO, MNDO and AM1 [26-31]. The complexity of these methods lies between empirical force-field and strictly *ab initio* calculations. Like force-field methods, they use some experimentally-derived parameters for improving calculation efficiency; like *ab initio* methods, they are based on solving the Schrödinger equation. Since a lot of time-consuming integrals are neglected or replaced by experimental data, semiempirical methods are computationally much faster than *ab initio* methods. Therefore, they can treat a molecular system that contains several hundred atoms. However, because of the same reason, these methods are very rough, and fail in the evaluation of dispersion and repulsion interactions in intermolecular interaction energy calculations. Some improved semiempirical methods, such as PDDG/PM3 and PDDG/MNDO [32] have been developed to partially overcome this deficiency. In this method, a Pairwise Distance Directed Gaussian function (PDDG) is added into the Core Repulsion Function (CRF) to eliminate the excessive core-core repulsion. Hence more accurate interaction energies can be obtained, especially for hydrogen-bonded molecular systems.

The definition of semiempirical methods was extended in recent years. QM/MM [33-39], a hybrid method combining molecular mechanical and quantum mechanical calculations, has also been included. This method was first introduced by Warshel and Levitt in1976. The idea is to divide a molecular system into a QM

region and an MM region with an appropriate boundary treatment to connect these two parts. Thus the total energy of the system can be written as

$$E_{int} = E_{QM} + E_{MM} + E_{QM/MM,\,elec} + E_{QM/MM,\,vdW} \qquad \textbf{(1.10)}$$

where E_{QM} and E_{MM} are energies of the QM and MM parts, and $E_{QM/MM,elec}$ and $E_{QM/MM,vdW}$ are the boundary electronic and vdW energy on the boundary. The key in this method is the treatment of the boundary energy, which represents the interaction of the MM atom cores with the electron cloud of the QM atoms when interacting with MM atoms. It is found that a Lennard-Jones term must be added to the QM atoms to obtain good intermolecular interaction energies.

The QM/MM methods are normally employed to study biomolecules and other condensed-phase systems, in which it is necessary to treat some parts of them rigorously. A good example is enzyme reactions. In most cases, the active site of an enzyme accounts for only a relatively small portion of the total system. The active site is computed by a QM method while other regions are treated by an MM scheme.

The most accurate methods for intermolecular interaction energy calculations are the *ab initio*, based on solving the time-independent Schrödinger equation with several approximations (non-relativistic approximation, Born-Oppenheimer, *etc.*):

$$\hat{H}\Psi = E\Psi \qquad \textbf{(1.11)}$$

where Ψ is a wave function and $\hat{H}$ is the Hamiltonian of the system. For a molecular system, the Hamiltonian (in atomic units) is defined as shown in Eq. (1.12):

$$\hat{H} = -\frac{1}{2}\sum_i \nabla_i^2 - \sum_i \sum_A \frac{Z_A}{r_{iA}} + \sum_{A>B} \sum_B \frac{Z_A Z_B}{R_{AB}} + \sum_{i>j} \sum_j \frac{1}{r_{ij}} \qquad (1.12)$$

Z_A and Z_B are the charges on nuclei A and B, r_{iA} is the distance between electron i and nucleus A, R_{AB} and r_{ij} are the distances between two nuclei and two electrons, respectively.

Many *ab initio* methods, such as Hartree-Fock (HF), Møller-Plesset (MP) perturbation [40], couple-cluster (CC) [41] and density functional theory (DFT), have been developed. However, not all of them are qualified to describe intermolecular systems. (See Section 1.6)

1.4.   Perturbation and Supermolecular Methods

The study of intermolecular interactions is one of the most exciting fields in chemical science. Considerable progress has been achieved toward understanding the mechanisms of these interactions. Ab initio theory, as a power tool, plays a central role in this progress. There are two different approaches to studying intermolecular interactions in *ab initio* schemes: the perturbation method and the supermolecular method. The perturbation method treats the interaction between the subsystem wave functions as a perturbation and the interaction energy is evaluated by perturbation theory [42-46]. In this method, the electrostatic energy, exchange-repulsion energy, polarization energy, dispersion energy, exchange-induction energy and exchange-dispersion interaction energy can be calculated separately. The total interaction energy is a summation of these contributions. Alternatively, in

the supermolecular method [47-48], the interaction energy is given as the difference between the energies of the supersystem and those of the subsystems.

Perturbation Theory of Intermolecular Interactions

For a complex of two molecules 1 and 2, the total Hamiltonian of the system in the frame work of Rayleigh-Schrödinger perturbation theory (RSPT) may be written as

$$\hat{H} = \hat{H}_1 + \hat{H}_2 + \hat{V} \tag{1.13}$$

where $\hat{H}_1$ and $\hat{H}_2$ are the Hamiltonians of molecules 1 and 2, respectively. $\hat{V}$ is the intermolecular interaction operator, which is expressed as

$$\hat{V} = \sum_{A1}\sum_{B2}\frac{Z_A Z_B}{r_{AB}} - \sum_{A1}\sum_{b2}\frac{Z_A}{r_{Ab}} - \sum_{a1}\sum_{B2}\frac{Z_B}{r_{aB}} + \sum_{a1}\sum_{b2}\frac{1}{r_{ab}} \tag{1.14}$$

where A and B are nuclei of molecules 1 and 2; analogously, a and b are electrons of molecules 1 and 2. Furthermore, we assume that the ground-state wave functions are $\psi_{1,0}$ and $\psi_{2,0}$, and the exited-state wave functions are $\psi_{1,i}$ and $\psi_{2,j}$. The corresponding eigenvalues are denoted as $\varepsilon_{1,0}$, $\varepsilon_{2,0}$, $\varepsilon_{1,i}$ and $\varepsilon_{1,j}$ respectively. The RSPT expression for the total energy E_{tot} is written in the form

$$E_{tot} = E_0 + \sum_i E_i \tag{1.15}$$

where E_0 is the total unperturbed energy of the isolated molecules and E_i the interaction energy at the ith level. When the exchange effects are not included (polarization approximation [49]), the long-range contributions (electrostatic, polarization and dispersion energy) can be obtained [43]

$$\boldsymbol{E_{es}} = <\psi_{1,0}\psi_{2,0}\,|\,V\,|\,\psi_{1,0}\psi_{2,0}> \tag{1.16}$$

$$E_{pol} = \sum_{i>0} \frac{|< \psi_{1,0}\psi_{2,0} |V| \psi_{1,i}\psi_{2,0} >|^2}{\varepsilon_{1,0} - \varepsilon_{1,i}} + \sum_{j>0} \frac{|< \psi_{1,0}\psi_{2,0} |V| \psi_{1,0}\psi_{2,j} >|^2}{\varepsilon_{2,0} - \varepsilon_{2,e}} \quad \textbf{(1.17)}$$

$$E_{disp} = \sum_{i>0} \sum_{j>0} \frac{|< \psi_{1,0}\psi_{2,0} |V| \psi_{1,i}\psi_{2,j} >|^2}{\varepsilon_{1,0} + \varepsilon_{2,0} - \varepsilon_{1,i} - \varepsilon_{2,j}} \quad \textbf{(1.18)}$$

The polarization approximation neglects exchange effects and may lead to convergence problems [50-51]. In more complicated approaches such as symmetry-adapted perturbation theory (SAPT) [52] and intermolecular perturbation theory (IMPT) [43, 53], the exchange-repulsion terms are involved in the perturbation expansion. Usually, the exchange–repulsion energy is determined by fitting methods [54-58].

Supermolecular Theory of Intermolecular Interactions

In the supermolecular approach, the interaction energy is calculated in terms of its definition as

$$E_{int} = E_{complex} - \sum E_{molecule} \quad \textbf{(1.19)}$$

in which E_{int} is the intermolecular interaction energy, $E_{complex}$ the energy of the complex, and $\Sigma E_{molecule}$ the total energy of isolated molecules. The energies of the complex and molecules are obtained by *ab initio* methods. In most cases, the values of $E_{complex}$ and $\Sigma E_{molecule}$ differ only by 10^1 to 10^3 J/mole while the energy of medium size complexes is 10^6-10^8 J/mole [59]. Coulson compared this method to weighing a ship's captain by weighing the ship with and without him. Therefore, the energies of the subsystems and of the supersystem must be calculated at very high precision and also must be evaluated at the same level.

Both approaches have advantages and drawbacks. In the perturbation method, the interaction energy is calculated directly, which avoids any inconsistency originating from different descriptions of supersystems and subsystems. In addition, the individual terms of the interaction energy have a clear physical meaning，which can reflect the nature of intermolecular interaction. However, perturbation calculations are more time-consuming than supermolecular methods and thus have not yet been used for large molecular systems. This method also suffers sometimes from convergence problems. Convergence problems of the interaction energy are avoided and intermolecular exchange effects are automatically incorporated in the supermolecular approach. Furthermore, compared to the perturbation approach, the higher-order terms in the interaction potential are implicitly taken into account. Since the supermolecular approach is formally straightforward, standard chemical programs can be employed, which means that no additional programming is needed and many advanced methods and highly efficient codes are available. Because of these advantages, most calculations of intermolecular interaction energies are carried out by supermolecular method. The perturbation method is mainly used to construct accurate intermolecular potential surfaces.

Theoretically, the supermolecular and perturbation methods are equivalent. Using an infinite basis set and extending perturbation to infinite orders, identical interaction energies must be obtained. Practically, the basis set inconsistency in the supermolecular method and truncation of high orders in perturbation calculations make the results somewhat different from each other.

1.5. <u>Basis Set Superposition Error (BSSE)</u>

The supermolecular method is extensively used for interaction energy determination. However, there is a major drawback. Suppose that a supersystem and its subsystems are calculated with the same basis set and theoretical method. Since the supersystem is described by a larger basis set, this leads to a more negative total energy, in which a spurious attraction energy is included. The error caused by unequal basis sets of supersystem and subsystems is called basis set superposition error (BSSE). It is not for any physical reason but is only a purely artificial mathematical effect. For small basis sets, the BSSE dominates interaction energy calculation, while it disappears automatically with an infinite basis set. In the 1970s, Boys and Bernardi introduced the counterpoise method (CP) for eliminating the BSSE [60]. In their method, subsystem energies are calculated in the supersystem basis set. The interaction energy corrected for the BSSE (E_{int}^{C}) is written as follows

$$E_{\text{int}}^{c} = E_{complex} - \sum_{i} E_{complex}^{i} \tag{1.20}$$

where $E_{complex}$ is the energy of the supersystem and $E_{complex}^{i}$ is the energy of the subsystem i with the same basis set as the complex. In other words, the energy of each subsystem is calculated in the presence of the atomic orbitals of the other subsystems, but without including the electrons and nuclei of the other subsystems. These kinds of orbitals are named "ghost orbitals".

The counterpoise method has proved effective and is therefore widely used to correct the BSSE. Nevertheless, the accuracy of this method is controversial. It is said that the Boys-Bernardi method (CP) may overestimate the BSSE, because in the supersystem calculation, the occupied orbitals of each subsystem are not available to the electrons in other ones [61]. A corrected method, called VCP ("virtual" counterpoise method), using only the virtual orbitals of the other subsystems, has been suggested [62-64].

In some cases, the VCP method performs well. Nevertheless, it has also been criticized. Some calculations demonstrate that the VCP method does not eliminate the whole BSSE [65-66]. In these papers, Gutowski *et al* declared that the full counterpoise method has a very beneficial effect while the VCP method should be rejected.

The debate about the BSSE correction is still continuing. It is really a very complicated problem. Fortunately, with the development of computer techniques, *ab initio* calculations with large basis sets are feasible now, which can make the BSSE correction negligible.

1.6. __Effective Theoretical Methods for Supermolecular Approach__

In the supermolecular method, all *ab initio* methods can be employed for intermolecular interaction calculation. However, not all of them are suitable for supermolecule calculations.

The Hartree-Fock method completely misses the dispersion interaction, which involves electron correlation between electrons on different molecules. In *ab*

initio calculations, the total interaction energy can be divided into two parts: Hartree-Fock (ΔE_{HF}) and correlation energy (ΔE_{COR}):

$$\Delta E_{\text{int}} = \Delta E_{HF} + \Delta E_{COR} \tag{1.22}$$

ΔE_{COR} represents mainly the dispersion interaction energy. In post-Hartree-Fock methods, the correlation term can be evaluated. The effective ones should give accurate values of ΔE_{COR}.

Density functional theory is very attractive for intermolecular energy calculation because it is much less computationally demanding than post-Hartree-Fock methods. As the exchange-correlation functionals are naturally contained in DFT, it was believed that this method is suited to deal with intermolecular interactions. Disappointingly, current density-functional methods fail completely for the evaluation of dispersion energy. The reason is very simple: none of the existing correlation functionals can describe the dispersion interaction [67-68]. Although DFT works well for hydrogen-bonded systems, it needs to overcome the dispersion problem to achieve enough accuracy for intermolecular interaction calculations.

The most economical post Hartree-Fock method is second-order Møller-Plesset theory (MP2). Surprisingly, this method gives very accurate intermolecular correlation energies. This is due to mutual compensation of neglected higher-order contributions [69]. For interaction energy calculations of big molecular complexes, the local MP2 method (LMP2) was developed. This can deal with a molecular system with hundreds of atoms [70]. Additionally, the value of the BSSE in this method is smaller than for the normal MP2 method [71].

For complete investigation of interaction energies, the full configuration method (FCI) or coupled-cluster singles, doubles and triples method (CCSDT) [72] is recommended. However, these methods are presently too computationally expensive to be applied to normal intermolecular systems. Therefore, as a compromise between accuracy and economy, an approximate form of CCSDT, which is called CCSD(T) (coupled cluster method with single, double and noninteractive triple excitations), has been developed [73]. CCSD(T) provides a powerful tool for the evaluation of intermolecular interaction energies.

Finally, we should underline that *ab initio* methods for the supermolecular approach must be size-consistent, which means that the energy of the supermolecule at infinite separation must be equal to the sum of the energies of the isolated molecules [40]. The size-consistency restriction means that some common methods are not qualified. For instance, configuration interaction methods (CI) are not size-consistent in that double excitations on each subsystem are included, but the corresponding higher order excitations are excluded for the supermolecule.

1.7.   Basis Set Selection

The selected basis set should describe the complex as accurately as possible. It is found that large basis sets which contain polarization and diffuse functions must be used for reliable results. Nevertheless, the relationship between the size of basis sets and computation time is not linear but n^X ($X \geq 4$), which means that the size of basis sets must be limited. Among all sorts of basis sets, Dunning's correlation-consistent basis sets [74-75], augmented with polarization functions,

have recently been extensively used for intermolecular interactions, because the basis set limit can be extrapolated. They are referred to with acronyms such as aug-cc-pVnZ, with n = D, T, Q, 5, etc., for double-zeta, triple-zeta, quadruple-zeta, etc.

Dunning's correlation-consistent basis sets are general-purpose, and are not optimized for interaction energy calculation. Many special basis sets have been developed for better results. For example, specially-tailored basis sets are designed to reproduce monomer properties relevant to intermolecular forces; adding bond-centred basis functions, located at or near the midpoint of the Van der Waals bond, is effective in recovering most of the dispersion energy [76].

The size of basis sets determines the value of the BSSE directly. Generally, the larger the basis set, the smaller the BSSE. When an infinite basis set is used, the BSSE is equal to zero. Therefore, large basis sets can reduce the effects caused by the BSSE.

References

[1]. Lewis, G.N. *Valence and structure of Atoms and Molecules;* Chemical Catalog Co.; New York, **1923**.

[2]. Israelachvili, J. *Intermolecular & Surface Force*; Academic Press; **1991**.

[3]. London, F. *Z. Phys.Vhem. (B)* **1930**, 11, 222.

[4]. London, F. *Trans. Faraday Soc.***1937**, 33, 8.

[5]. Margenau, *H. J. Chem. Phys.* **1938**, 6, 896.

[6]. Hornig, J.F.; Hirschfelder, J. O. *J. Chem. Phys.* **1952**, 20, 1812.

[7]. Zeiss, G.D.; Meath, W. *J. Mol. Phys.* **1977**, 33, 1155.

[8]. Jhanwar, B. L.; Meath, W. *J. Chem. Phys.* **1982**, 67, 185.

[9]. Kumar, A.; Meath, W. *J. Mol. Phys.* **1985**, 54, 823.

[10]. Murrell, J.N. In *Orbital Theories of Molecules and Solids*; March, N. H., Ed.; Clarendon: Oxford, **1974.**

[11]. Cornell, W. D.; Cieplak, P., Bayly; C. I., Gould, I. R.; Merz, K. M. Jr., Ferguson, D. M. Spellmeyer, D. C., Fox, T., Caldwell, J. W., and Kollman, P. A. *J. Am. Chem. Soc*. 117, **1995**, 5179.

[12]. Pearlman, D. A.; Case, D. A., Caldwell; J. C., Seibel, G. L.; Singh, U. C., Weiner, P.; Kollman, P. A., AMBER 4.0, University of California, San Francisco, 1991.

[13]. Weiner, P. K.; Kollman, P. A. *J. Comp. Chem*. 2, **1981**, 287.

[14]. Weiner, S.J.; Kollman, P.A.; Case, D.A.; Singh, U.C.; Ghio, C.; Alagona, G.; Profeta, S., Jr.; Weiner, P.K. *J. Am. Chem. Soc*. 106, **1984**, 765.

[15]. Weiner, S. J.; Kollman, P. A.; Nguyen, D. T.; Case, D. A., *J. Comp. Chem.* 7, **1986**, 230.

[16]. Brooks, B.R.; Bruccoleri, R.E.; Olafson, B.D.; States, D.J.; Swaminathan, S.; Karplus, M. *J. Comp. Chem.* 4, **1983**, 187.

[17]. Feller et al., *Biophys*. J. 73, **1997**, 2269.

[18]. MacKerell, A D ; Bashford, D; Bellott, M; Dunbrack, R L; Eva seck, J D; Field, M J; Fischer, S; Gao, J; Guo, H; Ha, S; JosephMcCarthy, D; Kuc nir, L; Kuczera, K; Lau, F T K; Mattos, C; Michnick, S; Ngo, T; Nguyen, D T; Pro hom, B; Reiher, W E; Roux, B; Schlenkrich, M; Smith, J C; Stote, R; Straub, J; W tanabe, M; WiorkiewiczKuczera, J; Yin, D; Karplus, M. *J. Phys. Chem., B* 102, **1998**, 3586-3617

[19]. Mackerell A D ; Wiorkiewiczkuczera J; Karplus, M. *J. Amer. Chem. Soc.*117, **1995**, 11946

[20]. Momany, F. A.; Rone, R. *J. Comp. Chem.* 13, **1992**, 888.

[21]. Pavelites, J. J.; J. Gao; P.A. Bash and A. D. Mackerell, Jr. *J. Comp. Chem.* 18, **1997**, 221.

[22]. Schlenkrich et al. Empirical Potential Energy Function for Phospholipids: Criteria for Parameter Optimization and Applications in "Biological Membranes: A Molecular Perspective from Computation and Experiment," K.M. Merz and B. Roux, Eds. Birkhauser, Boston, **1996**.

[23]. Allinger, N. L. *J. Am. Chem. Soc.* 99, **1977**, 8127.

[24]. Allinger, N. L.; Kok, R. A.; Imam, M. R. J. Comp. Chem. 9, 1988, 591.

[25]. Lii, J-H.; Gallion,S.; Bender,C.; Wikstrom, H.; Allinger, N. L.; Flurchick, K. M.; Teeter, M. M. *J. Comp. Chem.* 10, **1989**, 503.

[26]. Dewar, M.J.S.; Thiel W. *J. Am. Chem. Soc.* 99, **1977**, 4899.

[27]. Dewar, M.J.S.; Thiel W. *J. Am. Chem. Soc.* 99, **1977**, 4907.

[28]. Dewar, M.J.S.; Zoebisch E.G., Healy E.F. et al. *J. Am. Chem. Soc.* 107, **1985**, 3902.

[29]. Stewart, J.J.P. *J. Comput. Chem.* 10, **1989**, 209.

[30]. Stewart, J.J.P. *J. Comput. Chem,* 10, **1989**, 221.

[31]. Thiel W.; Voityuk A.A. *J. Phys. Chem.* 100, **1996**, 616.

[32]. Repasky, M.P.; Chandrasekhar, J.; Jorgenson, W. *J. Comput, Chem,* 23, **2002**, 2001.

[33]. Warshel,A,; Levitt, M. *J. Mol. Biol.*, 103, 1976, 227.

[34]. Zhang, Y.; Liu, Y.; Yang, W. *J. Chem. Phys.*112, **2000**, 3483.

[35]. Gao, J. *Acc. Chem. Res.*, 29, **1996**, 298.

[36]. Bakowies, D.; Thie, W. *J. Phys. Chem.*, 100, **1996**, 10580.

[37]. Field, M.; Bash, P.; Karplus, M. *J. Comput. Chem*, 11, **1990**, 700.

[38]. Friesner, R.; Beachy, M. D. *Curr. Opin. Struct. Biol.*, 8, **1998**, 257.

[39]. Monard, G; Merz, K. M. *Acc. Chem. Res.*, 32, **1999**, 904.

[40]. Bartlett, R.J. *Ann. Rev. Phys. Chem.*, 32, **1981**, 359.

[41]. Bartlett, R.J. *J. Phys. Chem.*, 93, **1989**, 1697.

[42]. Buckingham, A. D. *Adv Chem. Phys*. 12, **1967**, 107.

[43]. Stone, A. J. *The theory of Intermolecular forces;* Pergamon: Oxford, **1996**.

[44]. Pitzer, K.S. *Adv Chem. Phys*. 2, **1959**, 59.

[45]. Van Lenthe, J.H.; van Duijneveldt-van de Rijdt, J.G. C. M.; van Duijneveldt, F. B. . *Adv Chem. Phys*. 69, **1987**, 521.

[46]. Rullman, J. A. C.; van Duijnen, P.T. *Rep. Mol. Theor.*1, **1990**, 1.

[47]. Hobza, P; Zahradnik, R. *Intermolecular Complexes;* Elsevier: Amsterdam, **1988**.

[48]. Hobza, P. *Ann. Rep. Prog. Phys. Chem.* 93, **1997**, 257.

[49]. Hirshfelder, J. O. *Chem. Phys. Lett.* 1, **1967**, 325.

[50]. Claverie, P. *Int. J. Quant. Chem.*5, **1971**, 273.

[51]. Kutzelnigg, W. J. *J. Chem. Phys.* 73, **1980**, 343.

[52]. Jezeiorski, B.; Moszynski, R; Szalewicz, K. *Chem. Rev.* 94, **1994**, 1887.

[53]. Hayes, I.C.; Stone, A. J. *Mol. Phys.* 53, **1984**, 83.

[54]. Brdarski,S.; Karlström, G. *J.Phys. Chem. A* 102, **1998**, 8182.

[55]. Millot, C.; Stone, A. J. *Mol. Phys.* 77, **1992**, 439.

[56]. Hodges. M. P.; Stone, A. J.; Cabaleiro Lago, E. *J.Phys. Chem. A* 102, **1998**, 2455.

[57]. Stone, A. J.; Tong, C. S. *J. Comput. Chem.* 15, **1994**, 1377.

[58]. Fraschini, E.; Stone, A. J. *J. Comput. Chem.* 19, **1998**, 847.

[59]. Hobza, P.; Zahradnik, R. *Chem. Rev.* 88, **1988,** 871.

[60]. Boys, S.F.; Bernardi, F. *Mol. Phys.* 19, **1970**, 553.

[61]. Johansson, A.; Kollman, P.; Rothenburg, S. *Theor. Chim, Acta.* 29, **1973**, 167.

[62]. Schwenke, D. W.; Truhlar, D. G. *J. Chem. Phys.* 82, **1985**, 2418.

[63]. Daudey, J. P.; Claverie, P.; Malrieu, J. P. *Int. J. Quantum Chem.* 8, **1974**, 1

[64]. Olivares del Valle, F. J.; Tolosa, S.; Esperilla, J. J.; Ojalvo, E. A.; Requena, A. *J. Chem. Phys*. 84, **1986**, 5077.

[65]. Gutowski, M.; van Duijneveldt, F.B.; Chalasinski, G.; Piela, L *Mol. Phys.*61, **1987**, 233.

[66]. Gutowski, M.; van Lenthe, J.H.; Verbeek, J.; van Duijneveldt, F.B.; Chalasinski, G. *Chem. Phys. Lett.* 124, **1986**, 370.

[67]. Hobza, P; Šponer, J.; Reschel, T. *J. Comput. Chem.*11, **1995**, 1315.

[68]. Kristian, S.; Pulay, P.*Chem. Phys. Lett.* 229, **1994**, 175.

[69]. Hobza, P; Müller-Dethlefs, K. *Chem. Rev.* 100, **2000**, 143.

[70]. Saebø, S; Pulay, P. *J. Chem. Phys.* 86, **1987**, 914.

[71]. Schütz, M; Rauhut, G; Weiner, H. J. *J. Phys. Chem. A* 102, **1998**, 5997.

[72]. Noga, J; Bartlett, R. J. *J. Chem. Phys.* 86, **1987**, 7041.

[73]. Raghavachari, K; Trucks, G. W.; Head-Gordon, M; Pople, J.A. *Chem.Phys. Lett.* 157, **1989**, 479.

[74]. Dunning, T. H. J., Jr. *Chem. Phys.* 90, **1989**, 1107.

[75]. Dunning, T. H. J., Jr. *ibid* 98, **1993**, 1358.

[76]. Burcl, R.; Chalasinski, G.; Bukowski, R.; Szczesniak, M. M. *J. Chem. Phys.* 103, **1995**, 1498.

CHAPTER 2. SOME PROBLEMS IN *AB INITIO* INTERMOLECULAR INTERACTION ENERGY CALCULATIONS

2.1.   <u>Historical Retrospection</u>

Ab initio methods provide a robust tool for studying the properties of molecular systems. They are extensively used to understand the nature of the chemical bond and chemical reactions. In this field, *ab initio* quantum theory is so successful that the accuracy of theoretical calculations is close to experimental data in many cases. Nevertheless, *ab initio* methods could only give a qualitative explanation for intermolecular interactions for a long time, largely because of the difficulty of calculating the dispersion contribution. Before the 1990s, although many researchers believed that quantum theory can describe noncovalent intermolecular interactions as successfully as covalent ones, they had to acknowledge that it is a "very difficult task" [1]. At that time, even experimental data were not plentiful, and accurate empirical potential surfaces existed only for noble gas pairs [2] and some simple molecular systems such as Ar-H [3] and Ar-HCl [4].

During the early years of the 1990s, a great deal of work was done on the spectroscopy of weakly-bonded complexes, especially in the mid-infrared and near-infrared ranges [5]. These experimental data were used to determine intermolecular potentials and even to build potential energy surfaces (PES).

At the same time, because of the growth of computer power, various *ab initio* methods with larger basis sets and more complete intermolecular correlation were employed for intermolecular interaction calculations. Their accuracy can also be evaluated in terms of spectral data. It was found that CCSD(T) and MP2 are suitable methods. Using these, most dispersion energy can be recovered; furthermore, they are not as time-consuming as their cousins such as CCSDT, MP4, *etc*. Large basis sets with polarization functions should be used for accurate results.

Now the *ab initio* theory of intermolecular interactions enters a quantitative era. The methodology can provide reliable intermolecular potential energy surfaces and accurate interaction energies.

2.2. <u>Problems in *ab initio* Intermolecular Interaction Calculations</u>

Despite the considerable progress,, there are still some unsolved problems in this field, which limit the development and application of *ab initio* intermolecular interaction theory severely.

One of the most important problems is the efficiency of *ab initio* methods. As we know, *ab initio* calculations are so time-consuming that they cannot be applied to large molecular systems. The problem is even worse in intermolecular interaction calculations: For electronic structures of isolated molecules, *ab initio* calculation may give reliable results at the HF level with small or medium size basis sets in many cases. In contrast, post-HF methods (MP2, MP4 and CCSD(T), etc.) must be employed and large basis sets with polarization functions must be used for intermolecular energy calculations. Despite the progress in computational

capabilities, accurate results can only be obtained for some small complexes. Since many important intermolecular systems are medium- or large-sized, it is a serious drawback. Unless there are some breakthroughs in fundamental theory, the application of *ab initio* methods is very limited.

In chapter 1, we mentiond that the BSSE was a significant error in the supermolecular approach. The main approach for BSSE correction is the counterpoise method, the validity of which is still being argued today. It seems that the BSSE originates from the "internal infection" of the supermolecular method [1]. Although the CP correction works in most cases, it cannot completely eliminate the error. Theoretically, the BSSE converges to zero with complete basis sets. However this is too computationally demanding for most molecular complexes.

Another important problem in the supermolecular approach is called basis-set saturation: The convergence is very slow for interaction energies, with a rapid increase in the number of basis functions. This effect originates in the Coulomb cusp condition, which is very slowly reproduced by an one-electron basis set expansion [6-7]. It is particularly serious for dispersion interactions. Several different methods are used to correct this problem; these include adding the interaction distance into a basis set [8-9] and using bond functions in the middle of the van der Waals bond [10-11]. However the former is too computationally demanding in actual applications and the latter is not appropriate for electric properties of the subsystems [12].

In summary, *ab initio* calculations are becoming a popular method for intermolecular interaction calculations. However, there are still some difficult

problems with this approach. The complexity of *ab initio* methods limits their application to large complex systems and post-HF methods and big basis sets exacerbate the difficulty. In the supermolecular approach, the most popular method for interaction energy calculations, the BSSE correction is still argued. Additionally, the use of huge basis sets causes basis set saturation, which also needs correction. In order to overcome the difficulties, we want to develop a new method in this dissertation, which is less computationally demanding for intermolecular interaction energy calculations. Furthermore, the BSSE effect can be avoided in this approach.

References

[1]. Hobza, P.; Zahradník, R. *Chem. Rev.* 88, **1988**, 871.

[2]. Aziz, R. A. ``Interatomic potentials for rare gases: pure and mixed interactions'', in *Inert Gases*, edited by M. L. Klein Springer; Berlin, **1984**.

[3]. Le Roy, R. J.; Hutson, J. M. *J. Chem. Phys.* 86, **1987**, 837.

[4]. Hutson, J. M. *J. Chem. Phys.* 89, **1988**, 4550.

[5]. Bacic, Z.; Miller, R.E. *J. Phys. Chem.* 100, **1996**, 12945.

[6]. Kutzelnigg, W. *Theor. Chim. Acta* 68, **1985**,445

[7]. Klopper, W. *The Encyclopedia of Computational Chemistry*, von Rague Schleyer, P.; Allinger, N. L.; Clark, T.; Gasteiger, J.; Kollman, P.A.; Schaefer, H. F. III.; Schreiner, R.; Eds. Wiley: Chichester, UK, **1988**.

[8]. Jeziorski, B.; Szalewicz, K.; Monkhorst. H.; Zabolitzky, J. G. *J. Chem. Phys.* 81, **1984**, 368.

[9]. Bukowski, R.; Jeziorski, B.; Szalewicz, K. *J. Chem. Phys.* 102, **1995**, 888.

[10]. Tao, F.-M.; Pan. Y.-K. *J. Chem. Phys.* 97, **1992**, 4989.

[11]. Koch, H.; Fernanderz, B.; Christiansen, O. *J. Chem. Phys.* 108, **1998**, 2784.

[12]. Burcl, R.; Chalasiński, G.; Bukowski, R.; Szczęśniak, M. M. *J. Chem. Phys.* 103, **1995**, 1498.

CHAPTER 3. CALCULATION OF ELECTROSTATIC INTERACTION ENERGIES FROM ELECTRONIC DENSITIES

3.1. <u>Introduction</u>

Electrostatic interactions are very important in intermolecular systems. In particular, they dominate ionic and hydrogen-bonded systems such as proteins and DNA. For some hydrogen-bonded systems, an electrostatic approximation was employed and it was found that the electrostatic energy agreed very well with the non-empirical SCF interaction energy in the entire range from large separation to the vdW minimum [1]. Therefore, in some cases, the electrostatic energy can be used for estimating the strength of a weakbond.

The easiest method for electrostatic interaction energy calculations is to determine the net atomic charges for each molecule. This kind of work started decades ago [2]. As the motion of electrons is ignored, this method is only a crude approximation. Actually, there is no rigorous way to define atomic charge. Some improved methods, including the interaction of higher multipole moments, were developed for better results [3-7]. However, the evaluation of multipoles is sophisticated. In this work, a more accurate approach is presented: the energy of the intermolecular electrostatic interaction is calculated directly from the electron densities of the monomers.

3.2.   Computational Methods

The electron density is a physical observable, which can be determined by experimental methods such as X-ray diffraction in crystals [8]. If a bridge between interaction energy and electron density is built, the electrostatic interaction energy can be obtained from experimental data directly. This is really very attractive for calculations of big complexes. Alternatively, the electron densities may come from theoretical computation. With the development of modern quantum chemistry, calculation the electron densities of many molecular systems is becoming a routine task.

According to the Hohenberg-Kohn theorem [10], the ground-state molecular energy is uniquely determined by the electron density. In other words, the ground-state energy E_0 is a functional of the electron density ρ.

$$E_0 = F(\rho)$$

(3.1)

What the Hohenberg-Kohn theorem guarantees is the existence of such a functional $F(\rho)$. However, it does not tell us how to calculate E_0 from ρ. Actually, an exact analytical form of the functional may not exist. Hence we have to find other approaches.

Fortunately, it is not difficult to calculate the electrostatic interaction energy from an electron density model based on Coulomb's law. First, we assume that a complex is composed of two molecules, A and B. The intermolecular electrostatic interaction energy between A and B is the sum of nucleus-nucleus, nucleus-electron, and electron-electron terms. In the view of quantum mechanics, the position of the

electrons in uncertain at a specific time, so the electron probability density, a time-average property, is employed here. The electrostatic interaction energy E_{es} between A and B is,

$$E_{es} = \sum_A \sum_B \frac{Z_A Z_B}{|\vec{R}_A - \vec{R}_B|} - \sum_A \int \frac{Z_A \rho_B^0(\vec{r}_B)}{|\vec{R}_A - \vec{r}_B|} d\vec{r}_B$$
$$- \sum_B \int \frac{Z_B \rho_A^0(\vec{r}_A)}{|\vec{R}_B - \vec{r}_A|} d\vec{r}_A + \iint \frac{\rho_A^0(\vec{r}_A) \rho_B^0(\vec{r}_B)}{|\vec{r}_A - \vec{r}_B|} d\vec{r}_A d\vec{r}_B$$

(3.2)

where Z_A, Z_B are atomic charges in molecules A and B, and ρ_A^0 and ρ_B^0 are the electron densities of isolated molecules A and B.

Eq. (3.2) can also be derived rigorously from the concept of electrostatic potential. The electrostatic potential of molecule A at any point $\vec{r}$ that is created by the nuclei and electrons of a system A is given by [10, 11]

$$V_A(\vec{r}) = \sum_A \frac{Z_A}{|\vec{R}_A - \vec{r}|} - \int \frac{\rho_A^0(\vec{r}_A)}{|\vec{r}_A - \vec{r}|} d\vec{r}_A$$

(3.3)

in which $V_A(\vec{r})$ is the electrostatic potential of molecule A at point $\vec{r}$, Z_A is the charge on each nucleus of molecule A; and $\rho_A^0(\vec{r}_A)$ is the equilibrium electron density of isolated A. The nucleus and electron charges of molecule B interact with the electrostatic potential of molecule A and the energy of the electrostatic interaction between two molecules A and B is therefore,

$$E_{es} = \sum_B E_{B,N} + \int \varepsilon_{B,e} d\vec{r}_B$$

(3.4)

$E_{B,N}$ are the electrostatic interaction energies at each nucleus of molecule B and $\varepsilon_{B,e}$ are electrostatic energy densities at each point $\vec{r}_B$:

$$E_{B,N} = V_A(\vec{r}_B)Z_B \tag{3.5}$$

$$\varepsilon_{B,N} = V_A(\vec{r}_B)\rho_B^0(\vec{r}_B) \tag{3.6}$$

Putting Eqs. (3.5) and (3.6) into Eq. (3.4), we obtain an expression for the electrostatic interaction energy between A and B, which has the same form as Eq. (3.2).

According to Eq. (3.2), the unperturbed electron density of each molecule and the geometry of the complex must be known for the calculation of the intermolecular interaction electrostatic energy. To evaluate the integrals in Eq. (3.2), we use a numerical integration scheme modeled, with slight modifications, after that of Gavezzotti [12]. Usually, the calculation includes following several steps and some approximations are used:

(1). Preparation of electron density

In the numerical integration, an electron charge distribution $\rho(\vec{r})$ is divided into a large number of tiny electron density units by means of a three dimensional grid which creates blocks (not necessary cubical) of volumes V, called electron pixels centered around points $\vec{r}_i$. These units were termed "e-pixels" by Gavezzotti; however, since pixel is an abbreviation for picture element, which is two-dimensional, the present three-dimensional units should properly be called "e-voxels" (electronic volume elements). Therefore, we shall always use the term "e-voxel" in the dissertation.

The electron density of each e-voxel is generated from molecular wave functions by Gaussian 98 (G98). The electron density can be generated directly

with the keyword "cube=density" or from a formatted check point file by the program "cubegen". The Cube subroutine allows one to establish the origin, stepsizes and extent of the grid; alternatively, one need only specify the total number of points desired and Cube will generate a corresponding rectangular grid enclosing the particular charge distribution. For example, "cube=80" means generating a file which includes around 512000 ($80 \times 80 \times 80$) e-voxels. All the information of the electron density is stored in a cube file.

Some unrealistic values of the electron charges may arise close to the nuclei. Since this is mainly brought about by the inner core electrons, the valence electron density is used instead of the full electron density to alleviate the problem.

(2). Boundary of electron density

The electron cloud diffuses in the whole space. In a cube file, the number of e-voxels is usually from several hundred thousands to a few millions. In order to keep the scope of the calculation within reasonable bounds, Gavezzotti invokes a minimum acceptable magnitude for the charge of each e-voxel. We choose instead to assign an outer boundary to the molecule, defined as an isodensity contour of $\rho(\vec{r})$, designated ρ_{min}. All e-voxels beyond the boundary are ignored (exceptions are discussed below). Many near-zero-density e-voxels are removed in this step.

(3). Condensation

In step 2, many e-voxels are screened out. However, the number of voxels is still too high for calculation of the electron-electron repulsion energy. The original ones are combined and new cubic "super e-voxels" are thus formed. Each of them consists of n^3 old e-voxels. This procedure is called condensation and n is the

condensation level. The charge of a super e-voxel, Q_i, is taken to be located at its center $\vec{r}_i$, and to equal the sum of the charges of its constituents: $Q_i = \sum_j q_{j,i}$. It might seem that using a larger step size in the generation of the electron density (step 1) could avoid the condensation step and simplify the calculation. Nevertheless, it may cause errors because of an inaccurate electron count [12].

The original number of e-voxels may not be an integer multiple of that of the new ones, which causes a small asymmetry in the condensed density in Gavezzotti's approach [12]. Our method is very simple and effective: If a super e-voxel has its center within the ρ_{min} boundary, but some of its constituents are beyond ρ_{min}, the are nevertheless included, even if they are screened out in step 2. The asymmetry can thus be eliminated.

(4). Renormalization

In previous steps, a small part of the electron count is lost. To keep charge neutrality, the total valence charge must be renormalized to fit the nuclear charge in the molecule. Although this procedure may increase some inner electron density, the error is negligible.

(5). Coordinate transformation

Since the coordinates of atoms in the isolated molecules are normally different from those in the complex, the former must be transformed into the latter. The procedure involves a series of appropriate translations and rotations of coordinate axes. The parameters of translation and rotation can be determined by comparing the coordinates of each atom in the isolated molecules and in the

complex. Then the coordinates of each e-voxel are transformed in terms of the parameters.

(6). Electrostatic energy calculation

In terms of the super e-voxels, the electrostatic interaction energy between two systems, A and B, as expressed by Eq. (3.2), becomes,

$$E_{es} = \sum_A \sum_B \frac{Z_A Z_B}{|\vec{R}_A - \vec{R}_B|} - \sum_A \sum_i \frac{Z_A Q_i}{|\vec{R}_A - \vec{r}_i|} \\ - \sum_B \sum_j \frac{Z_B Q_j}{|\vec{R}_B - \vec{r}_j|} + \sum_i \sum_j \frac{Q_i Q_j}{|\vec{r}_i - \vec{r}_j|}$$

(3.7)

Sometimes the distances $|\vec{r}_i - \vec{r}_j|$ in Eq. (3.7) can be very small, leading to unrealistic interaction energies. In order to avoid the errors caused by e-voxel overlap, a minimum distance (e.g. one-half of the grid stepsize) is chosen and all distances below the minimum are reset to a fixed value (eg. the minimum distance).

Figure 3.1 gives the flowsheet of the calculation of the electrostatic interaction energy. A FORTRAN program was prepared on the basis of the flowsheet. It reads the electron density files of each isolated molecule and the coordinates of the complex and then calculates the electrostatic energy between the molecules.

3.3.   The Calculation of the Electrostatic Interaction Energy for Water Dimer

The properties of water are of the utmost importance in a host of chemical and biological processes. Intimately related to these properties are intermolecular interactions. Thus the water dimer, as one of the simplest intermolecular pairs, is
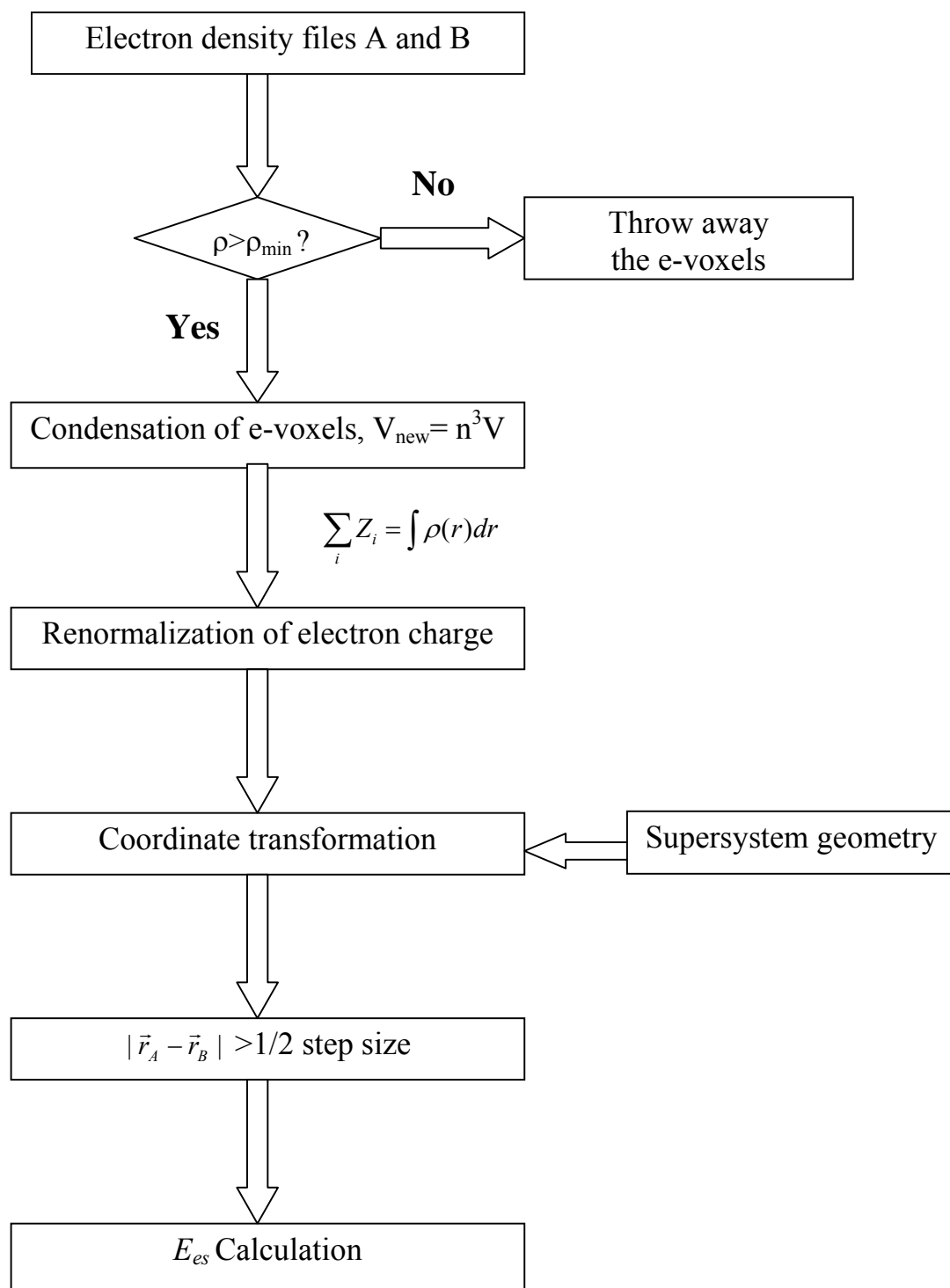
Figure 3.1 Flowsheet of the calculation of intermolecular electrostatic interaction
energy.

widely studied. In recent years, a lot of experimental work [13-16] and theoretical studies [17-25] focused on this topic and the structure and intermolecular interactions have been studied thoroughly.

The water dimer is an electrostatic-interaction-dominant complex. With the study of its intermolecular potential energy surface, ten stationary points were found and the nonplanar open C_s structure has the lowest energy among them [26]. In this dissertation, we always use the C_s structure.

The geometries of the dimer and the isolated molecules were optimized, respectively, at CCSD(T)/TZ2P(f,d)+dif and MP2/6-311G(d,p) levels [26], the hydrogen bond H---O distance was 1.9485 Å. The density cube files were prepared at different levels by single point calculations. Some parameters, such as the value of the isodensity boundary, condensation level and number of e-voxels in a cube file, may affect the results of calculation. In order to assess the influence caused by the various parameters, we calculated the electrostatic interaction energies of the water dimer with two different basis sets for various values of (a) ρ_{min} and (b) the number of e-voxels, using Hartree-Fock electron densities of the free molecules at their relative positions in the dimer.

The results are listed in Tables 3.1 and 3.2. Table 3.1 shows that $\rho_{min} \leq 1.0 \times 10^{-5}$ electrons/bohr^3 is sufficient for E_{es} to achieve convergence when the number of e-voxels equals 1.0×10^6. In most cases, the value of ρ_{min} is set from 10^{-5} to 10^{-6} electrons/bohr^3 for reliable results. As mentioned above, the number of e-voxels in a cube file can significantly affect the results: A small size cube file may lead to big errors. From Table 3.2, it is seen that 1.0×10^6 e-voxels is adequate for
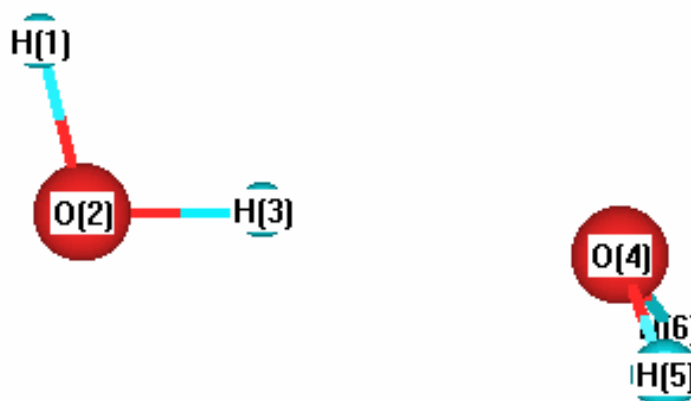
Figure 3.2   Optimized C_s structure of water dimer at CCSD(T)/TZ2P(f,d)+dif level. Intramonomer geometrical parameters: r_{H1O2} = 0.9581 Å; r_{O2H3} = 0.9653 Å; r_{O4H5} = 0.9597 Å; r_{O4H6} = 0.9597 Å; θ_{H1O2H3} = 104.45°; θ_{H5O4H6} = 104.58°. Intermonomer geometrical parameters: r_{H3O4} = 1.9485Å; θ_{O2H3O4} = 172.92°; θ_{H5O4O2} = 110.50°; θ_{H6O4O2} = 110.50°; $\tau_{O4H3O2H1}$ = 180.00°; $\tau_{H5O4O2H3}$ = 122.37°; $\tau_{H6O4O2H3}$ = -122.37°. $r_{XY,}$ θ_{XYZ} and τ_{WXYZ} represent distance, angle and dihedral angle respectively. Data are from ref. 26.

Computational	$\rho_{min,}$ electrons/bohr^3							
method	0.01	0.001	1.0×10^{-4}	5.0×10^{-5}	2.0×10^{-5}	1.0×10^{-5}	1.0×10^{-6}	1.0×10^{-7}
HF/6-31+G(d,p)	-8.12	-9.19	-9.56	-9.65	-9.81	-9.82	-9.83	-9.83
HF/aug-cc-pVQZ	-7.26	-7.40	-7.94	-8.02	-8.14	-8.17	-8.17	-8.17

Table 3.1   Electrostatic interaction energies E_{es} of $(H_2O)_2$, in kcal/mole, using various molecular boundaries ρ_{min}. Number of e-voxels is 1.00×10^6, stepsize is 0.0531 Å and condensation level is n=3. H_2O geometry optimization was MP2/6-311G(d,p); relative positions in dimer determined at CCSD(T)/TZ2p(f,d)+dif level.

reliable results when ρ_{min} =1.0×10^{-6} electrons/bohr^3. For most molecular systems,

"cube=100" (1.0×10^6 e-voxels) is a good choice. With regard to the number of

super e-voxels, our experience has been that at least 2000 are needed for E_{es} to be

stable. For example, for 1.0×10^6 e-voxels, the condensation level n should be no

larger than 7 ($1.0 \times 10^6/7^3$=2915).

Computational	Numer of e-voxels and condensation level[a]				
method	2.98×10^4 n=3	2.27×10^5 n=3	5.12×10^5 n=5	1.00×10^6 n=5	1.73×10^6 n=7
HF/6-31+G(d,p)	-10.91	-9.99	-9.74	-9.82	-9.78
HF/aug-cc-pVQZ	-9.29	-8.32	-8.09	-8.17	-8.16

Table 3.2　　Electrostatic interaction energies E_{es} of $(H_2O)_2$, in kcal/mole, for various number of e-voxels. Molecular boundary ρ_{min} is 1.0×10^{-6} electrons/bohr^3. H_2O geometry optimization was MP2/6-311G(d,p); relative positions in dimer determined at CCSD(T)/TZ2P(f,d)+dif level.

[a]Stepsizes range from 0.0441 Å for 1.73×10^6 e-voxels to 0.176 Å for 2.98×10^4.

　　　　Tables 3.1 and 3.2 indicate that the basis set can have a significant effect. To

further investigate the effect of basis sets and theoretical methods, we computed the

electrostatic interaction energies at different levels, with the electron charges of the

isolated water molecule and the geometry of the water dimer. As a comparison,

point-charge methods were also employed in this calculation: Here Mulliken

charges and CHelpG [27] (Charges from Electrostatic Potential using a Grid based

method) were obtained. Table 3.3 shows the charges on the oxygen atom.

　　　　From Table 3.3, it is found that the Mulliken charges fluctuate widely

(between −0.256 and −0.866) with different theoretical methods and basis sets.

Therefore, it is not reliable to determine the electrostatic interaction energy from

Mulliken charges. CHELPG makes the charges much less variable (between −0.675

and –0.870). The precision of this method thus is better than that of Mulliken charges.

Computational method	Mulliken Charge	E_{es}	CHELPG Charge	E_{es}
HF/3-21G	-0.7265	-4.89	-0.8703	-7.02
HF/6-31G(d)	-0.8655	-6.70	-0.8042	-6.00
HF/6-31+G(d,p)	-0.7312	-4.96	-0.8271	-6.34
HF/6-311++G(d,p)	-0.5104	-2.41	-0.8067	-6.03
HF/cc-pVDZ	-0.3068	-0.87	-0.7444	-5.13
HF/cc-pVQZ	-0.5271	-2.57	-0.7289	-4.92
HF/aug-cc-pVQZ	-0.5850	-3.17	-0.7198	-4.80
B3LYP/cc-pVDZ	-0.2556	-0.60	-0.6920	-4.44
B3LYP/cc-pVQZ	-0.4879	-2.21	-0.6911	-4.43
B3LYP/aug-cc-pVQZ	-0.5860	-3.18	-0.6751	-4.22
CBS-Q	-0.5113	-2.49	-0.7547	-5.28

Table 3.3. Mulliken and CHELPG charges on the oxygen atom and electrostatic interaction energies E_{es} (in kcal/mole) of $(H_2O)_2$ at various computational levels. H_2O geometry optimization was MP2/6-311 G(d,p); relative positions in dimer determined at CCSD(T)/TZ2P (f,d)+dif levels.

Table 3.3 also gives the electrostatic interaction energies of the water dimer by point-charge methods. Not surprisingly, poor results are obtained in the electrostatic energy calculation with Mulliken charges, from -0.60 to -6.70 kcal/mole. This is in agreement with the conclusion that charges derived from Mulliken population analysis are not suitable for electrostatic energy calculation [28]. CHELPG results are much better: the energies are from -4.22 to –7.02 kcal/mole. Compared to point-charge methods, the energies by our electron density method fluctuate less with basis sets and are much larger in magnitude (Table 3.4). The reason may be explained by the neglect of multipole interactions in the point-charge approach.

In Table 3.4, what is particularly interesting is that for a given basis set, the Hartree-Fock, B3LYP and MP2 results differ by no more than 0.65 kcal/mole. Especially, when huge basis sets are used, the electrostatic energies are almost the same with different computational methods. For example, with the basis set aug-cc-pVQZ, the electrostatic interaction energies are: Hartree-Fock (-8.17 kcal/mole), B3LYP (-8.04 kcal/mole) and MP2 (-8.08 kcal/mole).

Computational method	$\rho_{min}=1.0\times10^{-5}$ electrons/bohr^3	$\rho_{min}=1.0\times10^{-6}$ electrons/bohr^3
HF/3-21G	-8.74	-8.74
HF/6-31G(d)	-8.68	-8.68
HF/6-31+G(d,p)	-9.82	-9.83
HF/6-311++G(d,p)	-9.52	-9.52
HF/cc-pVDZ	-7.84	-7.84
HF/cc-pVQZ	-8.11	-8.13
HF/aug-cc-pVQZ	-8.17	-8.17
B3LYP/cc-pVDZ	-7.19	-7.19
B3LYP/cc-pVQZ	-7.87	-7.89
B3LYP/aug-cc-pVQZ	-8.04	-8.05
MP2/6-311++G(d,p)	-9.72	-9.72
MP2/cc-pVDZ	-7.51	-7.52
MP2/aug-cc-pVQZ	-8.08	-8.08
CBS-Q	-9.27	-9.27

Table 3.4   Electrostatic interaction energies E_{es} of $(H_2O)_2$, in kcal/mole, at various computational levels. Number of e-voxels is 1.00×10^6, stepsize is 0.0531 Å and condensation level is n=3. H_2O geometry optimization was MP2/6-311G(d,p); relative positions in dimer determined at CCSD(T)/TZ2P(f,d)+dif level.

Different basis sets give different electronic densities and then different electrostatic energies. Table 3.4 shows that the electrostatic energies vary from -7.19 to -9.82 kcal/mole ($\rho_{min}=1.0\times10^{-5}$ electrons/bohr^3). For a particular computational method, e.g. HF or MP2, the range of E_{es} values for various basis sets are less than 2 kcal/mole. Also it is found that the diffusion functions play an

important role in E_{es} calculation. Obviously, the use of diffusion functions increases the electron density in outer regions. For the water dimer, it gives larger electrostatic interaction energies. Furthermore, the size of basis sets may affect the results: More accurate electron densities are generated by larger basis sets and thus more accurate electrostatic energies can be obtained.

3.4. <u>Evaluation of the Electron Density Method</u>

We have derived the expression for the electrostatic interaction energy from electron densities and made calculations for the water dimer. To verify the validity of this method, we have compared it to other theoretical methods.

There are several different ways to analyze electrostatic interaction energies of various complexes. In the perturbation approach, electrostatic energy can be obtained directly [29-35]. In the supermolecular approach, the total interaction energy can be decomposed into different parts. One of the most frequently used methods is the Kitaura-Morokuma (KM) scheme [36-37]. Briefly, it is an energy decomposition scheme for intermolecular interactions within the Hartree-Fock approximation. The interaction energy is divided into four components — electrostatic E_{es}, polarization E_{pol}, exchange E_{ex} and charge-transfer E_{et}. (The Hartree-Fock interaction energy does not include a dispersion term.) Each component is defined as follows:

Electrostatic: the classical electrostatic interaction between occupied MO's which does not cause any mixing of MO's.

Polarization: the interaction which causes the mixing between the occupied and vacant MO's within each molecule.

Exchange: the interaction between occupied MO's which causes electron exchange and delocalization between molecules.

Charge Transfer: the interaction which causes intermolecular delocalization by mixing the occupied MO's of one molecule with the vacant MO's of the other and vice versa.

The physical meaning of each interaction may be expressed by Fig. 3.3.

Following the definition of electrostatic interaction in the KM scheme, the equation for the electrostatic interaction energy can be derived. Suppose there are two closed-shell molecules A and B in a complex. Both of them are in the ground state. The total Hamiltonian of the complex is

$$\hat{H} = \hat{H}_A + \hat{H}_B + \hat{H}_{AB} \tag{3.8}$$
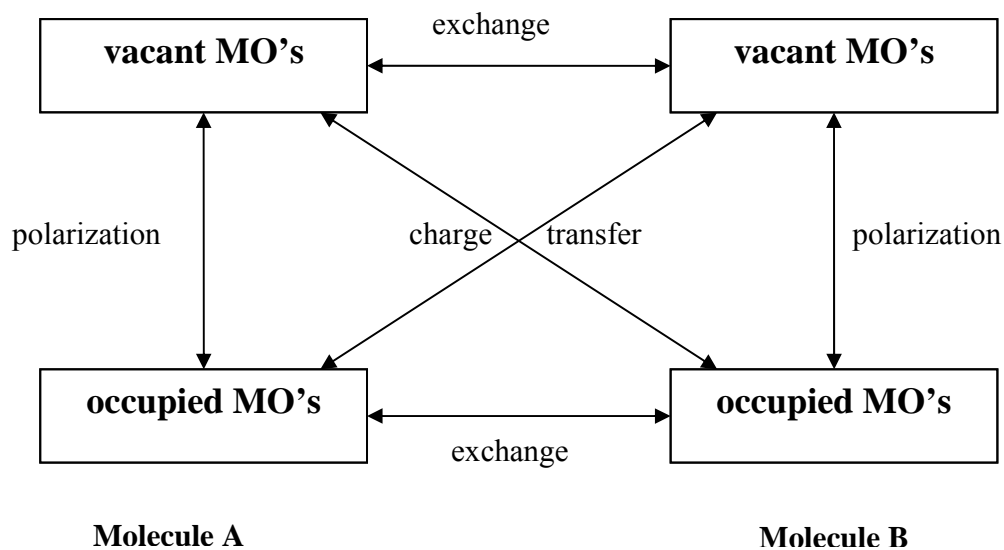
Figure 3.3   Interaction and mixing of MO's via various components of molecules

(see ref. 36).

where $\hat{H}_A$ and $\hat{H}_B$ are the Hamiltonians for the isolated molecules and $\hat{H}_{AB}$ is the interaction term between the two molecules. Since the electrostatic term is caused by unmixed MO's, the wave function of the complex may be written as

$$\psi_1 = \psi_A^0 \psi_B^0 \tag{3.9}$$

ψ_A^0 and ψ_B^0 are the wave functions of the isolated molecules. The total energy of the complex considering only electrostatic interaction is given by

$$
\begin{aligned}
E_1 &=< \psi_1 | \hat{H} | \psi_1 > \\
&=< \psi_1 | \hat{H}_A | \psi_1 > + < \psi_1 | \hat{H}_B | \psi_1 > + < \psi_1 | \hat{H}_{AB} | \psi_1 > \\
&=< \psi_A^0 | \hat{H}_A | \psi_A^0 > + < \psi_B^0 | \hat{H}_B | \psi_B^0 > + < \psi_1 | \hat{H}_{AB} | \psi_1 >
\end{aligned}
\tag{3.10}
$$

where ψ_A^0 and ψ_B^0 are normalized. On the other hand, the total energy of the unperturbed state is the sum of the Hartree-Fock ground state energies of molecules A and B

$$E_0 =< \psi_A^0 | \hat{H}_A | \psi_A^0 > + < \psi_B^0 | \hat{H}_B | \psi_B^0 > \tag{3.11}$$

The electrostatic interaction energy is

$$
\begin{aligned}
E_{es} &= E_1 - E_0 \\
&=< \psi_1 | \hat{H}_{AB} | \psi_1 >
\end{aligned}
\tag{3.12}
$$

The interaction operator $\hat{H}_{AB}$ can be expressed as

$$
\hat{H}_{AB} = \frac{e^2}{4\pi\varepsilon_0} \left(\sum_A \sum_B \frac{Z_A Z_B}{|\vec{R}_A - \vec{R}_B|} - \sum_A \sum_{j=1}^{N} \frac{Z_A}{|\vec{R}_A - \vec{r}_{B,j}|} \right.
$$
$$
\left. - \sum_B \sum_{i=1}^{M} \frac{Z_B}{|\vec{R}_B - \vec{r}_{A,i}|} + \sum_{i=1}^{M} \sum_{j=1}^{N} \frac{1}{|\vec{r}_{A,i} - \vec{r}_{B,j}|} \right)
\tag{3.13}
$$

where M and N are the number of electrons in A and B, respectively. It is easy to prove the equality of electrostatic interaction energy in the KM scheme and the E_{es} described by Eq. (3.2). Combining Eqs. (3.9), (3.12) and (3.13), we have

$$E_{es} = \frac{e^2}{4\pi\varepsilon_0} \left\langle \psi_A^0 \psi_B^0 \left| \begin{array}{l} \displaystyle\sum_A \sum_B \frac{Z_A Z_B}{|\vec{R}_A - \vec{R}_B|} - \sum_A \sum_{j=1}^{N} \frac{Z_A}{|\vec{R}_A - \vec{r}_{B,j}|} \\ \displaystyle - \sum_B \sum_{i=1}^{M} \frac{Z_B}{|\vec{R}_B - \vec{r}_{A,i}|} + \sum_{i=1}^{M} \sum_{j=1}^{N} \frac{1}{|\vec{r}_{A,i} - \vec{r}_{B,j}|} \end{array} \right| \psi_A^0 \psi_B^0 \right\rangle \quad (3.14)$$

Since ψ_A^0 and ψ_B^0 are normalized, the electrostatic energy E_{es} can be written as follows further

$$\begin{aligned} E_{es} = \frac{e^2}{4\pi\varepsilon_0} (&\sum_A \sum_B \frac{Z_A Z_B}{|\vec{R}_A - \vec{R}_B|} - \sum_A \sum_{j=1}^{N} \int \cdots \int \psi_B^{0*} \frac{Z_A}{|\vec{R}_A - \vec{r}_{B,j}|} \psi_B^0 d\vec{r}_B d\vec{r}_{B,2} \cdots d\vec{r}_M \\ &- \sum_B \sum_{i=1}^{M} \int \cdots \int \psi_A^{0*} \frac{Z_B}{|\vec{R}_B - \vec{r}_{A,i}|} \psi_A^0 d\vec{r}_A d\vec{r}_{A,2} \cdots d\vec{r}_N \\ &+ \sum_{i=1}^{M} \sum_{j=1}^{N} \int \cdots \int \psi_A^{0*} \psi_B^{0*} \frac{1}{|\vec{r}_{A,i} - \vec{r}_{B,j}|} \psi_A^0 \psi_B^0 d\vec{r}_A d\vec{r}_{A,2} \cdots d\vec{r}_N d\vec{r}_B d\vec{r}_{B,2} \cdots d\vec{r}_M) \end{aligned} \quad (3.15)$$

The electron densities of A and B can be defined as

$$\rho_A^0(\vec{r}_A) = N \int \cdots \int |\psi_A^0(\vec{r}_A, \vec{r}_{A,2}, \cdots, \vec{r}_{A,N})|^2 \ d\vec{r}_{A,2} \cdots d\vec{r}_N d\vec{r}_A \quad (3.16)$$

$$\rho_B^0(\vec{r}_B) = M \int \cdots \int |\psi_B^0(\vec{r}_B, \vec{r}_{B,2}, \cdots, \vec{r}_{B,M})|^2 \ d\vec{r}_{B,2} \cdots d\vec{r}_M d\vec{r}_B \quad (3.17)$$

Eq. (3.15) thus can be expressed by electron densities

$$E_{es} = \frac{e^2}{4\pi\varepsilon_0}(\sum_A\sum_B\frac{Z_AZ_B}{|\vec{R}_A-\vec{R}_B|}-\sum_A\int\sum_{j=1}^{N}\frac{1}{N}\frac{Z_A}{|\vec{R}_A-\vec{r}_{B,j}|}\rho_B^0(\vec{r}_B)d\vec{r}_B$$

$$-\sum_B\int\sum_{i=1}^{M}\frac{1}{M}\frac{Z_B}{|\vec{R}_B-\vec{r}_{A,i}|}\rho_A^0(\vec{r}_A)d\vec{r}_A \qquad \textbf{(3.18)}$$

$$+\iint\sum_{i=1}^{M}\frac{1}{M}\sum_{j=1}^{N}\frac{1}{N}\frac{\rho_A^0(\vec{r}_A)\rho_B^0(\vec{r}_B)}{|\vec{r}_{A,i}-\vec{r}_{B,j}|}d\vec{r}_Ad\vec{r}_B)$$

Since electrons are indistinguishable, Eq. (3.18) has the same form as Eq. (3.2). Thus the equality of the electrostatic interaction energies in the KM scheme and the electron density method is demonstrated.

In our method, several approximations are used to improve the computational efficiency. However, they may also reduce the accuracy of the results. Fortunately, the electrostatic energy obtained from electron densities can be evaluated against that from the KM scheme. The electrostatic energies for six noncovalently-bound dimers were calculated. The dimer geometries (see Figure 3.4) were obtained at the HF/6-31+G(d,p) level and the monomer geometries were extracted from the optimized dimer structure; density cube files with the option "cube=100" generated at the HF/6-31+G(d,p) level were used. The electrostatic energies with KM decomposition scheme are from Kairys and Jensen's work [38].

Table 3.5 gives the electrostatic interaction energies from the electronic density calculations. As a comparison, the results from the KM scheme and distributed multipole calculations are also listed. Despite the use of several approximations, the results show great agreement between our method and the Kitaura-Morokuma values, which means the approximations are reasonable; the small discrepancies may be caused by slight differences in the optimized

(H2O)$_2$ C$_s$ [Me(OH)]$_2$ C$_i$

(Me$_2$SO)$_2$ C$_i$ (CH$_2$Cl$_2$)$_2$ C$_1$

(Me$_2$CO)$_2$ C$_{2h}$ (MeCN)$_2$ C$_{2h}$
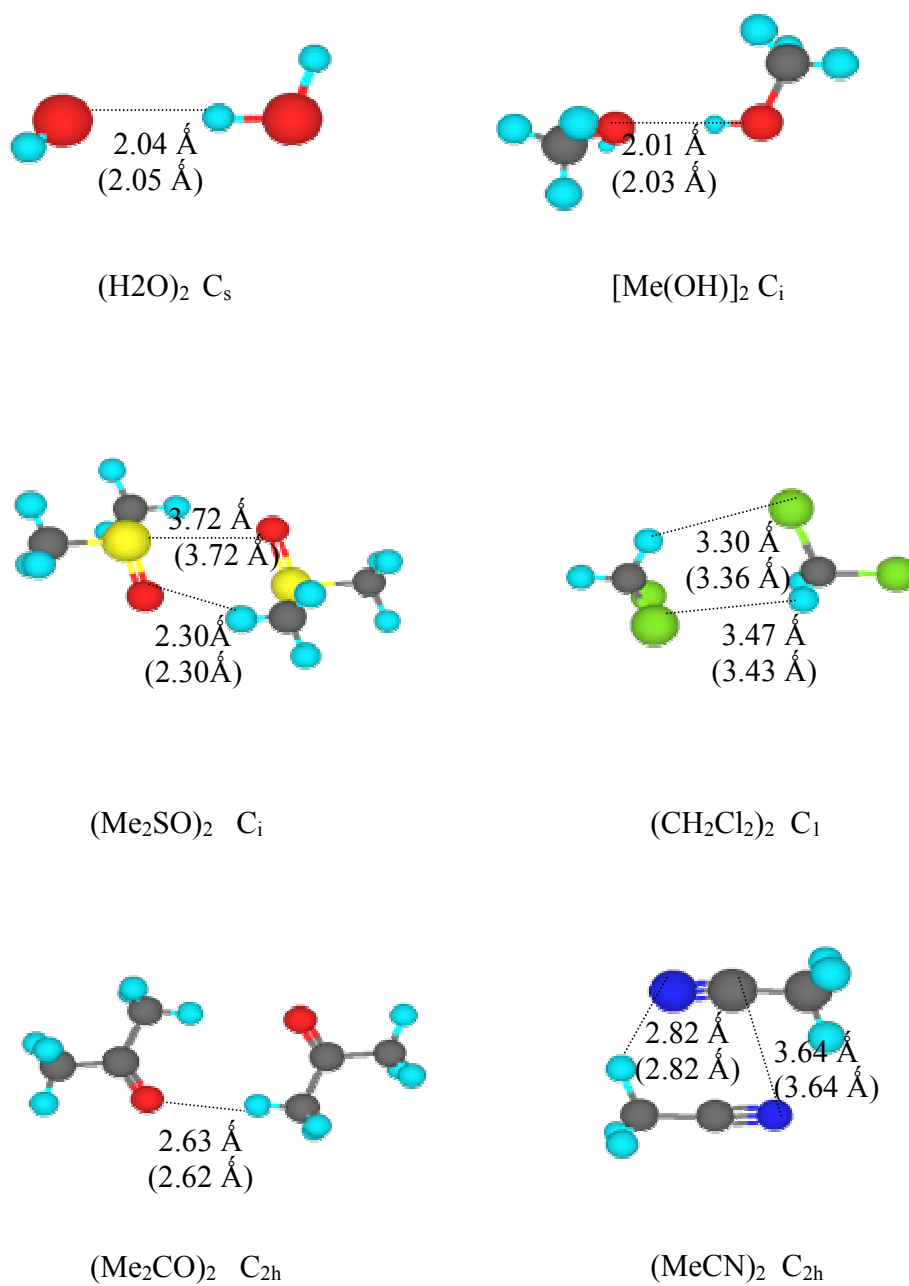
Figure 3.4 Dimer geometries calculated at HF/6-31+G(d,p) level. Electron density obtained at HF/6-31+G(d,p). The values in parentheses correspond to the geometries in ref. 38.

System	Eq. (8).[a]		Kitaura-Morukuma[b]	Distributed multipole method[b]
	$\rho_{min}=1.0\times10^{-5}$ electrons/bohr^3	$\rho_{min}=1.0\times10^{-6}$ electrons/bohr^3		
$(H_2O)_2$	-8.13	-8.14	-8.21	-7.12
$(CH_3OH)_2$	-8.47	-8.49	-8.12	-6.88
$(CH_2Cl_2)_2$	-1.67	-1.66	-1.73	-1.47
$(CH_3CN)_2$	-5.12	-5.26	-5.12	-4.54
$(CH_3COCH_3)_2$	-3.38	-3.46	-3.33	-2.65
$(CH_3SOCH_3)_2$	-11.9	-12.0	-10.88	-8.41

Table 3.5 Electrostatic interaction energies E_{es}, in kcal/mole, computed by different procedures. Geometry optimizations and other calculations were at HF/6-31+G(d,p) level.

[a]Number of e-voxels in each case is approximately 1.0×10^6, condensation level is n=3 or n=5 and stepsizes range from 0.0531 Å to 0.0964 Å.
[b]Ref. 38.

geometries and the valence charge approximation. Different software packages were used in this work and ref. 38. Slightly different geometries were generated and then different electrostatic energies were obtained. As mentioned above, some unrealistic electron densities very close to the nuclei are obtained with Gaussian 98. The use of the valence charge density can mitigate this problem. Nevertheless, it cannot eliminate the problem completely, even for those molecules containing atoms with many core electrons(e.g. S, Cl, etc.). In Table 3.5, the E_{es} of the DMSO dimer has the largest deviation from the KM electrostatic energy (-1.0 kcal/mole when $\rho_{min}=10^{-5}$ electrons /bohr^3; -1.1 kcal/mole when $\rho_{min}=10^{-6}$ electrons/bohr^3). This may indicate that the electron density near the S atom may not be evaluated accurately with Gaussian 98.

Table 3.5 also clealy shows that the electron density method is a better choice than distributed multipole calculations. The errors of the multipole method range from 11.3% for the acetonitrile dimer to 22.7% for the DMSO dimer, which is much larger than those of electron density calculations. The multipole expansion is not valid inside a charge distribution and may cause errors for interaction energy calculations with overlapping charge distributions [38]. For correcting the errors, a charge penetration term must be added.

3.5.   Electrostatic Interaction Energy Study of Stacked Uracil Dimer

Knowledge of DNA and RNA structures is a foundation stone of modern life science. The double helix structure of DNA has been investigated extensively for its great value in understanding genetics and molecular biology. However, the intra- and intermolecular energies which may affect the structure of DNA are still not known quantitatively. The difficulty consists in the complexity of the huge molecular systems. In order to simplify this problem, the properties of the base pairs are studied widely. The structures and interaction energies of stacked DNA and RNA base pairs have been evaluated by experimental [39, 40] and theoretical methods [41, 42].

The force-field method shows that the face-to-face and face-to-back structures are minima for stacked uracil dimers [43]. Furthermore, the accurate structures and binding energies of these two stacked uracil dimers by *ab initio* calculation at MP2 and CCSD(T) levels has been reported recently [44]. (See Figure 3.5).

The molecular electrostatic potential was examined for DNA base pairs. It is found that the electrostatic interaction energies agree reasonably well with the self-consistent-field (SCF) values [45]. Additionally, it is possible to identify the binding energy with the SCF energy for H-bonded complexes, because the BSSE and dispersion energy may compensate for each other [28]. Although this approximation is rough, it is valid in most cases. In general, the electrostatic energy can reflect the stabilization energy for many electrostatic-dominant molecular systems.

As the reliability of the electron density method has been demonstrated in section 3.4, it can be employed for electrostatic energy calculations. In order to find the contribution of the electrostatic interaction in stacked uracil dimers, we computed the intermolecular electrostatic energies between two stacked uracil molecules. The geometries of the dimers were taken from ref. 44, optimized at the MP2/TZ2P(f,d)++ level. The basis set TZ2P(f,d)++ consisted of the Huzinaga-Dunning set of triple-ζ Gaussian functions with two sets of p-type and one set of d-type functions on all hydrogen atoms and two sets of d-type and one set of f-type polarization functions on each first-row atom (Li-Ne). The individual structures were extracted from the dimers geometries and the electron densities were computed with the parameter "cube=100" using Dunning's correlation-consistent basis sets. Since the uracil molecule is larger than the others that we have considered, our first step was to calculate E_{es} for a series of ρ_{min}, to ascertain its convergence behavior. This was done for both dimers, at Hartree-Fock levels (results in Table 3.6). We concluded that $\rho_{min} \leq 1.0 \times 10^{-6}$ electrons/bohr^3 is now
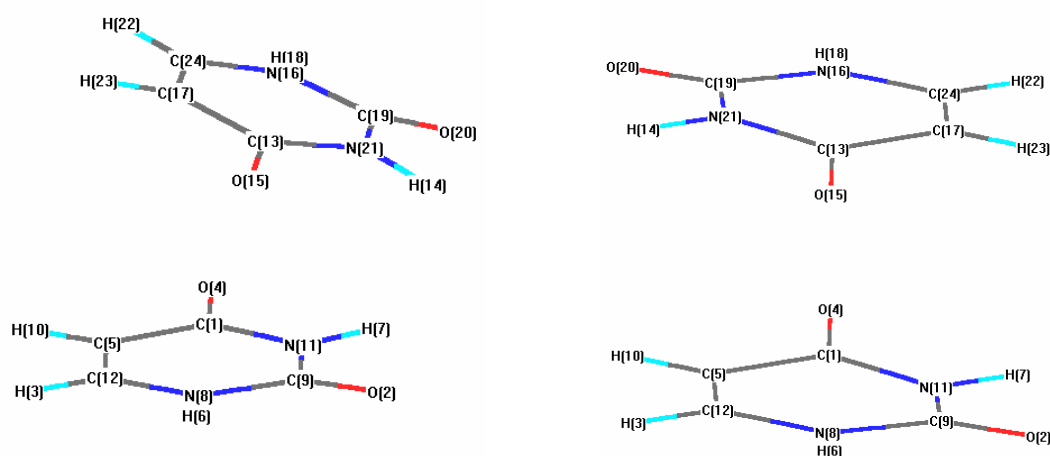
Figure 3.5 Face-to-face and face-to-back uracil dimers.

Computational level		$\rho_{min,}$ electrons/bohr^3				
		1.0×10^{-3}	1.0×10^{-4}	1.0×10^{-5}	1.0×10^{-6}	1.0×10^{-7}
Face-to-face dimer	HF/aug-cc-pVDZ	-6.69	-10.06	-11.79	-12.07	-12.07
	HF/aug-cc-pVTZ	-6.56	-10.30	-12.24	-12.42	-12.42
	HF/aug-cc-pVQZ	-6.34	-10.08	-12.10	-12.26	-12.26
Face-to-back dimer	HF/aug-cc-pVDZ	-4.46	-4.28	-4.95	-5.16	-5.16
	HF/aug-cc-pVTZ	-4.19	-5.69	-5.01	-5.11	-5.11
	HF/aug-cc-pVQZ	-3.98	-4.02	-5.01	-5.10	-5.10

Table 3.6   Electrostatic interaction energies E_{es}, in kcal/mole, for stacked uracil dimers with different ρ_{min}. Uracil molecular structure taken from MP2/TZ2P(f,d)++ dimer geometries.[a] Number of e-voxel is $1.01 \times 10^6 (115 \times 107 \times 82)$, condensation level is n=5 or 7, stepsize is 0.0860Å.

[a]Ref. 44.

required, rather than $\rho_{min} \leq 1.0 \times 10^{-5}$ electrons/bohr^3, which suffices for the smaller

molecules. We proceeded to determine E_{es} for each dimer from Hartree-Fock

electron densities obtained with six different basis set. The results are listed in Table 3.7.

For each complex, the magnitude of E_{es} initially increases as the basis become larger, but then levels off. The electrostatic interaction is consistently stronger, by more than a factor of two, for the face-to-face dimer. This can be explained by considering their different structures: in the face-to-face dimer, there are four positive-negative N-H---O charge pairs (O15-H6, O2-H14, O20-H7 and O4-H18), where as in the face-to-back, there are only two of that kind of pairs (O15-H6 and O4-H18), the other two being the weak C-H---O.

Computational level	Face-to-face dimer	Face-to-back dimer
HF/cc-pVDZ	-8.91	-4.26
HF/cc-pVTZ	-10.46	-4.93
HF/cc-pVQZ	-12.30	-5.30
HF/aug-cc-pVDZ	-12.07	-5.16
HF/aug-cc-pVTZ	-12.42	-5.11
HF/aug-cc-pVQZ	-12.26	-5.10

Table 3.7   Electrostatic interaction energies E_{es}, in kcal/mole, for stacked uracil dimers. Uracil molecular structure taken from MP2/TZ2P(f,d)++ dimer geometries.[a] Number of e-voxel is 1.01×10^6, condensation level is n=5, stepsize is 0.0860Å, and $\rho_{min}=1.0\times10^{-6}$ electrons/bohr^3.

[a]Ref. 44.

For the face-to-face dimer, the electrostatic energies are -8.91 — -12.42 kcal/mole computed with different basis sets. The values with augmented basis sets are much more consistent (from -12.07 to -12.42 kcal/mole) than those with non-

augmented basis sets. The electrostatic interaction energy is much smaller (-4.26—
-5.30 kcal/mole) for the face-to-back complex. Leininger *et al* computed the MP2
stabilization energies, extrapolated these to the infinite basis set limits and then
included higher-order correlation effects, finally estimating $\mathit{\Delta E_{stab}}$ to be -9.7
kcal/mole for the face-to-face complex and -8.8 for the face-to-back. Since Table
3.7 indicates that E_{es} for these systems is about -12.4 and -5.1 kcal/mole,
respectively, it follows that any contributions of $\mathit{\Delta E_{stab}}$, besides E_{es}, are overall
stabilizing in the face-to-back dimer but destabilizing in the face-to-face. It seems
likely that the exchange-repulsion term is significantly larger in the latter instance;
it is frequently viewed as being proportional to the overlap of the components'
charge distribution [6, 46, 47], and Leininger *et al*'s structures do show the two
uracil rings to be tilted toward each other in the face-to-face dimer, on the side
having adjacent N-H---O interactions, whereas they are approximately parallel in
the face-to-back.

Clearly, the face-to-face complex is a strongly electrostatic molecular
system. However, it is not an electrostatic-dominant system because other
interactions are also strong. In the face-to-back structure, the dispersion
contribution even dominates the binding energy although the electrostatic energy
plays an important role [39].

3.6.   Summary

The equation for electrostatic interaction energies between two molecules
has been derived from the electrostatic potential $V(\vec{r})$, in terms of the electron

densities. With several approximations, procedures for electrostatic interaction energy calculations, using a numerical integration technique slightly different from Gavezzotti's, have been developed. The equality of the electrostatic interaction energy by our electron density method and by Kitaura-Morokuma analysis was rigorously demonstrated. The validity of the approximations was tested by calculations for some inter-molecular systems. In this method, E_{es} are determined from the electron densities of complex and its components, and thus can be obtained with generally satisfactory accuracy and relatively inexpensively (in term of computational resources), as well as from experimental (diffraction) measurements.

References

[1]. Alagona, G.; Tani, A. *J. Chem. Phys.* 74, **1981**, 3980.

[2]. Williams, D.E. *Acta Crystallogr.* A30, **1974**, 71.

[3]. Buckingham, A. D.; Fowler, P. W. *Can. J. Chem.* 63, **1985**, 2018.

[4]. Buckingham, A. D.; Fowler, P. W. *J. Chem. Phys.* 79, **1983**, 6426.

[5]. Price, S. L. *J. Chem. Soc., Faraday Trans.* 92, **1996**, 2997.

[6]. Nobeli, I.; Price, S. L. *J. Phys. Chem.* 103, **1999**, 6448.

[7]. Coombes, S.; Price, S. L.; Willock, D. J.; Leslie, M. *J. Phys. Chem.* 100, **1996**, 7352.

[8]. Koritsanszky, T. S.; Coppens, P. *Chem.Rev.* 101, **2001**, 1583.

[9]. Hohenberg, P.; Kohn, W. *Phys. Rev. B* 136, **1964**, 864.

[10]. Politzer, P.; Murray, J. S. Reviews in Computational Chemistry, Vol. 2; Lipkowitz, K. B.; Boyd, D. B., Eds.; VCH Publishers: New York, **1991**.

[11]. Murray, J. S.; Sen, K., Eds. Molecular Electrostatic Potentials: Concepts and Applications; Elsevier: New York, **1996**.

[12]. Gavezzotti, A. *J. Phys. Chem. B.* 106, **2002**, 4145.

[13]. Dyke, T.R.; Mack, K. M.; Muenter, J. S. *J. Chem. Phys.* 66, **1977**, 498.

[14]. Odutola, J.A.; Dyke, T. R.; *J. Chem. Phys.* 72, **1980**, 5062.

[15]. Curtiss, L.A.; Frurip, D. J.; Blander, M. *J. Chem. Phys.* 71, **1979**, 2703.

[16]. Reimers, J.; Watts, R.; Klein, M. *Chem. Phys.* 64, **1982**, 95.

[17]. Diercksen, G. H.F.; Kraemer, W. P.; Roos, B. O. *Theor. Chim. Acta* 36, **1975**, 249.

[18]. Baum, J.O.; Finnery, J. L. *Mol. Phys.* 55, **1985**, 1097.

[19]. Frisch, M. J.; Del Bene, J. E.; Binkley, J.S.; Schaefer, H. F., III. *J. Chem. Phys.* 84, **1986**, 2279.

[20]. Xantheas, S.S.; Dunning, T. H., Jr. *J. Chem. Phys.* 99, **1993**, 8774.

[21]. Feller, D.; Glendening, E. D.; Peterson, K.A. *J. Chem. Phys.* 100, **1994**, 4981.

[22]. Feyereisen, M.W.; Feller, D.; Dixon, D.A. *J. Phys. Chem.* 100, **1996**, 2993.

[23]. Smith, B. J.; Swanton, D. J.; Pople, J. A.; Schaefer, H. F., III.; Radom, L. *J. Chem. Phys.* 92, **1990**, 1240.

[24]. Fellers, R. S.; Braly, C. L. L. B.; Brown, M. G.; Saykally, R. J. *Science*, 284, **1999**, 945.

[25]. Mas, E. M.; Bukowski, R.; Szalewicz, K.; Groenenboom, G. C.; Wormer, P. E. S.; van der Avoird, A. *J. Phys. Chem.* 113, **2000**, 6687.

[26]. Tschumper, G.: Leininger, M. Hoffman, B. C.; Valeev, E. F.; Schaefer, H. F., III.; Quack, M. *J. Chem. Phys.* 116, **2002**, 690.

[27]. Breneman, C. M.; Wiberg, K. B. *J. Comp. Chem.* 11, **1990**,361.

[28]. Hobza, P.; Zahradník, R. *Chem. Rev.* 88, **1988**, 871.

[29]. Jeziorski, B.; Kolos, W. In *Molecular Interactions*; Ratajczak H. and Orville-Thomas, eds.; vol. 3 Wiley, New York **1982**.

[30]. Jeziorski, B.; van Herment, M. *Mol. Phys.* 31, **1976**, 713.

[31]. Arrighimi, P. *Intermolecular forces and their evaluation by perturbation theory*, vol. 25. Springer-Verlag, Berlin **1981**.

[32]. Szalewicz, K.; Jeziorski, B.; Rybak, S. *Int. J. Quantum, Chem.* QBS18, **1991**, 23.

[33]. Williams, H. L.; Mas, E. M.; Szalewicz, K.; Jeziorski, B. *J. Chem. Phys.* 103, 1995, 7374.

[34]. Buckingham, A. D. In *intermolecular interactions: From Diatomics to Biopolymers;* Pullman, B. eds.; Wiley, New York, **1978**.

[35]. Claverie, P. In *intermolecular interactions: From Diatomics to Biopolymers;* Pullman, B. eds.; Wiley, New York, **1978**.

[36]. Kitaura, K.; Morokuma, K. *Int. J. Quantum Chem.* Vol X, **1976**, 325.

[37]. Morokuma, K.; Kitaura, K. In*Chemical Applications of Atomic and Molecular Electrostatic Potentials;* Politzer, P.; Truhlar, D. G., eds.; Plenum, New York, **1981**.

[38]. Kairys, V; Jensen, J. *Chem. Phys. Lett.* 315, **1999**, 140.

[39]. Guckian, K. M.; Schweitzer, B. A.; Ren. R. X. –F.; Sheils, C. J.; Tahmassebi, D. C.; Kool, E. T. *J. Am. Chem. Soc.* 122, **2000**, 2213.

[40]. Makey, S. L.; Haptonstall, B.; Gellman, S. H. *J. Am. Chem. Soc.* 122, **2000**, 2213.

[41]. Luo, R.; Gilson, H. S. R.; Potter, M. J. Gilson, M. K. *Biophys. J.* 80, **2001**, 140.

[42]. Hobza, P.; Šponer, J. *Chen. Rev.* 99, **1999**, 3247.

[43]. Kratochvíl, M.; Engkvist, O.; Šponer, J.; Jungwirth, P.; Hobza, P. *J. Phys. Chem. A* 102, **1998**, 6921.

[44]. Leininger, M. L.; Nielson, I. M. B.; Colvin, M.E.; Janssen, C. L. *J. Phys. Chem. A* 106, **2002**, 3850.

[45]. Hobza, P.; Sandorfy, C. *J. Am. Chem. Soc.* 109, **1987**, 1302.

[46]. Engkvist, O.; Astrand, P.-O.; Karlstrom, G. *Chem. Rev.* 100, **2000**, 4087.

[47]. Murrell, J. N.; Teixeira-Dias, J. J. C. *Mol. Phys.* 19, **1970**, 521.

CHAPTER 4. EVALUATION OF POLARIZATION ENERGIES FROM ELECTRONIC DENSITIES

4.1. <u>Introduction</u>

As mentioned in Chapter 1, when a molecule is placed in a static electric field, induced electric multipoles can be generated due to distortion of the charge distribution. When only the lowest order is considered, a dipole moment $\vec{\mu}$ is induced:

$$\vec{\mu} = \alpha \cdot \vec{E} \tag{4.1}$$

The dipole moment is proportional to the static field $\vec{E}$ and the direction of the vector is parallel to $\vec{E}$. α is a tensor, called the electronic polarizability. For a non-polar molecule, the polarization arises from the displacement of its negatively charged electron cloud relative to the positively charged nuclei under the influence of an external electric field. For a polar molecule, there is an additional contribution, called orientational polarization, which arises from the effect of an external field on the Boltzmann-average orientations of the rotating dipole [1]. The orientational polarizability α_{orient} is given by

$$\alpha_{orient} = \mu^2 / 3k\text{T} \tag{4.2}$$

where μ is the permanent dipole moment of the polar molecule and k is the Boltzmann constant. The polarization energy E_{pol} generated by an induced dipole moment $\vec{\mu}$ in an external electric field $\vec{E}$ can be expressed as

$$E_{pol} = -\int_o^E \vec{\mu} \cdot d\vec{E} = -\frac{1}{2}\alpha E^2 \qquad \textbf{(4.3)}$$

It is difficult to accurately evaluate the polarization energy between two molecules by Eq. (4.3). First, evaluating the polarizability of a molecule is not an easy task [2]. Although it may be obtained approximately as the sum of the polarizabilities of its covalent bonds, this is not true in many cases. For example, for those molecules which have delocalized or lone pair electrons, this approach causes significant errors. Second, the electric field emanating from other molecules is very complicated for most molecular systems. In general, the strength of the electric field changes at different positions of a molecule. One possible treatment is the use of an average electric field instead. Other methods include the use of "point polarizability" [3, 4]. In this approach, the polarizability at each point of a molecule is defined by some specific rules and thus the polarization energy at each point can be determined. The total polarization energy is taken as the sum of the polarization energies at each point. Several defects discussed in ref. 4 may affect the accuracy of this method. Finally, Eq. (4.3) does not contain the interaction of high order moments. Briefly, Eq. (4.3) is only a crude approximation for polarization energy calculations.

In perturbation theory, the polarization energy for a pair of molecules A and B can be written as follows [5]

$$E_{pol} = \frac{1}{4\pi\varepsilon_0}(\int \Psi_A^{0*}\Psi_B^{0*}\sum_{ij}\frac{e_i^A e_j^B}{R_{ij}}\Psi_A^0\Psi_B^1 d\tau_A d\tau_B +$$

$$\int \Psi_A^{0*}\Psi_B^{0*}\sum_{ij}\frac{e_i^A e_j^B}{R_{ij}}\Psi_A^1\Psi_B^0 d\tau_A d\tau_B) \qquad \textbf{(4.4)}$$

where Ψ_A^0 and Ψ_B^0 are the unperturbed ground state wave functions of molecules A

and B, Ψ_A^1 is the first-order change in the wave function of molecule A induced by

the electric field of molecule B, and R_{ij} is the distance between the charge e_i^A in A

and the charge e_j^B in B. If overlap effects are neglected, the polarization energy

between two molecules is given by Eq. (4.4). The polarization energy can also be

defined by other quantum chemical methods. For example, in the Kitaura-

Morokuma analysis, it is defined as the interaction which causes the mixing

between occupied and vacant MOs within each molecule [5]. In all these

approaches, the wave function change of a molecule caused by the external electric

field must be known.

The polarization energy can also be derived based on the concept of electron

density. First, we will give the rigorous definition of the polarization energy

between two molecules.

4.2.   The Electron Density Expression of Polarization Energy

Suppose there are two molecules, A and B, in a complex. Both of them are

closed-shell molecules in the ground state. In the isolated state, their electron

densities are ρ_A^0 and ρ_B^0, respectively. In the complex A···B, the electron densities

may change because of the polarization effect. The electron densities of molecules

A and B in the complex can be written as

$$\rho_A^1 = \rho_A^0 + \Delta\rho_A^{pol} \tag{4.5}$$

$$\rho_B^1 = \rho_B^0 + \Delta\rho_B^{pol} \tag{4.6}$$

where $\Delta\rho_A^{pol}$ and $\Delta\rho_B^{pol}$ are electron density changes caused by polarization. The interaction energy including electrostatic and polarization contributions between the two molecules is

$$E_1 = \sum_A \sum_B \frac{Z_A Z_B}{|\vec{R}_A - \vec{R}_B|} - \sum_A \int \frac{Z_A \rho_B^1(\vec{r}_B)}{|\vec{R}_A - \vec{r}_B|} d\vec{r}_B$$
$$- \sum_B \int \frac{Z_B \rho_A^1(\vec{r}_A)}{|\vec{R}_B - \vec{r}_A|} d\vec{r}_A + \iint \frac{\rho_A^1(\vec{r}_A)\rho_B^1(\vec{r}_B)}{|\vec{r}_A - \vec{r}_B|} d\vec{r}_A d\vec{r}_B$$

(4.7)

E_1 is the sum of electrostatic and polarization energy:

$$E_1 = E_{es} + E_{pol}$$

(4.8)

Combining Eqs. (4.5), (4.6) and (4.7), we have

$$E_1 = \sum_A \sum_B \frac{Z_A Z_B}{|\vec{R}_A - \vec{R}_B|} - \sum_A \int \frac{Z_A(\rho_B^0(\vec{r}_B) + \Delta\rho_B^{pol}(\vec{r}_B))}{|\vec{R}_A - \vec{r}_B|} d\vec{r}_B$$
$$- \sum_B \int \frac{Z_B(\rho_B^0(\vec{r}_B) + \Delta\rho_B^{pol}(\vec{r}_B))}{|\vec{R}_B - \vec{r}_A|} d\vec{r}_A$$
$$+ \iint \frac{(\rho_B^0(\vec{r}_B) + \Delta\rho_B^{pol}(\vec{r}_B))(\rho_B^0(\vec{r}_B) + \Delta\rho_B^{pol}(\vec{r}_B))}{|\vec{r}_A - \vec{r}_B|} d\vec{r}_A d\vec{r}_B$$

(4.9)

Subtracting the electrostatic term (see Eq. (3.2)) from Eq. (4.9), the polarization energy between molecules A and B is obtained

$$E_{pol} = -\sum_A \int \frac{Z_A \Delta\rho_B^{pol}(\vec{r}_B)}{|\vec{R}_A - \vec{r}_B|} d\vec{r}_B - \sum_B \int \frac{Z_B \Delta\rho_A^{pol}(\vec{r}_A)}{|\vec{R}_B - \vec{r}_A|} d\vec{r}_A$$
$$+ \iint \frac{\rho_A^0(\vec{r}_A)\Delta\rho_B^{pol}(\vec{r}_B)}{|\vec{r}_A - \vec{r}_B|} d\vec{r}_A d\vec{r}_B + \iint \frac{\rho_B^0(\vec{r}_B)\Delta\rho_A^{pol}(\vec{r}_A)}{|\vec{r}_A - \vec{r}_B|} d\vec{r}_A d\vec{r}_B$$
$$+ \iint \frac{\Delta\rho_A^{pol}(\vec{r}_A)\Delta\rho_B^{pol}(\vec{r}_B)}{|\vec{r}_A - \vec{r}_B|} d\vec{r}_A d\vec{r}_B$$

(4.10)

Eq. (4.10) gives the exact form of the polarization energy between two molecules in term of the electron densities of the isolated components and the changes in these

due to polarization. Now the problem is how to put it into practical calculations. According to Eq. (4.10), for the polarization energy computation, ρ_A^0, ρ_B^0, $\Delta\rho_A^{pol}$ and $\Delta\rho_B^{pol}$ must be known. As discussed in Chapter 3, ρ_A^0 and ρ_B^0 can be obtained by theoretical or experimental methods. The difficulty focuses on the measure of $\Delta\rho_A^{pol}$ and $\Delta\rho_B^{pol}$.

The total electron density of a complex can be known from quantum chemical calculations. However, the relationship between the total electron density ρ and the electron density change caused by polarization is indirect. ρ may be expressed as follows

$$
\begin{aligned}
\rho = {} & \rho_A^0 + \Delta\rho_A^{pol} + \Delta\rho_A^{ex} + \Delta\rho_A^{disp} \\
& + \rho_B^0 + \Delta\rho_B^{pol} + \Delta\rho_B^{ex} + \Delta\rho_B^{disp}
\end{aligned}
\tag{4.11}
$$

where $\Delta\rho^{pol}$, $\Delta\rho^{ex}$ and $\Delta\rho^{disp}$ are the electron density changes by polarization, exchange and dispersion effects, respectively. As the dispersion term does not exist in the Hartree-Fock method, $\Delta\rho^{disp}$ can be neglected within the HF approximation. Bader *et al.* suggested that the electron isodensity surface provided a useful theoretical definition of the size and shape of an isolated molecule [7]. They also proposed the 0.002 electrons/bohr^3 density contour as the boundary of molecules. In a supermolecular complex, the molecular electron clouds interpenetrate each other. However, it is still possible to obtain a prescription for molecular size in which mutual penetration is minimal if the boundary of the molecule is defined properly [8]. The exchange-repulsion energy is equal to zero when the electron densities of two molecules do not overlap each other. If an isodensity boundary is well defined,

the exchange effect may be neglected. Within the Hartree-Fock approximation, Eq. (4.11) may be written as

$$\rho_{HF} \approx \rho_A^0 + \Delta\rho_A^{pol} + \rho_B^0 + \Delta\rho_B^{pol} \tag{4.12}$$

Eq. (4.12) gives the relationship between the HF electron density and electron density changes by polarization effects. However, it is impossible to resolve $\Delta\rho_A^{pol}$ and $\Delta\rho_B^{pol}$ using just one equation. Additional approximations are necessary for $\Delta\rho_A^{pol}$ and $\Delta\rho_B^{pol}$.

The supermolecular complex A⋯B is divided into three spatial regions: one is associate only with A, another only with B, and the third with the overlap with A and B (Figure 4.1). Although the exchange-repulsion interaction arises from the overlap of the electron clouds, it can be well controlled (see the discussion of section 4.4). In the two nonoverlap regions, each of which contains no electronic charge from the other component. $\Delta\rho_A^{pol}$ and $\Delta\rho_B^{pol}$ thus can be defined

$$\Delta\rho_{A,nonoverlap}^{pol} = \rho_{HF} - \rho_A^0 \tag{4.13}$$

$$\Delta\rho_{B,nonoverlap}^{pol} = \rho_{HF} - \rho_B^0 \tag{4.14}$$

The second approximation is about charge transfer effects. We assume that there is no charge transfer for each molecule in the complex. Accordingly, for each molecule, the number of electrons does not change from the isolated state to the bound state:

$$\int \rho_A^0(\vec{r})d\vec{r} = N_A \tag{4.15}$$

$$\int \rho_A(\vec{r})d\vec{r} = N_A \tag{4.16}$$
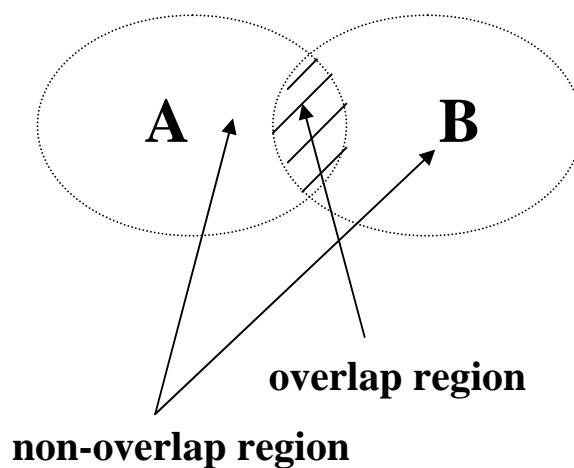
Figure 4.1 Overlap and nonoverlap regions in a complex.

where N_A is the number of electrons of molecule A. According to the previous approximations, using Eq. (4.16) minus Eq. (4.15), we have

$$\int \Delta \rho_A^{pol}(\vec{r})d\vec{r} = 0 \tag{4.17}$$

$$\int \Delta \rho_B^{pol}(\vec{r})d\vec{r} = 0 \tag{4.18}$$

The third approximation gives the electron density change in the overlap region. Since the electron density for each molecule is composed of two parts, Eq. (4.17) can be rewritten

$$\int \Delta \rho_{A,overlap}^{pol}(\vec{r})d\vec{r} + \int \Delta \rho_{A,nonoverlap}^{pol}(\vec{r})d\vec{r} = 0 \tag{4.19}$$

For series of noncovalently-bound complexes, Bentley has made a detailed study of the density difference function $\Delta \rho_{AB}(\vec{r})$ [8], defined as

$$\Delta\rho_{AB}(\vec{r}) = \rho(\vec{r}) - \rho_A^0(\vec{r}) - \rho_B^0(\vec{r}) \qquad \textbf{(4.20)}$$

He found that $\Delta\rho_{AB}(\vec{r})$ is very small and relatively slow-varying in the intermolecular region of significant overlap. We will assume that $\Delta\rho_A^{pol}$ and $\Delta\rho_B^{pol}$ can be treated as being constant. Thus, from Eq. (4.19), $\Delta\rho_{A,overlap}^{pol}$ and $\Delta\rho_{B,overlap}^{pol}$ are given as

$$\Delta\rho_{A,overlap}^{pol} = -\frac{\int \Delta\rho_{A,nonoverlap}^{pol}(\vec{r})d\vec{r}}{V_{overlap}} \qquad \textbf{(4.20)}$$

$$\Delta\rho_{B,overlap}^{pol} = -\frac{\int \Delta\rho_{B,nonoverlap}^{pol}(\vec{r})d\vec{r}}{V_{overlap}} \qquad \textbf{(4.21)}$$

where $V_{overlap}$ is the volume of overlap region. Eqs. (4.12), (4.13), (4.20) and (4.21) provide an approximate form of $\Delta\rho_A^{pol}$ and $\Delta\rho_B^{pol}$. Knowing these, as well as ρ_A^0 and ρ_B^0, it is possible to calculate E_{pol} from Eq. (4.10).

4.3. Procedure for Polarization Energy Calculation

With several approximations, the polarization energy can be obtained from Eq. (4.10). The calculation is programmed with a numerical integration method, which is similar to the electrostatic energy computation described in Chapter 3. The procedure of polarization energy calculation is performed in the following steps:

(1). Generation of electron density files

The files containing the information about electron densities can be generated by the Gaussian software package. The basic unit in the files is called an e-voxel, the number and size of which can be adjusted with different parameters. Only the valence charge density is included in order to mitigate the unrealistic electron density around the nuclei. For the polarization energy calculation, electron density files of the complex and the monomers are needed.

The size of the e-voxels used for the complex is the same as that for the monomers, for convenience. The counterpoise method is employed for the monomers in order to eliminate the BSSE [9].

(2). Boundary of electron density

Choosing a proper isodensity boundary is very important for the polarization energy calculation. The boundaries of the isolated components are defined by assigning a value for ρ_{min}. The overlap region is determined by identifying those e-voxels that are simultaneously within the boundaries of both components, and the remaining e-voxels within these boundaries constitute the two nonoverlap regions. In Chapter 3, we discussed the effect of the isodensity boundary. It was found that a smaller ρ_{min} led to a more accurate value of the electrostatic energy. The problem is more complicated for the polarization energy calculation: with a small ρ_{min}, the molecular volume increases and then the overlap region enlarges. This may cause a significant exchange-repulsion effect between two molecules and lead to big errors in the evaluation of $\Delta\rho^{pol}$. On the other hand, the use of a big ρ_{min} may lose some

outer e-voxel and lead to inaccuracy of ρ^0. Therefore, the value of ρ_{min} should be selected carefully and it can be neither too small nor too big.

(3). Condensation of e-voxels

The number of e-voxels is too high for electron-electron repulsion interaction evaluation and must be reduced to a reasonable level. The method used here is the same as that described in Chapter 3. For convenience of the $\Delta\rho^{pol}$ calculation, the condensation level of the complex must be equal to that of the monomers. Normally, there are only several thousand super e-voxels left after condensation.

(4). Charge renormalization

A small part of the electron count is lost in the previous steps. In order to maintain the balance between positive and negative charges, the total valence charge is renormalized. Before renormalization, the electron densities of the complex and monomers can not be used for $\Delta\rho^{pol}$ calculation directly, because their normalization coefficients are different.

(5). Coordinate transformation

The electron densities for the complex and the monomers may be based on different coordinate systems. However, a corresponding relationship must be built between each of the e-voxels in the complex and those in the monomers for the polarization energy calculation. Therefore, the coordinate system of each monomer must be transformed to that of the complex. The process involves a series of translations and rotations of coordinate axes.

(6). Calculation of $\Delta\rho^{pol}$

Before the calculation of $\Delta\rho^{pol}$, the overlap and nonoverlap regions are measured. Each e-voxel is assigned according to its position in the coordinate system. Then $\Delta\rho^{pol}$ can be obtained with Eqs. (4.13), (4.14), (4.20) and (4.21).

(7). Polarization energy calculation

With numerical integration, the polarization energy can be calculated by Eq. (4.10). ρ^0, the distances between the two points and $\Delta\rho^{pol}$ are given in steps 4, 5 and 6 respectively. In the calculation, the near zero voxel-voxel or voxel-atom distances are reset to avoid unrealistic energies. The flow sheet of the polarization energy calculation is given in Figure 4.2.

4.4.   Polarization Energy Calculation For Water Dimer

The polarization interaction is seldom dominant in intermolecular interaction energies and thus can often be ignored in comparison with the electrostatic and other contributions [10]. However, the polarization interaction still plays an important role in some molecular systems [11].

The polarization energy, E_{pol}, for the water dimer has been studied by Chen and Gordon with the Kitaura-Morokuma technique and also an alternative energy partition scheme, the reduced variational space self-consistent-field (RVS SCF) method of Stevens and Fink [12,14]. Using the procedure discribed in sections 4.2 and 4.3, we computed the E_{pol} for the water dimer and compared it with Chen and Gorden's results. The water dimer structures were optimized at several different levels, consistent with Chen and Gordon; the individual H_2O geometries were taken from the dimers. All the charge densities were generated by Gaussian 98.

Figure 4.2 Flowsheet of polarization energy calculation.

Electron density files of the isolated molecules and complex

Making isodensity surfaces

Condensation of electron voxels

$$\sum_i Z_i = \int \rho(\mathbf{r})d\mathbf{r}$$

Renormalization of electron charge

Coordinate transformation

Geometries of the isolated molecules and complex

$\Delta\rho^{pol}$ Calculation
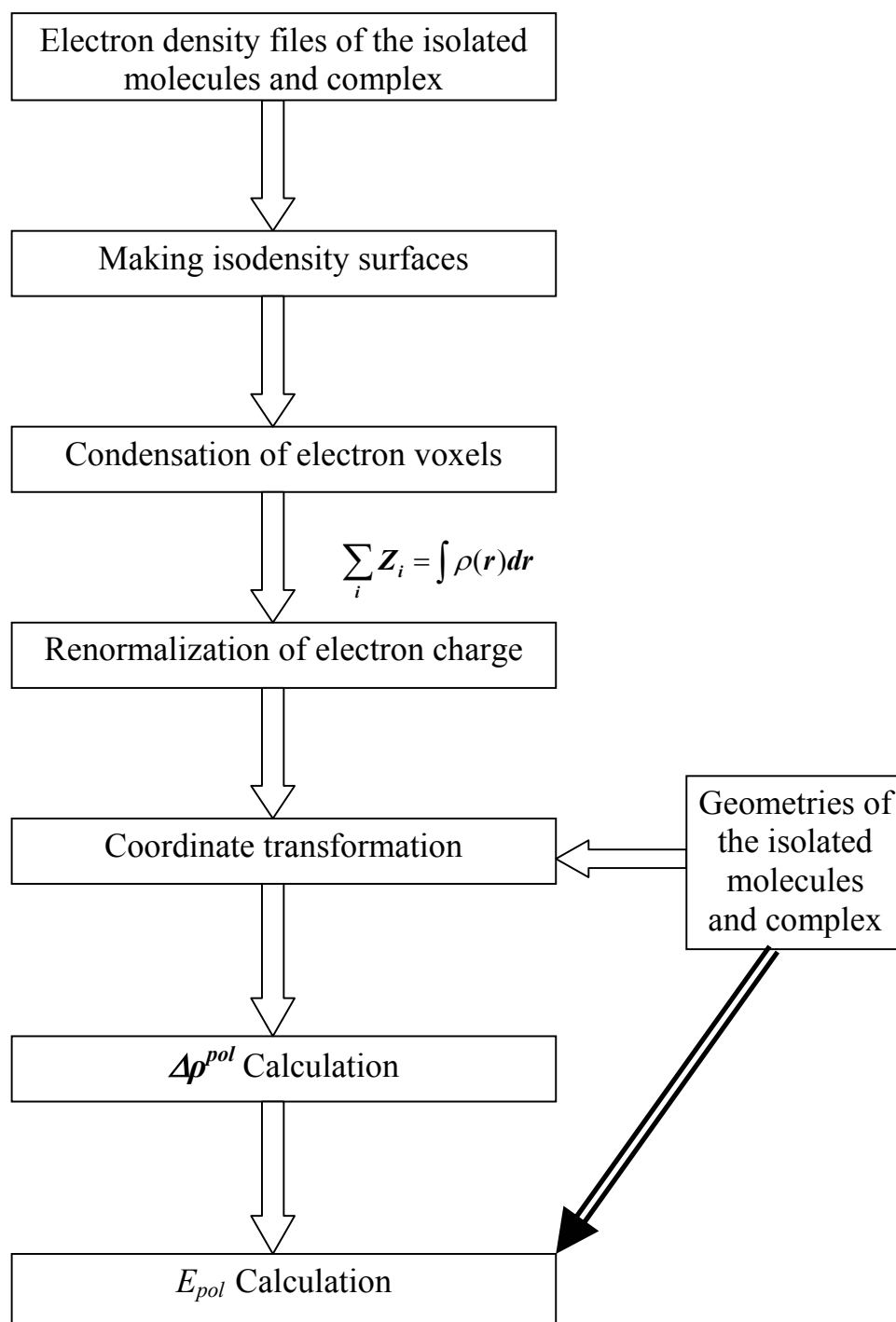
E_{pol} Calculation

Figure 4.2 Flowsheet of polarization energy calculation.

The counterpoise method was used in the monomer calculations for BSSE corection. The results are in Table 4.1.

Computational method	Eq. (4.10)[a]			Morokuma-Kitaura[b]	RVS SCF[b]
	$\rho_{min}=0.01$	$\rho_{min}=0.001$	$\rho_{min}=0.0001$		
HF/6-31G(d,p)//HF/6-31G(d,p)	-0.94	-1.36	-1.09	-0.47	-0.60
HF/cc-pVDZ// HF/6-31G(d,p)	-0.53	-1.19	-0.83	-0.44	-0.56
HF/aug-cc-pVDZ//HF/6-31G(d,p)	-0.86	-1.19	-1.32	-1.12	-0.77
HF/6-31++G(d,p)//HF/6-31G(d,p)	-0.77	-1.07	-1.19	-0.84	-0.65
HF/6-31++G(2d,p)//HF/6-31G(d,p)	-0.82	-1.17	-1.32	-0.91	-0.71
HF/cc-pVDZ//HF/cc-pVDZ	-0.57	-1.28	-0.91	-0.45	-0.58
HF/aug-cc-pVDZ//HF/cc-pVDZ	-0.86	-1.28	-1.30	-1.09	-0.78
HF/aug-cc-pVDZ//HF/aug-cc-pVDZ	-0.69	-1.11	-1.35	-0.89	-0.67
HF/6-31++G(d,p)//HF/6-31++G(d,p)	-0.73	-1.11	-1.23	-0.77	-0.66
HF/6-31++G(2d,p)//HF/6-31++G(2d,p)	-0.71	-1.09	-1.33	-0.78	-0.66

Table 4.1 Polarization interaction energies E_{pol} of $(H_2O)_2$, in kcal/mole, computed by different procedures. Number of e-voxels is 1.00×10^6, stepsize is 0.065Å, and condensation level is n=3.

[a]Values of ρ_{min} are in electrons/bohr^3.
[b]Ref. 12.

In Table 4.1, the number of e-voxels is about 1.00×10^{-6} and the condensation level is set to 3. The results show that E_{pol} is not highly sensitive to basis set. In section 4.3, we discussed the importance of ρ_{min}, which can be neither too big nor too small for reasonable results. We tested some values of ρ_{min} and found that the approximations are valid compared to other results [12] if ρ_{min} is between 10^{-2} to 10^{-4} electrons/bohr^3. Since the overlap region is only 0.1% of the total volume for each monomer when $\rho_{min}=10^{-2}$ electrons/bohr^3, the exchange-repulsion can be neglected. Surprisingly, the overlap part increases to 23% of the

volume when $\rho_{min}=10^{-4}$ electrons/bohr^3 and the results are still satisfactory. However, when $\rho_{min}=10^{-5}$ electrons/bohr^3, the approximations are not effective and give wrong polarization energies. This demonstrated that our model is applicable for the slight or moderate overlap of electron clouds.

Our E_{pol} for $\rho_{min}=0.01$ electrons/bohr^3 are in very good agreement with the RVS SCF and, for the most part, with the Kitaura-Morokuma as well; the average absolute differences are 0.09 and 0.16 kcal/mole, respectively. For the other ρ_{min}, they are 0.52 and 0.41 kcal/mole. These clearly indicate that the volume of the overlap region is the most important factor for the calculation. It should be noted that Bentley's analysis of the electron densities of noncovalent complexes shows that $\rho=0.01$ electrons/bohr^3 is an appropriate boundary surface for a constituent of a hydrogen-bonded system, as is $(H_2O)_2$. For weaker interactions, he suggested $\rho \approx 0.01$ electrons/bohr^3. Thus, the data in Table 4.1 suggest that, for $(H_2O)_2$, the magnitude of E_{pol} is overestimated at $\rho=0.001$ and 0.0001 electrons/bohr^3.

4.5. <u>Summary</u>

The exact expression for polarization interaction energies between two molecules is derived in terms of the electron densities. As $\Delta\rho^{pol}$ cannot be obtained directly, it is necessary to make some approximations. Procedures for polarization energy calculations are proposed and a program is formulated, using a numerical integration technique. The validity of the approximations is supported by calculations for the water dimer. The result is quite reliable in comparison with

other theoretical results. This method provides a new way for evaluation of polarization energies.

References

[1]. Israelachvili, J. *Intermolecular & Surface Force*, Chapter 5; Academic Press: San Deigo; **1991**.

[2]. Stone, A. J. *The Theory of Intermolecular Forces;* Clarendon: Oxford, **1996**.

[3]. Gavezzotti, A. *J. Phys. Chem. B* 106, **2002**, 4154.

[4]. Gavezzotti, A. *J. Phys. Chem. B* 107, **2003**, 2344.

[5]. Buckingham, A. D. In *Intermolecular Force: From Diatomics to Biopolymers;* Pullman, B., Ed.; Wiley: New York, **1978**.

[6]. Kitaura, K.; Morokuma, K. *Int. J. Quantum Chem.* Vol X, **1976**, 325.

[7]. Bades, R. F. W.; Hennecker, W. H.; Cade, P.E. *J. Chem. Phys.* 46, **1967**, 3341.

[8]. Bentley, J. *J. Phys. Chem. A* 102, **1998**, 6043.

[9]. Boys, S. F.; Bernardi, F. *Mol. Phys.* 19, **1970**, 553.

[10]. Buckingham, A. D.; Fowler, P.W., Hutson, J. M. *Chem Review*, 88, **1988**, 963.

[11]. Ferenczy, G. G.; Reynolds, C. A. *J. Phys. Chem. A.* 105, **2001**, 11470.

[12]. Chen, W.; Gordon, M. S. *J. Phys. Chem.* 100, **1996**, 14316.

[13]. Bagus, P. S.; Hermann, K.; Bauschlicher, C. W., Jr. *J. Chem. Phys.* 80, **1984**, 4378.

[14]. Stevens, W. J.; Fink, W. H. *Chem. Phys. Lett.* 139, **1987**, 15.

CHAPTER 5. DETERMINATION OF NONCOVALENT INTERACTION ENERGIES FROM ELECTRONIC DENSITIES

5.1. <u>Introduction</u>

Noncovalent interactions are of key importance in many areas, including salvation [1, 2], liquid and solid properties [3, 4], DNA and Protein structure [5, 6], biological molecular recognition processes [7, 8], supermolecular chemistry [9], physical adsorption [8, 10], etc. Hydrogen bonding is a particularly prominent example of a noncovalent interaction [11, 12].

The stabilization energy ΔE_{stab} of a noncovalent complex AB can be defined as the difference between the energies of the complex and the isolated molecules A and B:

$$\Delta E_{stab} = E_{AB} - (E_A + E_B) \tag{5.1}$$

Since ΔE_{stab} is usually several orders of magnitude smaller than E_{AB} and $(E_A + E_B)$, any errors in the values of these latter energies are considerably magnified in ΔE_{stab}. Accordingly, E_{AB}, E_A and E_B have to be computed at a high level of accuracy. This is often not feasible for those relatively large systems. Another problem caused by this approach is called BSSE, which has been discussed in Chapters 1 and 2.

Instead of calculating ΔE_{stab} from Eq. (5.1) (called the supermolecular method), a popular alternative which does not require taking a difference between computed quantities is to use perturbation theory to directly obtain the interaction energy E_{int}. Unlike ΔE_{stab}, E_{int} normally refers to interactions between rigid systems, A and B having the same geometries in the complex as in their isolated states; in contrast, ΔE_{stab} corresponds to AB, A and B having their equilibrium structures [13-16]. The difference between ΔE_{stab} and E_{int} will be discussed in section 5.3. Generally, E_{int} is composed of 4 components, which are usually designated as electrostatic, polarization, exchange-repulsion and dispersion. Various techniques have been used to evaluate these terms [13-18].

In terms of the concept of electron density, some methods have been developed for calculating noncovalent interaction energies. In Chapters 3 and 4, we computed electrostatic and polarization energies from electronic densities. Exchange-repulsion energy can be evaluated by the overlap model, which assumes that the exchange energy between two closed shell molecules A and B is proportional to the overlap of the isolated molecule electron densities [19, 20],

$$E_{ex} = K \int \rho_A^0(r)\rho_B^0(r)dr \qquad (5.2)$$

where K is an adjustable parameter and ρ_A^0 and ρ_B^0 are the electron densities of the isolated molecules A and B. The validity of this model has been tested explicitly for some intermolecular systems, such as pairs of rare gas atoms [21], rare gas atoms with halide ions [22], and $(F_2)_2$, $(N_2)_2$, $(Cl_2)_2$ [23], etc. Compared to *ab initio* calculations, this method is less computationally demanding. However, the overlap model is only a semiempirical method. The parameter K is normally obtained by

fitting, which may affect the accuracy of calculations. The dispersion energy may be also expressed in term of electron densities. Recently, Gavezzotti developed a method called semi-classical density sums (SCDS) for the calculation of intermolecular interaction energies [24]. In his approach, the polarizability at each e-voxel and the ionization energy are defined by semi-empirical methods. Intermolecular energies are calculated as a sum of voxel-voxel terms in a London-type expression.

The Hohenberg-Kohn theorem states that the electron density determines all the ground state properties of a molecular system. Therefore, the interaction energy may be calculated from the electron densities of a supermolecular system and its components. In this work, we develop an alternative method for the calculation of intermolecular interaction energy, which only requires a knowledge of the electronic density of the complex.

In 1998, Bentley explored the behavior of 50 interaction pairs and found that the total electron density was well represented by the sum of the density functions of the isolated molecules in the reaction region [25]. The results suggest that the approximate electron densities of the subsystems may be obtained from the electron density of the supersystem. Hence the calculation of the electronic density of the isolated molecules may be omitted.

Our calculation is based on the Hellmann-Feynman electrostatic theorem, which describes the nature of the forces acting on nuclei in molecular systems. It states that the effective force acting on a nucleus in a molecular system can be calculated by simple electrostatics as the sum of the Coulombic forces exerted by

other nuclei and by the electron density found by solving the Schrödinger equation [26]. In the spirit of the electrostatic theorem, we propose a new method for interaction energy calculations.

5.2. **The Hellmann-Feynman Electrostatic Theorem**

The generalized Hellmann-Feynman theorem [27, 28] has the following form,

$$\frac{\partial E}{\partial \lambda} = \int \psi^* \frac{\partial \hat{H}}{\partial \lambda} \psi d\tau \tag{5.3}$$

where ψ is an exact eigenfunction of a Hamiltonian $\hat{H}$, E is the corresponding eigen energy and λ is any parameter that appear in the Hamiltonian.

Now we apply the Hellmann-Feynman theorem to a molecular system. Suppose there are N nuclei and m electrons in the system. For any nucleus α, its Cartesian coordinates can be written as (X^α, Y^α, Z^α), (α=1, …N). First, in a Cartesian coordinate system, considering the force f_X^α, exerted on nucleus α in the X direction. According to Eq. (5.3), we have

$$f_X^\alpha = -\frac{\partial E}{\partial X^a} = -\int \psi^* \frac{\partial \hat{H}}{\partial X^\alpha} \psi d\tau \tag{5.4}$$

The Hamiltonian consists of the kinetic energy operator $\hat{T}$ and the potential energy operator $\hat{V}$, $\widehat{H} = \hat{T} + \hat{V}$. Since $\hat{T}$ is independent on the nuclear Cartesian coordinates, Eq. (5.4) is written as

$$f_X^\alpha = -\int \psi^* \frac{\partial \hat{V}}{\partial X^\alpha} \psi d\tau \tag{5.5}$$

$\hat{V}$ is made up of three terms: the interactions of the nuclei with each other $\hat{V}_{NN}$, of the nuclei and electrons $\hat{V}_{Ne}$, and of the electrons $\hat{V}_{ee}$

$$\hat{V} = \hat{V}_{NN} + \hat{V}_{Ne} + \hat{V}_{ee} \tag{5.6}$$

$\hat{V}_{NN}$, $\hat{V}_{Ne}$ and $\hat{V}_{ee}$ can be expressed as follows

$$\hat{V}_{NN} = \sum_\beta \sum_{\alpha > \beta} \frac{Z_\alpha Z_\beta}{[(X^\alpha - X^\beta)^2 + (Y^\alpha - Y^\beta)^2 + (Z^\alpha - Z^\beta)^2]^{1/2}} \tag{5.7}$$

$$\hat{V}_{Ne} = -\sum_\alpha \sum_i \frac{Z_\alpha e}{[(X^\alpha - x^i)^2 + (Y^\alpha - y^i)^2 + (Z^\alpha - z^i)^2]^{1/2}} \tag{5.8}$$

$$\hat{V}_{ee} = -\sum_i \sum_{j>i} \frac{e^2}{[(x^j - x^i)^2 + (y^j - y^i)^2 + (z^j - z^i)^2]^{1/2}} \tag{5.9}$$

where x^i, y^i and z^i are the coordinates of the electrons. Following Eqs. (5.7), (5.8) and (5.9), we have

$$\frac{\partial \hat{V}_{NN}}{\partial X^\alpha} = \sum_{\beta \neq \alpha} \frac{Z_\alpha Z_\beta (X^\beta - X^\alpha)}{R_{\alpha\beta}^3} \tag{5.10}$$

$$\frac{\partial \hat{V}_{Ne}}{\partial X^\alpha} = \sum_i \frac{Z_\alpha e(X^\alpha - x^i)}{R_{\alpha i}^3} \tag{5.11}$$

$$\frac{\partial \hat{V}_{ee}}{\partial X^\alpha} = 0 \tag{5.12}$$

where $R_{\alpha\beta}$ is the distance between two nuclei α and β, and $R_{\alpha i}$ is the distance from nucleus α to electron i.

$$R_{\alpha\beta} = [(X^\alpha - X^\beta)^2 + (Y^\alpha - Y^\beta)^2 + (Z^\alpha - Z^\beta)^2]^{1/2} \tag{5.13}$$

$$R_{\alpha i} = [(X^\alpha - x^i)^2 + (Y^\alpha - y^i)^2 + (Z^\alpha - z^i)^2]^{1/2} \tag{5.14}$$

If ψ is normalized, Eq. (5.5) becomes

$$f_X^\alpha = -\sum_{\beta \neq \alpha} \frac{Z_\alpha Z_\beta (X^\beta - X^\alpha)}{R_{\alpha\beta}^3} - \sum_i Z_\alpha e \int \psi^* \psi \frac{X^\alpha - x^i}{R_{\alpha i}^3} d\tau$$

$$= -\sum_{\beta \neq \alpha} \frac{Z_\alpha Z_\beta (X^\beta - X^\alpha)}{R_{\alpha\beta}^3} - \int \sum_i \frac{Z_\alpha e(X^\alpha - x^i)}{R_{\alpha i}^3} [\int ' \psi^* \psi dv] d\tau$$

$$\text{(5.15)}$$

$\int ' \psi^* \psi dv$ means the integral over the coordinates of all electrons except those of

electron i. This integral is equal to ρ/m (m is the number of electrons in the system).

Thus Eq. (5.15) can be further written as

$$f_X^\alpha = -\sum_{\beta \neq \alpha} \frac{Z_\alpha Z_\beta (X^\beta - X^\alpha)}{R_{\alpha\beta}^3} - \frac{1}{m} \sum_{i=1}^m Z_\alpha e \int \rho \frac{X^\alpha - x^i}{R_{\alpha i}^3} d\tau \qquad \text{(5.16)}$$

As the integrals in Eq. (5.16) have the same value no matter the value of i is, the

equation is simplified to the following form:

$$f_X^\alpha = -\sum_{\beta \neq \alpha} \frac{Z_\alpha Z_\beta (X^\beta - X^\alpha)}{R_{\alpha\beta}^3} + Z_\alpha e \int \rho \frac{x^i - X^\alpha}{R_{\alpha i}^3} d\tau \qquad \text{(5.17)}$$

The force on nucleus α is the gradient of the potential energy at point α:

$$\vec{F}_\alpha = \vec{\nabla} E = f_X^\alpha \vec{i} + f_Y^\alpha \vec{j} + f_Z^\alpha \vec{k} \qquad \text{(5.18)}$$

Therefore, the effective force exerted on nucleus α is written

$$\vec{F}_\alpha = -\sum_{\beta \neq \alpha} \frac{Z_\alpha Z_\beta \vec{R}_{\alpha\beta}}{R_{\alpha\beta}^3} + Z_\alpha e \int \rho \frac{\vec{R}_{\alpha i}}{R_{\alpha i}^3} d\tau \qquad \text{(5.19)}$$

Eq. (5.19) is called the electrostatic theorem. As described above, the force on a

nucleus is just the classical interaction exerted on the nucleus by the other nuclei

and by the electron density distribution of all of the electrons. It is easy to explain

the formation of covalent bonds by the electrostatic theorem. The attractive forces

between two nuclei originate from the second term in Eq. (5.19): The electron

density distribution between the two nuclei gives the strong attraction between two atoms and leads to a covalent bond.

The electrostatic theorem can also be used to explain intermolecular interactions. Feynman interpreted the dispersion force [28]. He said, "The Schrödinger perturbation theory for two interacting atoms at a separation R, large compared to the radii of the atoms, leads to the result that the charge distribution of each is distorted from central symmetry, a dipole moment of order $1/R^7$ being induced in each atom. The negative charge distribution of each atom has its center of gravity moved slightly toward the other. It is not the interaction of these dipoles which leads to van der Waals' force, but rather the attraction of each nucleus for the distorted charge distribution of its own electrons that gives the attractive $1/R^7$ force."

The electrostatic theorem provides the classical interpretation that intermolecular interactions come from the electrostatic forces between the nuclei and the electrons whose distribution is determined by the electron density of the system. Hirschfelder and Eliason calculated the long-range interaction of two ground state hydrogen atoms with the use of the Hellmann-Feynman electrostatic theorem [29]. They found that the exact C_6 coefficient was obtained with highly accurate approximate wavefunctions. This confirms Feynman's suggestion that the force on the nucleus is due to its attraction to the centroid of its "own" electron cloud.

5.3. A New Model for Calculation of Noncovalent Interaction Energy

In this section, we shall use Eq. (5.19) to express the stabilization energy ΔE_{stab}. Assume that a complex AB is composed of two molecules, A and B. Both of them are in the ground state. The intermolecular interaction energy is equal to the work in moving A from infinite distance from B to the separation in the complex. The molecule A can be divided into two parts, nuclei and electrons. According to the electrostatic theorem, the work done by each nucleus α in A, W_α is given as

$$W_\alpha = \int_\infty^{R_\alpha} \vec{F}_{\alpha B} \cdot d\vec{R}$$
$$= -\int_\infty^{R_{\alpha B}} \sum_B \frac{Z_\alpha Z_B \vec{R}_{\alpha B}}{R_{\alpha B}^3} \cdot d\vec{R}_{\alpha B} + \int_\infty^{r_{\alpha B}} Z_\alpha e \int \rho_B(\vec{r}_{\alpha B}, \vec{r}_B) \frac{\vec{r}_{\alpha B}}{r_{\alpha B}^3} d\vec{r}_B \cdot d\vec{r}_{\alpha B}$$

(5.20)

where $R_{\alpha B}$ is the distance from nucleus α to the nucleus B in molecule B, $r_{\alpha B}$ the distance from nucleus α to r_B where the electron density of molecule B is ρ_B. However, the calculation of the second integral is difficult, in that the electron density ρ_B changes with intermolecular distance. Hence we divided the second integral of Eq. (5.20) into two terms: In the first term, the electron density is always equal to electron density of molecule B in the complex; the second one is a correction term. Hence Eq. (5.20) can be written as

$$W_\alpha = -\int_\infty^{R_{\alpha B}} \sum_B \frac{Z_\alpha Z_B \vec{R}_{\alpha B}}{R_{\alpha B}^3} \cdot d\vec{R}_{\alpha B} + \int_\infty^{r_{\alpha B}} Z_\alpha e \int \rho_B(\vec{r}_B) \frac{\vec{r}_{\alpha B}}{r_{\alpha B}^3} d\vec{r}_B \cdot d\vec{r}_{\alpha B} + \Delta E_{\alpha B}^{cor}$$
$$= \sum_B \frac{Z_\alpha Z_B}{R_{\alpha B}} - Z_\alpha e \int \frac{\rho_B(\vec{r}_B)}{r_{AB}} d\vec{r}_B + \Delta E_{\alpha B}^{cor}$$

(5.21)

and the work done by all nuclei in molecule A is

$$W_N = \sum_{\alpha \in A} W_\alpha = \sum_A \sum_B \frac{Z_A Z_B}{R_{AB}} - \sum_A Z_A e \int \frac{\rho_B(\vec{r}_B)}{|\vec{R}_A - \vec{r}_B|} d\vec{r}_B + \sum_A \Delta E_{AB}^{cor}$$

(5.22)

Now we consider the work done by the electrons in molecule A. For an electron i, the effective force on it due to the nuclei and electrons of molecule B is,

$$\vec{F}_i = \sum_B \frac{Z_B e \vec{R}_{Bi}}{R_{Bi}^3} - e^2 \int \rho_B(\vec{r}_{Bi}, \vec{r}_B) \frac{\vec{r}_{Bi}}{r_{Bi}^3} d\vec{r}_B \tag{5.23}$$

where R_{Bi} is the distance between nucleus B to electron i, and r_{Bi} is the distance between electron i and a point B with the electron density ρ_B. The work made by electron i can be written as

$$\begin{aligned}
W_i &= \int_\infty^{R_{Bi}} \sum_B \frac{Z_B e \vec{R}_{Bi}}{R_{Bi}^3} \cdot d\vec{R}_{Bi} - \int_\infty^{r_{Bi}} e^2 \int \rho_B(\vec{r}_B) \frac{\vec{r}_{Bi}}{r_{Bi}^3} d\vec{r}_B \cdot d\vec{r}_{Bi} + \Delta E_{Bi}^{cor} \\
&= -\sum_B \frac{Z_B e}{R_{Bi}} + e^2 \int \frac{\rho_B(\vec{r}_B)}{r_{Bi}} d\vec{r}_B + \Delta E_{bi}^{cor}
\end{aligned} \tag{5.24}$$

ΔE_{Bi}^{cor} is a correction term. In Eq. (5.24), the electron i is treated as a stationary point. According to quantum mechanics, an electron can appear in any position and the probability is determined by the electron density. Therefore, Eq. (5.24) may be expresszd as

$$W_i = -\sum_B \int \frac{Z_B e}{R_{Bi}} \rho_i(\vec{R}_{Bi}, \vec{r}_i) dr_i + e^2 \int\int \frac{\rho_B(\vec{r}_B)\rho_i(\vec{r}_{Bi}, \vec{r}_i)}{r_{Bi}} d\vec{r}_i d\vec{r}_B + \Delta E_{bi}^{cor} \tag{5.25}$$

where ρ_i is the electron density of i. Since ρ_i is also a function of intermolecular distance, we use the same treatment described above. Thus two correction terms are added

$$\begin{aligned}
W_i &= -\sum_B \int \frac{Z_B e}{R_{Bi}} \rho_i(\vec{r}_i) d\vec{r}_i + \Delta E_{Bi}^{cor} \\
&+ e^2 \int\int \frac{\rho_B(\vec{r}_B)\rho_i(\vec{r}_i)}{r_{Bi}} d\vec{r}_i d\vec{r}_B + \Delta E_{ib}^{cor} + \Delta E_{bi}^{cor}
\end{aligned} \tag{5.26}$$

The work by all of the electrons in molecule A can be given as

$$W_e = \sum_{i \in A} W_i$$
$$= \sum_B \int \frac{Z_B e}{|\vec{R}_B - \vec{r}_A|} \rho_A(\vec{r}_A) d\vec{r}_A + e^2 \iint \frac{\rho_B(\vec{r}_B)\rho_A(\vec{r}_A)}{|\vec{r}_A - \vec{r}_B|} d\vec{r}_A d\vec{r}_B \qquad \textbf{(5.27)}$$
$$+ \sum \Delta E_{BA}^{cor} + \sum \Delta E_{ab}^{cor} + \sum \Delta E_{ba}^{cor}$$

The stabilization energy is the sum of W_N and W_e. Combining Eq. (5.22) and Eq. (5.27), we obtain the expression of stabilization energy between two molecules:

$$\Delta E_{stab} = W_N + W_e$$
$$= \sum_A \sum_B \frac{Z_A Z_B}{R_{AB}} - \sum_A \int \frac{Z_A e \rho_B(\vec{r}_B)}{|\vec{R}_A - \vec{r}_B|} d\vec{r}_B + \sum_B \int \frac{Z_B e \rho_A(\vec{r}_A)}{|\vec{R}_B - \vec{r}_A|} d\vec{r}_A \qquad \textbf{(5.28)}$$
$$+ e^2 \iint \frac{\rho_B(\vec{r}_B)\rho_A(\vec{r}_A)}{|\vec{r}_A - \vec{r}_B|} d\vec{r}_A d\vec{r}_B + \Delta E^{cor}$$

Eq. (5.28) indicates that the stabilization energy ΔE_{stab} can be expressed as the sum of the classical electrostatic energy and the correction energy ΔE^{cor}. As the electronic densities depend on intermolecular distance, ΔE^{cor} should be included to describe the effect. If we neglect the dependence and use ρ_A and ρ_B at the equilibrium state in the complex AB, the energy that we obtain is not rigorously ΔE_{stab} but rather represents the intermolecular interaction of A and B as they are in the complex, which is designated E_{int}^*. Eq. (5.28) accordingly becomes,

$$E_{int}^* = \sum_A \sum_B \frac{Z_A Z_B}{R_{AB}} - \sum_A \int \frac{Z_A e \rho_B(\vec{r}_B)}{|\vec{R}_A - \vec{r}_B|} d\vec{r}_B + \sum_B \int \frac{Z_B e \rho_A(\vec{r}_A)}{|\vec{R}_B - \vec{r}_A|} d\vec{r}_A$$
$$+ e^2 \iint \frac{\rho_B(\vec{r}_B)\rho_A(\vec{r}_A)}{|\vec{r}_A - \vec{r}_B|} d\vec{r}_A d\vec{r}_B \qquad \textbf{(5.29)}$$

Eq. (5.29) expressed the interaction energy solely in term of classical electrostatics, involving the charge distributions of the components as they are in the complex. Conceptually, E_{int}^*, E_{int} and ΔE_{stab} differ from one another: ΔE_{stab} refers to AB, A

and B in their equilibrium states, E_{int}^* corresponds to A and B having geometries and electronic densities as in the complex, and E_{int} uses ground-state geometries for the monomers A and B but attempts to approximate their electronic densities in AB. The effects of these distinctions are usually quite small [30]. For example, The energies required to distort both components in $(H_2O)_2$ and $(HF)_2$ from isolated equilibrium to their states in the dimers were found to be 0.09 kcal/mole [31] and 0.03 kcal/mole [32], respectively. To those larger systems such as face-to-face dimer of uracil [33], we found the energy to be 0.79 kcal/mole at MP2/6-31+G* level. The effect may be significantly greater for ion-molecule interactions, e.g. F⁻ (H_2O) [31].

The relationship between ΔE_{stab} and E_{int}^*, and the physical meaning of the correction energy ΔE^{cor} is denoted in Figure 5.1. We design a two-step path to describe the binding process. In the first step, the geometries and electronic densities of the isolated molecules change to those in binding state; In the second step, A and B form the complex A···B. Therefore, the interaction energy is given as

$$\Delta E_{stab} = E_{int}^* + \Delta E_A^* + \Delta E_B^* \qquad \textbf{(5.30)}$$

Comparing (5.30) and (5.28), we find

$$\Delta E^{cor} = \Delta E_A^* + \Delta E_B^* \qquad \textbf{(5.31)}$$

It gives the binding energy between two separated molecules with the same geometries and electronic densities as those in the complex. ΔE_A^* and ΔE_B^*, designated relaxation energies, are the differences in energy between the unperturbed isolated state and the hypothesized state with the geometry and

electronic density in the complex. Since the geometries and electronic densities vary little in this process, ΔE^{cor} is usually much smaller than E_{int}^* and can be ignored in many cases.

$$\text{A}(\rho_{A,0}) + \text{B}(\rho_{B,0}) \xrightarrow{\Delta E_{stab}} \text{A}\cdots\text{B}(\rho_A + \rho_B)$$

$$\Delta E_A^* \downarrow \qquad \Delta E_B^* \downarrow \qquad E_{int}^*$$

$$\text{A}^*(\rho_A) + \text{B}^*(\rho_B)$$
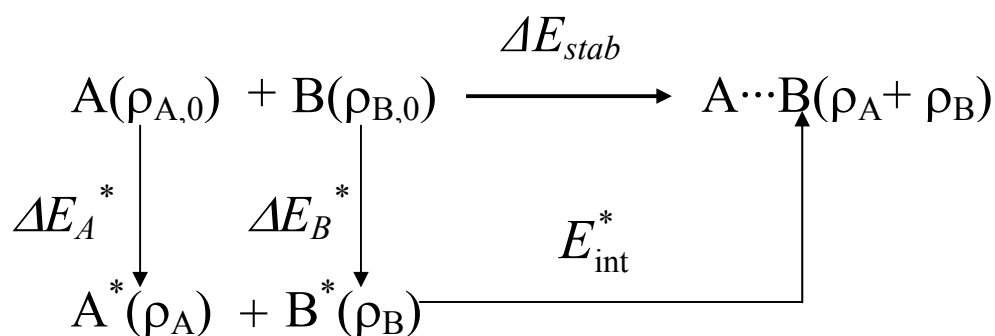
Figure 5.1 Relationship between ΔE_{stab} and E_{int}^*, and physical meaning of the correction energy.

Since Eq. (5.29) is to be applied by computing the electronic density of the complex and then partitioning it into those of the monomers, a key problem now is how to carry out the latter step. The approach and integration technique shall be described in the next section.

5.4. Approximate Approach for Calculation of Interaction Energy

According to Eq. (5.29), E_{int}^* can be computed if ρ_A and ρ_B are known. However, only the total electron density of the system is available. It is impossible to resolve ρ_A and ρ_B strictly by one equation. Fortunately, the binding between the molecules in a complex is normally very weak, which means their electron clouds

only overlap and penetrate each other slightly. Thus the total electron density ρ may be decomposed to ρ_A and ρ_B directly. First, a molecular boundary surface for the complex should be established in term of an isodensity contour $\rho_{\min}$. A lot of work has been done in this field: Bader *et al.* suggested a value of 0.001 electrons/bohr^3 as best describing molecular dimensions in the gas phase [34]. Wiberg *et al.* used a value of 0.0004 electrons/bohr^3 for reproducing liquid molar volumes [35]. Bentley found that the 0.002 electrons/bohr^3 can be used to define the size and shape of a molecule for weakly interacting systems in condensed states [25]. Here we choose 0.001-0.0001 electrons/bohr^3 as the boundary of the molecular electron clouds.
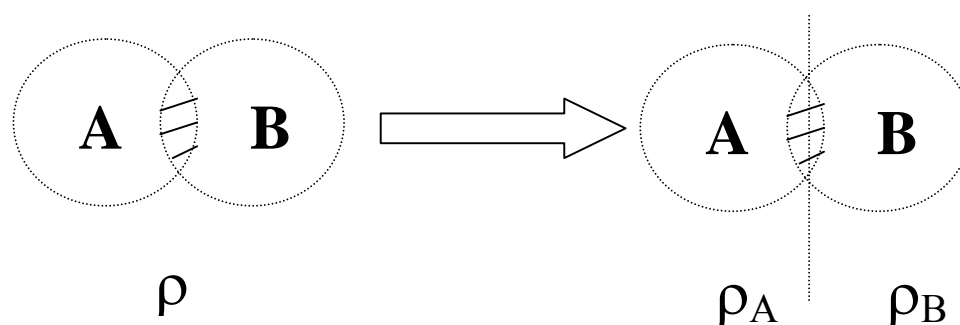
Figure 5.2 Decomposition of the electron density of a complex.

The size and shape of the electron clouds for the complex are defined when an isocontour is given. For obtaining the approximate electronic densities ρ_A and ρ_B, we assume that the electronic density at any point can only be owned by one molecule. Thus ρ_A and ρ_B can be determined by assigning each point in the complex. A simple method is implemented for the assignment: For each point p in the complex, we evaluate the ratios of its distance from each nucleus divided by van

der Waals radius of that atom (R_{pN}/R_{NvDW}, where R_{pN} is the distance between p and the nucleus of atom N, and R_{NvDW} is the vDW radius of atom N.). The point and the corresponding electronic density are assigned to the atom with the lowest value of R_{pN}/R_{NvDW}. In terms of the position of the atom, the assignment of each point can be determined.

The procedure for E_{int}^{*} calculation is similar to that described in Chapters 3 and 4. The integrations are carried out numerically, which consists of several steps: (1). For each molecule in the complex, the boundary of the electron cloud is defined in term of an isodensity contour. (2). Each point in the complex is assigned to a molecule in the complex and the electronic density of each molecule is thus obtained. (3). The electronic charge distribution is divided into a large number of small units, "e-voxels", via a three dimension grid. Since unrealistic values may arise near the nuclei, only the valence electrons are included. (4). Cubic "super e-voxels" are generated by combining n^3 old ones for each molecule. Each super e-voxels has a charge equal to the sum of those of its constituents, which is taken to be located at its center. If some of the constituent e-voxels are beyond ρ_{min}, they are nevertheless included in order to avoid asymmetry. (5). Charge renormalization is carried out for each molecule, so that overall charge neutrality is preserved. (5). The interaction energy is calculated using Eq. (5.29). Since the distance between two super e-voxels is very small sometimes, we choose a minimum distance, e.g. one-half of the grid stepsize, below which this term is forced to equal the minimum.

On the basis of the procedure mentioned above, a computer program was written to implement this numerical integral method. It reads an electron density

file generated by Gaussian 98 and computes E_{int}^* between any two molecules in the complex.

5.5. Interaction Energy Calculations for (H₂O)₂ and (HF)₂

In Chapters 3 and 4, we discussed the electrostatic and polarization interaction energies for the water dimer. Here we calculate E_{int}^* of these hydrogen-bonded systems. The nonplanar C_s geometry of the water dimer optimized at the CCSD(T)/TZ2P(f,d)+dif level was used [36]. Electronic density files for the water dimer were generated by single point calculations. Four different theoretical methods (HF, MP2, B3LYP and B3PW91) were employed, with three basis sets (cc-pVXZ, (X=D, T, Q)) for each method. The number of e-voxels of each cube file is 1.0×10^6 and the condensation level is 3. E_{int}^* were computed with four different ρ_{min} varying from 0.01 to 0.00001 electrons/bohr^3.

E_{int}^* for another strong hydrogen-bonded system — the hydrogen fluoride dimer, was also evaluated. The geometry of the (HF)₂ has been investigated by theoretical calculations [32, 38-47] and experimental methods [48-50]. It was found that the theoretical results agreed well with those estimated from experiments (R_{FF}=2.72±0.03Å; $\angle H_3F_4F_2$ = 117±6°; $\angle H_1F_2F_4$=10±6°). Here we used the best estimated geometry obtained from the CCSD(T) calculations by Peterson *et al* [32] (see Figure 5.3). The dimer electronic densities and E_{int}^* were also computed at several different theoretical levels, with Dunning's correlation-consistent basis sets

(CC-pVXZ, X=D, T, Q). The number of e-voxels, the condensation level and ρ_{min} are as same as those for $(H_2O)_2$.

Method	$\rho_{min} =$	10^{-2} au	10^{-3} au	10^{-4} au	10^{-5} au
HF/cc-pVDZ		-7.18	-6.26	-6.07	-6.04
HF/cc-pVTZ		-7.30	-6.19	-5.95	-5.91
HF/cc-pVQZ		-7.29	-6.20	-5.92	-5.88
MP2/cc-pVDZ		-6.63	-5.82	-5.62	-5.58
MP2/cc-pVTZ		-6.76	-5.65	-5.39	-5.36
MP2/cc-pVQZ		-6.77	-5.63	-5.33	-5.29
B3LYP/cc-pVDZ		-6.48	-5.68	-5.49	-5.45
B3LYP/cc-pVTZ		-6.65	-5.59	-5.33	-5.29
B3LYP/cc-pVQZ		-6.62	-5.55	-5.26	-5.22
B3PW91/cc-pVDZ		-6.48	-5.71	-5.53	-5.49
B3PW91/cc-pVTZ		-6.63	-5.61	-5.37	-5.34
B3PW91/cc-pVQZ		-6.63	-5.60	-5.32	-5.28
best estimate of ΔE_{stab}[c]		-5.0 to -5.4			

Table 5.1 Calculated E_{int}^* for $(H_2O)_2$, in kcal/mole, using CCSD(T) optimized dimer geometry and Eq. (5.29).[a, b]

[a] Geometry taken from Ref. 36.
[b] Number of e-voxels=1.0×10^6; grid stepsize=0.0615 Å; n=3.
[c] Ref. 37.

There is a long history of efforts to determine ΔE_{stab} for $(H_2O)_2$. Correlated *ab initio* methods (MP2, MP4, CI, with correlation consistent basis sets) have tend to give values between -4.2 and -4.8 kcal/mole (corrected for BSSE) [37, 51], while an experimentally- based (thermal conductivity) prediction is -5.44±0.7 kcal/mole [52]. Feyereisen *et al* concluded that the MP2 complete basis set limit is -5.0 kcal/mole, so that the true ΔE_{stab} is between -5.0 and -5.4 kcal/mole. $(HF)_2$ has also been studied extensively. High-level (MP4, CI, CC) calculated ΔE_{stab} are primarily in the range -4.3 to -5.3 kcal/mole [32, 45, 50]. Klopper *et al*'s analysis of computed and IR data led to a best estimate of 5.57±0.05 kcal/mole.
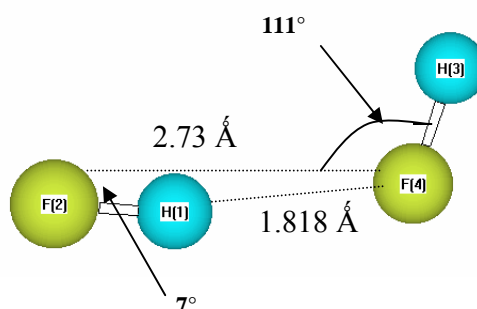
Figure 5.3 The best estimated C_s structure of HF dimer from CCSD(T) calculations
(Ref. 32).

Table 5.1 and Table 5.2 give the E_{int}^* for $(H_2O)_2$ and $(HF)_2$, respectively. It is found that the magnitude of E_{int}^* decreases as ρ_{min} becomes smaller, which expands the molecular boundary. The reason can be explained reasonably: since more peripheral electron voxels are included when a smaller ρ_{min} used, more short e-voxel pairs are involved in the calculation. This process yields a larger electron-

Method	$\rho_{\min} =$	10^{-2} au	10^{-3} au	10^{-4} au	10^{-5} au
HF/cc-pVDZ		-6.69	-5.08	-4.83	-4.80
HF/cc-pVTZ		-7.10	-5.12	-4.75	-4.70
HF/cc-pVQZ		-7.27	-5.30	-4.83	-4.77
MP2/cc-pVDZ		-6.13	-4.61	-4.36	-4.33
MP2/cc-pVTZ		-6.42	-4.49	-4.13	-4.09
MP2/cc-pVQZ		-6.62	-4.63	-4.15	-4.10
B3LYP/cc-pVDZ		-6.07	-4.63	-4.38	-4.35
B3LYP/cc-pVTZ		-6.41	-4.52	-4.15	-4.11
B3LYP/cc-pVQZ		-6.55	-4.61	-4.13	-4.07
B3PW91/cc-pVDZ		-6.06	-4.64	-4.39	-4.36
B3PW91/cc-pVTZ		-6.42	-4.55	-4.19	-4.15
B3PW91/cc-pVQZ		-6.55	-4.67	-4.21	-4.15
best estimate of ΔE_{stab} [c]		-4.57			

Table 5.2 Calculated E_{int}^{*} for $(HF)_2$, in kcal/mole, using CCSD(T) optimized dimer geometry and Eq. (5.29).[a, b]

[a] Geometry taken from Ref. 32.
[b] Number of e-voxels=1.0×10^{6}; grid stepsize=0.0573 Å; n=3.
[c] Ref. 50.

electron repulsion and then a smaller interaction energy. For $(H_2O)_2$ and $(HF)_2$, E_{int}^{*} converge when $\rho_{\min}$ is less than 10^{-4} electrons/bohr^3. Surprisingly, different theoretical methods, HF, MP2 and DFT give close results. With the same basis set,

the biggest difference of E_{int}^* is only about 0.7 kcal/mole. Also it is noted that the Hartree-Fock E_{int}^* are more negative than the others, for $(H_2O)_2$ and $(HF)_2$, the differences are about $0.4 - 0.7$ kcal/mole. The discrepancy could be caused by following reasons: (1). As the electronic densities are obtained from the approximate wave functions generated by a numerical method, the accuracy of the electronic densities may be not as good as that of other calculated properties such as energies and geometries. The inaccuracy of the electronic densities may affect the results. (2). Because several approximations are used in the decomposition of the electronic densities, it is not a rigorous approach. For electronic densities produced by different theoretical methods, different errors may be introduced in this process. (3). In our scheme, ΔE_{stab} consists of two terms, E_{int}^* and ΔE^{cor}. The correction energy is neglected in the calculation. However, the MP2, B3LYP and B3PW91 E_{int}^* are usually quite similar. Additionally, for a given computational method (HF, MP2, B3LYP or B3PW91), E_{int}^* show only small basis set dependence. We computed E_{int}^* for $(HF)_2$ and found that the MP2 E_{int}^* vary by 0.25 kcal/mole from cc-pVDZ to cc-pV5Z; and the DFT E_{int}^* change a little more, about 0.35 kcal/mole. Especially, there is little difference between the results given by the larger basis sets (cc-pVTZ, cc-pVQZ and cc-pV5Z).

In comparing our results to the estimated ΔE_{stab}, we shall focus upon E_{int}^* for $\rho_{min} \leq 10^{-4}$ electrons/bohr^3. For $(H_2O)_2$ and $(HF)_2$, The E_{int}^* are in good agreement with the best estimated stabilization energy: e.g., for the water dimer,

MP2 and DFT give the E_{int}^* in the range -5.28 to -5.62 kcal/mole with different basis sets.

5.6.   Interaction Energy Calculations for (MeOH)$_2$ and (HCOOH)$_2$

Ab initio calculations have been widely employed to study intermolecular interactions. With the use of high level post-Hartree-Fock methods and large basis sets, the results agree well with the experimental data [37, 53]. In order to test the performance of E_{int}^*, we computed the interaction energies for two other hydrogen-bonded systems: (MeOH)$_2$ and (HCOOH)$_2$ and compared them to the experimental results.

The geometries of the complexes were optimized at the MP2/6-311G** level by Gaussian 98. The geometries of (MeOH)$_2$ and (HCOOH)$_2$ are C$_1$ and C$_{2h}$, respectively. (Figure 5.4) The electronic densities were obtained at several theoretical levels (HF, MP2, B3LYP and B3PW91) with Dunning's correlation-consistent basis sets (CC-pVXZ, X=D, T, Q). The number of e-voxels in each cube file is about 1.0×10^6. Four electron density isocontours (ρ_{min}) were tested and the condensation level was set to 3.

Experimental ΔH have been reported for the formation of (MeOH)$_2$ and (HCOOH)$_2$, although with some degrees of uncertainty: Curtiss *et al* reported that the ΔH of the (MeOH)$_2$ is 3.2—4.1 kcal/mole [54]. Bizzarri *et al* gave the result ΔH=3.2±0.1 kcal/mole [55]. The bonding enthalpy of the (HCOOH)$_2$ was reported by Lazaar *et al* as no more than 12 kcal/mole [56]. Henderson estimated the value is 11.45±0.10 kcal/mole [57]. All these values are based on IR and NMR studies.

Tsuzuki *et al* added zero-point and thermal contributions to arrive at estimates of ΔE_{stab} at 0K [58]: -4.6 to -5.9 kcal/mole for $(CH_3OH)_2$ and -13.2 kcal/mole for $(HCOOH)_2$.

The E_{int}^* were computed by the procedures described in this chapter. Tables 5.3 and 5.4 give the calculated E_{int}^* of the hydrogen-bonded complexes. The E_{int}^* decrease as ρ_{min} becomes smaller and converge for $\rho_{min} \leq 10^{-4}$ electrons/bohr^3, which are similar to those of $(H_2O)_2$ and $(HF)_2$. The Hartree-Fock E_{int}^* are more negative than the others, approximately by 15-20% margin; while the MP2, B3LYP and B3PW91 E_{int}^* are much closer.
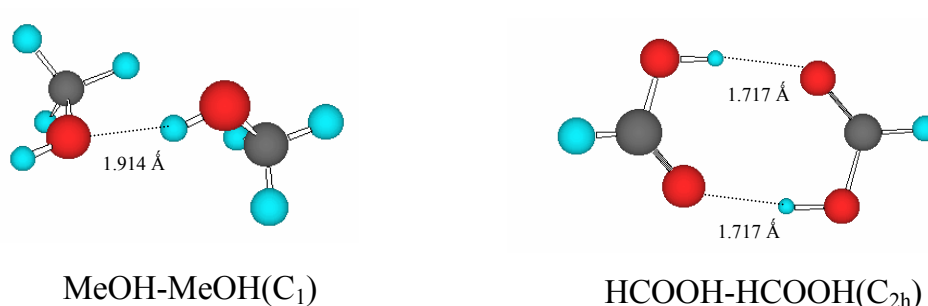

MeOH-MeOH(C_1)   HCOOH-HCOOH(C_{2h})

Figure 5.4 *Ab initio* (MP2/6-311G**) optimized structures of $(MeOH)_2$ and $(HCOOH)_2$.

The E_{int}^* are also independent of basis set size for all the theoretical methods. The deviation is usually under 5% from cc-pVDZ to cc-pVQZ. It was reported that the small cc-pVDZ basis set considerably underestimates the

dispersion interactions for the MP2 method [53]. However, this is not reflected in our electronic density method. We note that the MP2, B3LYP and B3PW91 E_{int}^* are

Method	$\rho_{min} =$	10^{-2} au	10^{-3} au	10^{-4} au	10^{-5} au
HF/cc-pVDZ		-4.32	-3.59	-3.43	-3.40
HF/cc-pVTZ		-4.52	-3.61	-3.39	-3.35
HF/cc-pVQZ		-4.57	-3.61	-3.38	-3.34
MP2/cc-pVDZ		-3.75	-3.08	-2.88	-2.85
MP2/cc-pVTZ		-3.79	-3.06	-2.83	-2.79
MP2/cc-pVQZ		-3.86	-3.07	-2.85	-2.80
B3LYP/cc-pVDZ		-3.59	-2.98	-2.80	-2.77
B3LYP/cc-pVTZ		-3.68	-3.02	-2.78	-2.74
B3LYP/cc-pVQZ		-3.70	-3.00	-2.76	-2.72
B3PW91/cc-pVDZ		-3.66	-3.02	-2.85	-2.82
B3PW91/cc-pVTZ		-3.71	-3.04	-2.83	-2.79
B3PW91/cc-pVQZ		-3.68	-3.04	-2.82	-2.78
best estimate of ΔE_{stab} [c]		-4.6 to -5.9			

Table 5.3 Calculated E_{int}^* for $(MeOH)_2$, in kcal/mole, using MP2/6-311G(d,p) optimized dimer geometry and Eq. (5.29).[a]

[a] Number of e-voxels=1.0×10^6; grid stepsize=0.0843 Å; n=3.
[b] Ref. 58.

smaller in magnitude than the reported ΔE_{stab} by roughly 2 to 3 kcal/mole. There are several possible reasons for these discrepancies: (1). The definition of E_{int}^* is

	$\rho_{min} =$	10^{-2} au	10^{-3} au	10^{-4} au	10^{-5} au
Method					
HF/cc-pVDZ		-16.48	-13.00	-12.38	-12.29
HF/cc-pVTZ		-17.46	-13.88	-13.11	-13.01
HF/cc-pVQZ		-17.51	-14.07	-13.21	-13.09
MP2/cc-pVDZ		-13.43	-10.15	-9.47	-9.37
MP2/cc-pVTZ		-14.47	-10.93	-10.12	-10.00
MP2/cc-pVQZ		-14.65	-11.18	-10.26	-10.12
B3LYP/cc-pVDZ		-14.03	-10.99	-10.33	-10.24
B3LYP/cc-pVTZ		-14.92	-11.49	-10.69	-10.57
B3LYP/cc-pVQZ		-15.01	-11.66	-10.74	-10.61
B3PW91/cc-pVDZ		-12.42	-10.31	-9.73	-9.65
B3PW91/cc-pVTZ		-13.36	-10.78	-10.06	-9.96
B3PW91/cc-pVQZ		-13.45	-10.96	-10.15	-10.03
best estimate of ΔE_{stab} [c]		-13.2			

Table 5.4 Calculated E_{int}^* for $(HCOOH)_2$, in kcal/mole, using MP2/6-311G(d,p) optimized dimer geometry and Eq. (5.29).[a]

[a] Number of e-voxels=1.0×10^6; grid stepsize=0.0718 Å; n=3.
[b] Ref. 58.

different from that of ΔE_{stab}: ΔE_{stab} refers to the complex and its components in their equilibrium ground states; while E_{int}^* corresponds to the components having same geometries and electronic densities as in the complex. According to Eq. (5.28), ΔE_{stab} is the sum of E_{int}^* and the correction energy, ΔE^{cor}. In our approach, ΔE^{cor} is

not included. (2). Our computed dimer structures are likely somewhat different from those used in the measurements upon which the ΔE_{stab} are based. (3). The electronic densities of the components, generated by several approximations, are not exact. (4) There is some uncertainty in the literature values.

We have presented the results which support the approach described in Sections 5.3 and 5.4. However, there continues to be a need for further exploration of the effects of such factors as the number of e-voxels, the value of ρ_{min}, and the level of condensation n, in relation to the sizes and shapes of the molecules. For this purpose, it is important to apply our new approach to larger intermolecular systems. In next Chapter, we will compute the interaction energies for an energetic explosive — RDX.

5.7.   **Summary**

Based on the electrostatic Hellmann-Feynman theorem, an expression is derived, for the intermolecular interaction energy in forming a noncovalently-bound complex.   In this approach, only classical electrostatics, involving the charge distributions of the components as they are in the complex, is invoked. The definition of our E_{int}^* is slightly different from ΔE_{stab} and E_{int}. Their relationships have been discussed.

An approximate method for the calculation of E_{int}^* has been proposed. The electronic densities of the components are obtained by a decomposition procedure and integration over the electronic densities is carried out by a numerical method. We calculate the interaction energies for four molecular dimers at a variety of

computational levels. The results are analyzed and compared to the best estimated values available in the literature. This method may open a new window for interaction energy calculations.

References

[1]. Cramer, C.J.; Truhlar, D. G. *Chem. Rev.* 99, **1999**,2161.

[2]. Tomasi, J.; Mennucci, B.; Cammi, R. in *Molecular Electrostatic Potential: Concepts and Applications*, edit by Murray, J. S.; Sen, K. (Elsevier, Amsterdam, 1996), ch. 1.

[3]. Allen, M. P.; Tildesley, D. J. *Computer Simulation of Liquids* (Oxford University Press, Oxford, 1987).

[4]. Karle, J.; Huang, L. *J. Mol. Struct.* 647, **2003,** 9.

[5]. Saenger, W. *Principle of Nucleic-Acid Structure* (Springer-Verlag, New York, 1984).

[6]. Hunter, C. A.; Singh, J.; Thornton, J. M. *J. Mol. Biol.* 218, **1991**, 837.

[7]. Politzer, P.; Laurence, P. R.; Jayasuriya, K. *Env. Health Persp.* 61, **1985**, 191.

[8]. Naray-Szabo, G.; Ferenczy, G. G. *Chem. R*ev. 95, **1995**, 829.

[9]. Fyfe, M. C. T.; Stoddart, J. F. *Acc. Chem. Res.* 30, **1997**, 393.

[10]. Sauer, J.; Ugliengo, P.; Garrone, E.; Saunders, V. R. *Chem. Rev.* 94, **1994**, 2095.

[11]. Legon, A.C.; Millen, D. J. *Acc. Chem. Res.* 20, **1987**, 39.

[12]. Desiraju, G. R. *Acc. Chem. Res.* 35, **2002**, 565.

[13]. Jeziorski, B.; Moszynski, R.; Szalewicz, K. *Chem. Rev.* 94, **1994**, 1887.

[14]. Jeziorski, B.; Szalewicz, K. *The Encyclopedia of Computational Chemistry,* vol 2, edited by Schleyer, P. von R. (Wiley, New York, **1998**), 1376.

[15]. Rngkvist, O.; Astrand, P. O.; Karlstrom, G. *Chem. Rev.* 100, **2000**, 4087.

[16]. Chalasinski, G.; Szczesniak, M. M. G. *Chem. Rev.* 100, **2000**, 4227.

[17]. Langlet, J.; Caillet, J.; Berges, J.; Reinhardt, P. *J. Chem. Phys.* 118, **2003**, 6157.

[18]. Chipot, C.; Dehez, F.; Angyan, J.; Millot, C.; Orozco, M.; Luque, F. J. *J. Phys. Chem. A* 105, **2001**, 11505.

[19]. Wheatley, R. *J. Chem. Phys. Lett.* 294, **1998**, 487.

[20]. Nobeli, I.; Price, S. L. *J. Phys. Chem. A* 103, **1999**, 6448.

[21]. Kim, Y. S.; Kim, S. K.; Lee, W. D. *Chem. Phys. Lett.* 80, **1981**, 574.

[22]. Kita, S.; Noda, K.; Inouye, H. *J. Chem. Phys.* 64, **1976**, 3446.

[23]. Wheatley, R.J.; Price, S. L. *Mol. Phys.* 69, **1990**, 507.

[24]. Gavazzotti, A. *J. Chem. Phys. B* 107, **2003**, 2344.

[25]. Bentley, J. *J. Phys. Chem. A* 102, **1998**, 6043.

[26]. Levine, I. N. *Quantum Chemistry*; Prentice-Hall, **1995**.

[27]. Hellman, H. *Einfuhrung in die Quantenchemie;* Franz Deuticke, Leipzig, Germany, **1937**.

[28]. Feynman, R. P. *Phys. Rev.* 56, **1939**, 340.

[29]. Hirschfelder, J. O.; Eliason, M.A. *J. Chem. Phys.* 47, **1967**, 1164.

[30]. Szalewicz, K.; Jeziorski, B. *J. Chem. Phys.* 109, **1998**, 1198.

[31]. Xantheas, S.S. *J. Chem. Phys.* 104, **1996**, 8821.

[32]. Peterson, K. A.; Dunning, T.H., Jr. *J. Chem. Phys.* 102, **1995**, 2032.

[33]. Leininger, M.L.; Nielsen, I. M. B.; Colvin, M.E.; Janssen, C. L. *J. Phys. Chem. A* 106, **2002**, 3850.

[34]. Bader, R. F. W.; Carroll, M. T.; Cheeseman, J.R.; Chang, C. J. *J. Am. Chem. Soc.* 109, **1987**, 7968.

[35]. Wiberg, K. B.; Keith, T. A.; Frisch, M. J.; Murcko, M. *J. Phys. Chem.* 99, **1995**, 9072.

[36]. Tschumper, G.: Leininger, M. Hoffman, B. C.; Valeev, E. F.; Schaefer, H. F., III; Quack, M. *J. Chem. Phys.* 116, **2002**, 690.

[37]. Feyereisen, M. W.; Feller, D.; Dixon, D. A. *J. Phys. Chem.* 100, **1996**, 2993.

[38]. Barton, A. E.; Howard, B. J. *Faraday Discuss. Chem. Soc.* 73, **1982**, 45.

[39]. Gaw, J. F.; Yamaguchi, Y.; Vincent, M. A.; Schaefer, H. F. III *J. Am. Chem. Soc.* 106, **1984,** 3133.

[40]. Michael, D. W.; Dykstra, C. E.; Lisy, J. M. *J. Chem. Phys.* 81, **1984**, 5998.

[41]. Frisch, M. J.; Del Bene, J. E.; Binkley, J. S.; Schaefer, H. F. III *J. Chem. Phys.* 84, **1986**, 2279.

[42]. Hancock, G. C.; Truhlar, D. G.; Dykstra, C. E. *J. Chem. Phys.* 88, **1988**, 1786.

[43]. Kofranek, M.; Lischka, H.; Karpfen, A. *J. Chem. Phys.* 121, **1988**, 137.

[44]. Bunker, P.R.; Jensen, P.; Karpfen, A.; Kofranek, M.; Lischka, H. *J. Chem. Phys.* 92, **1990**, 7432.

[45]. Racine, S. C.; Davidson, E. R. *J. Phys. Chem.* 97, **1993**, 6367.

[46]. Novoa, J. J.; Planas, M.; Whangbo, M. *Chem. Phys. Lett.* 225, **1994**, 240.

[47]. Tschumper, G. S.; Yamaguchi, Y.; Schaefer, H. F. III *J. Chem. Phys.* 106, **1997**, 9627.

[48]. Howard, B. J.; Dyke, T. R.; Klemperer, W. *J. Chem. Phys.* 81, **1984**, 5417.

[49]. Gutowsky, H. S.; Chuang, C.; Keen, J. D.; Klots, T. D.; Emilsson, T. *J. Chem. Phys.* 83, **1985**, 2070.

[50]. Klopper, W.; Quack, M.; Suhm, M. A. *J. Chem. Phys.* 108, **1998**, 10096.

[51]. Chakravorty, S. J.; Davidson, E. R. *J. Phys. Chem.* 97, **1993**, 6373.

[52]. Curtiess, L. A.; Frurip, D. J.; Blander, M. *J. Chem. Phys.* 71, **1979**, 2703.

[53]. Tsuzuki, S.; Lüthi, H. P. *J. Chem. Phys.* 114, **2001**, 3949.

[54]. Curtiss, L. A.; Blander, M. *Chem. Rev.* 88, **1988**, 827.

[55]. Bizzarri, A.; Stolte, S.; Reuss, J.; van Duijneveldt-van de Rijdt, J. G. C. M.; van Duijneveldt, F.B. *Chem. Phys.* 143, **1990**, 423.

[56]. Lazzar, K. I.; Bauer, S. H. *J. Am. Chem. Soc.* 107, **1985**, 3769.

[57]. Henderson, G. *J. Chem. Educ.* 64, **1987**, 88.

[58]. Tsuzuki, S.; Uchimaru, T.; Matsumura, K.; Mikami, M.; Tanabe, K. *J. Chem. Phys.* 110, **1999**, 11906.

CHAPTER 6. APPLICATION: INTERMOLECULAR ENERGETICS FOR RDX CRYSTAL

6.1. **Introduction**

Hexahydro-1,3,5,-trinitro-s-triazine (RDX) is one of the most widely used explosives. Its structure is shown in Figure 6.1. There are two known polymorphic forms [1], designated I and II or α and β in literature. The second, II or β, is very unstable; it is therefore α-RDX that is of interest. The details of the crystal structure of α-RDX are known from neutron diffraction [1]. The unit cell of α-RDX is orthorhombic and contain 8 molecules, which have a chair-AAE conformation. AAE Means that two NO_2 groups are oriented axially (A) while the third is equatorial (E).
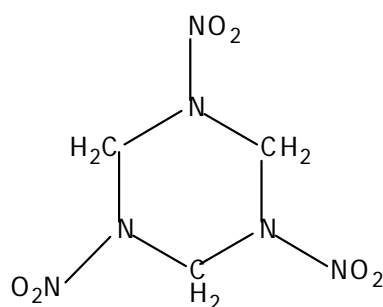

Figure 6.1 Structure of the RDX molecule.

Classical molecular dynamics (MD) simulations provide a promising route to achieving a better understanding of the factors and processes involved in the initiation and propagation of detonation in energetic solids. There has indeed been considerable activity in this area, as reviewed recently on several occasions [2-4]. A key challenge is to identify and develop inter/intramolecular potentials which can satisfactorily describe both molecular and crystal properties and behavior, including crystal growth, lattice defect formation, impact/shock-induced vibrational excitation and molecular dissociation *etc*. Some work of this kind has been applied to the study of the properties of RDX, such as intermolecular potential and conformation [5-7].

As discussed in Chapter 1, the total intermolecular interaction energy is frequently expressed as the sum of four primary elements: electrostatic, polarization (induction), dispersion and exchange-repulsion. In molecular dynamics simulations, the intermolecular potential is usually taken to be composed of a point-charge Coulombic term together with a Lennard-Jones or Buckingham expression to represent non-bonded interactions. Since the Lennard-Jones and the Buckingham potentials each contain both an attractive (dispersion) and a repulsive contribution (exchange-repulsion), three of the four elements are taken into account in some manner. Polarization generally is not, although techniques for doing so do exist; for example, the magnitudes of the point charges could periodically be changed [8].

It should be noted that the molecular dynamics formulation does not reflect any distortion of the molecules' geometries that may accompany crystal formation; their equilibrium gas phase structures are often used for the calculations. The effect

of neglecting such distortion upon the interaction energy is often quite small [9], however, for the uracil dimer, our calculation shows that the energy required to convert two free uracil molecules to their states in the dimer is 0.8 kcal/mole at the MP2/6-31+G* level.
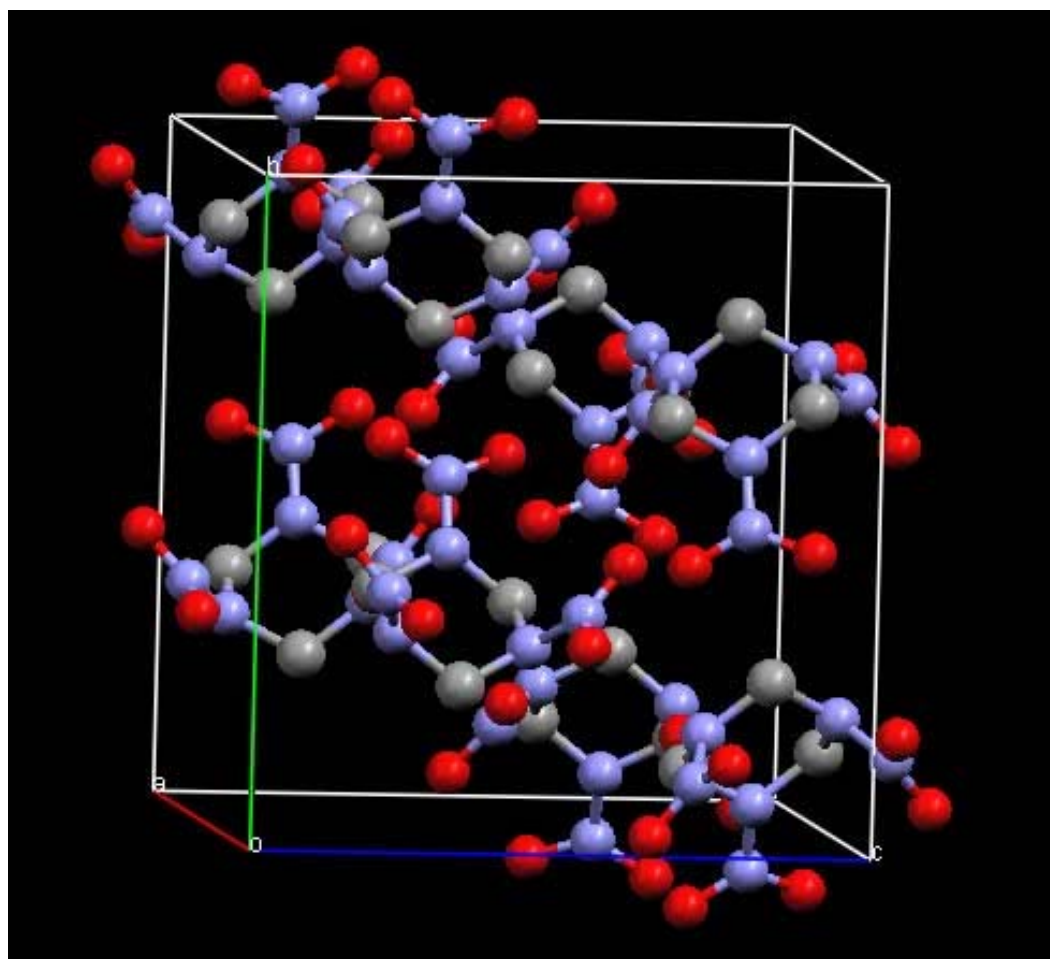

Figure 6.2 Unit cell of RDX, containing 8 molecules in two series of interlocked pairs. Oxygens are red, nitrogens blue and carbons gray. Hydeogens are not shown in this figure.

In this work, we have focused on the pairwise intermolecular interactions in the crystal lattice of RDX. We evaluate both the electrostatic and total interaction

energies. Our objectives include (a) obtaining accurate values for these, and (b) assessing how effectively they are reproduced by typical molecular dynamics methodology.
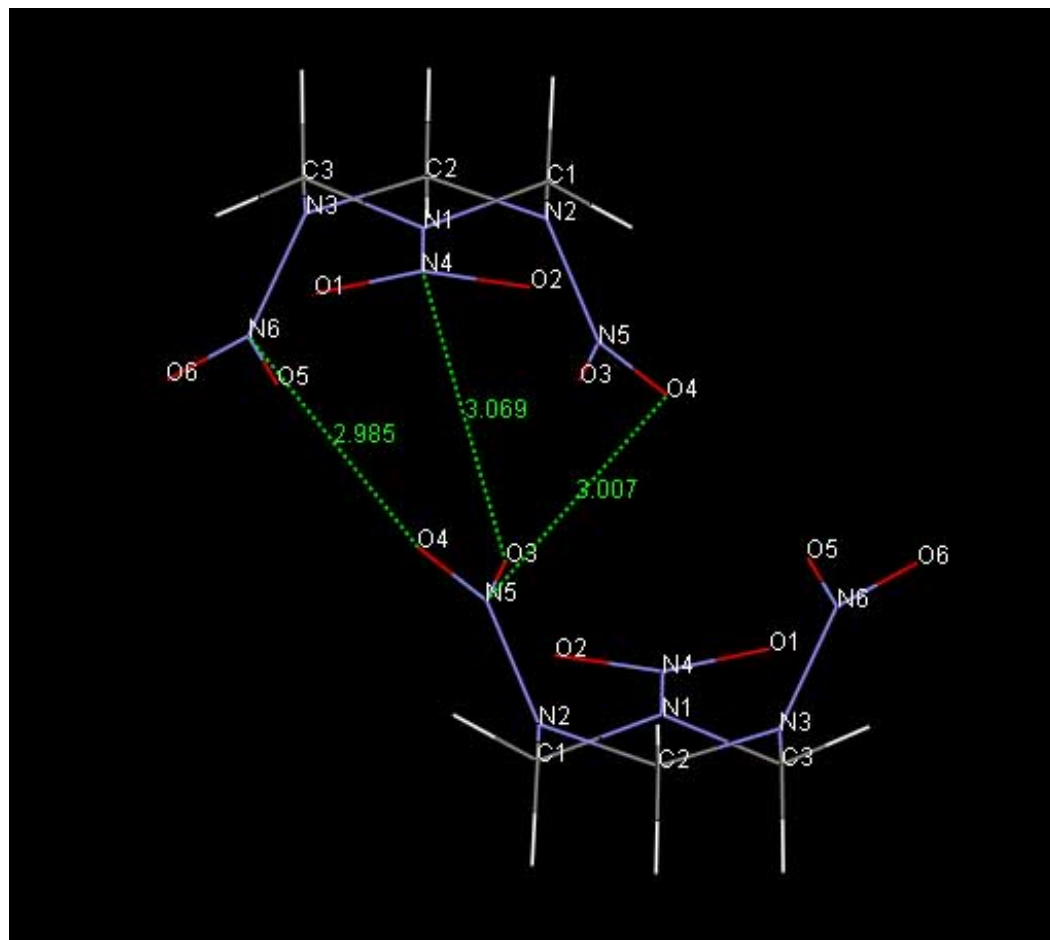
Figure 6.3 An interlocked pair of molecules in the crystal lattice of RDX. Shortest N(nitro)---O distances are given in Angstroms.

Karpowicz and Brill pointed out that the lattice can be viewed as composed of series of interlocked molecules, adjoining pairs having several N(nitro)---O electrostatic interactions, with fewer and weaker ones between the pairs of neighboring series [10]. This is shown in Figures 6.2-6.4. We will look at both

types of interactions between two RDX molecules: first, when they comprise an interlocked pair (Figure 6.3) and second, when they are members of neighboring interlocked pairs (Figure 6.4). The geometries of the two molecules and their positions relative to each other will be taken from the experimental crystal structure of α-RDX [1, 11].

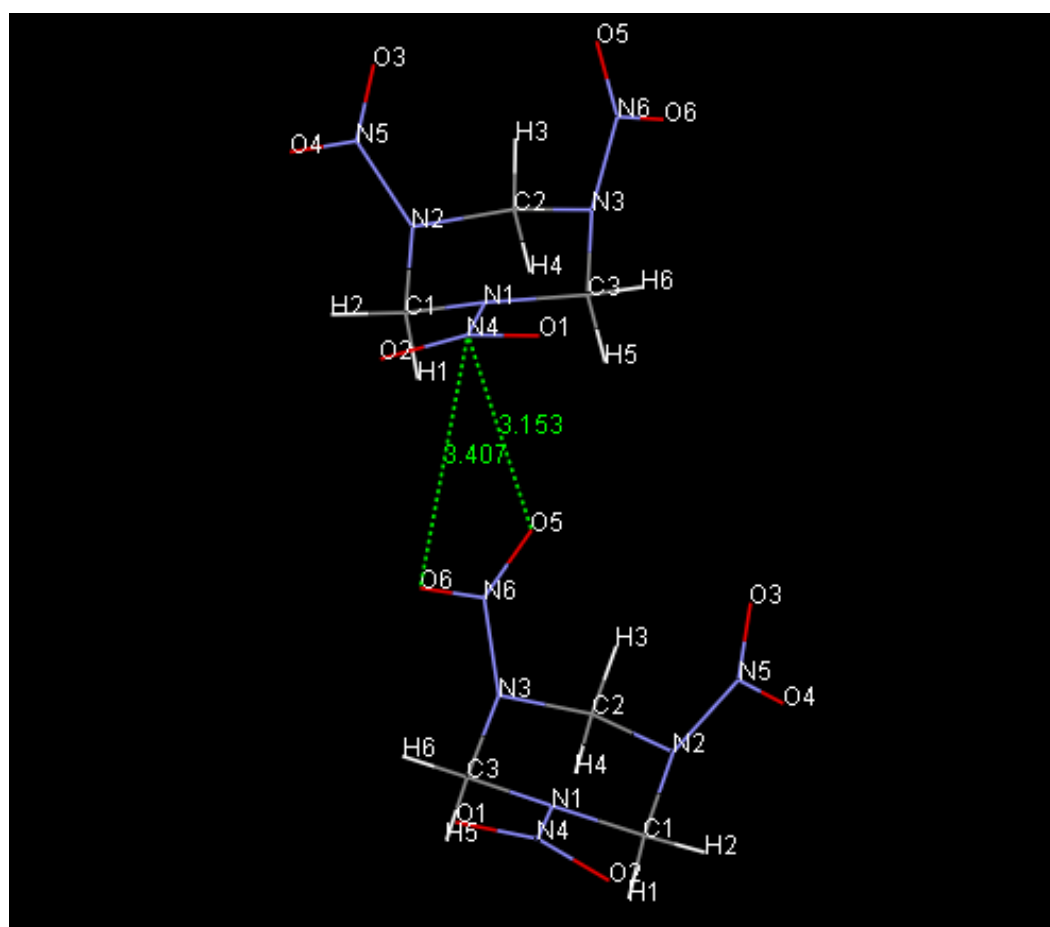Figure 6.4 Two molecules in neighboring interlocked pairs in the crystal lattice of RDX. Shortest N(nitro)---O distances are given in Angstroms.

6.2. <u>Energy Expressions</u>

In molecular dynamics, a common approach to calculating the electrostatic interaction energy, E_{es}, between two unperturbed molecules A and B is to treat them as collections of point charges:

$$E_{es} = \sum_i \sum_j \frac{Q_i Q_j}{R_{ij}}$$

(6.1)

in which Q_i and Q_j are the net charges on atoms i in A and j in B, and R_{ij} is their distance. The atomic charges may be obtained by one of the variety of techniques that have been proposed [12-15], or they can be treated as parameters, to be determined by some fitting procedure. In molecular dynamics simulations of energetic solids, the charges are frequently established by requiring that they reproduce the molecules' electrostatic potentials [4, 13, 14]. The representation of E_{es} by Eq. (1) could of course be improved, but at greater computational cost, by adding dipole and higher-order multipole terms [16]. In Chapter 3, we derived a rigorous expression for E_{es}:

$$E_{es} = \sum_A \sum_B \frac{Z_A Z_B}{|\vec{R}_A - \vec{R}_B|} - \sum_A \int \frac{Z_A \rho_B^0(\vec{r}_B)}{|\vec{R}_A - \vec{r}_B|} d\vec{r}_B$$
$$- \sum_B \int \frac{Z_B \rho_A^0(\vec{r}_A)}{|\vec{R}_B - \vec{r}_A|} d\vec{r}_A + \iint \frac{\rho_A^0(\vec{r}_A)\rho_B^0(\vec{r}_B)}{|\vec{r}_A - \vec{r}_B|} d\vec{r}_A d\vec{r}_B$$

(6.2)

where Z_A and Z_B refer to the charges on nuclei of molecules A and B, respectively; $\vec{R}_A$ and $\vec{R}_B$ are their locations, and ρ_A^0 and ρ_B^0 are the electronic densities of the unperturbed molecules.

In reality, the interacting molecules do polarize each others' charge distributions, so that their electronic densities are no longer described by ρ_A^0 and ρ_B^0. The associated energy effect, E_{pol}, is one of the contributions to the total energy of the interaction between A and B. Various approaches to estimating E_{pol} have been proposed [16-20]. In Chapter 4, we developed a formulation of E_{pol} which is based on writing the polarized electronic densities of the molecules as $\rho_A^0 + \Delta\rho_A^{pol}$ and $\rho_B^0 + \Delta\rho_B^{pol}$; $\Delta\rho_A^{pol}$ and $\Delta\rho_B^{pol}$ are the changes due to mutual polarization:

$$
\begin{aligned}
E_{pol} = &-\sum_A \int \frac{Z_A \Delta\rho_B^{pol}(\vec{r}_B)}{\left|\vec{R}_A - \vec{r}_B\right|}d\vec{r}_B - \sum_B \int \frac{Z_B \Delta\rho_A^{pol}(\vec{r}_A)}{\left|\vec{R}_B - \vec{r}_A\right|}d\vec{r}_A \\
&+ \iint \frac{\rho_A^0(\vec{r}_A)\Delta\rho_B^{pol}(\vec{r}_B)}{\left|\vec{r}_A - \vec{r}_B\right|}d\vec{r}_A d\vec{r}_B + \iint \frac{\rho_B^0(\vec{r}_B)\Delta\rho_A^{pol}(\vec{r}_A)}{\left|\vec{r}_A - \vec{r}_B\right|}d\vec{r}_A d\vec{r}_B \\
&+ \iint \frac{\Delta\rho_A^{pol}(\vec{r}_A)\Delta\rho_B^{pol}(\vec{r}_B)}{\left|\vec{r}_A - \vec{r}_B\right|}d\vec{r}_A d\vec{r}_B
\end{aligned}
\tag{6.3}
$$

In Eq. (6.3), we have used an approximate approach to represent $\Delta\rho_A^{pol}$ and $\Delta\rho_B^{pol}$ (see Chapter 4). They are obtained from the total electronic density of the pair after interaction.

In Chapter 5, we derived the total noncovalent interaction energy between two molecules, E_{int}^*, from the Hellmann-Feynman electrostatic theorem [21, 22], which can be expressed in a manner similar to Eq. (6.2) but in which ρ_A^0 and ρ_B^0 are replaced by the electronic densities of the molecules after interaction, ρ_A and ρ_B,

$$E_{\text{int}}^* = \sum_A \sum_B \frac{Z_A Z_B}{R_{AB}} - \sum_A \int \frac{Z_A e \rho_B(\vec{r}_B)}{|\vec{R}_A - \vec{r}_B|} d\vec{r}_B + \sum_B \int \frac{Z_B e \rho_A(\vec{r}_A)}{|\vec{R}_B - \vec{r}_A|} d\vec{r}_A$$
$$+ e^2 \iint \frac{\rho_B(\vec{r}_B) \rho_A(\vec{r}_A)}{|\vec{r}_A - \vec{r}_B|} d\vec{r}_A d\vec{r}_B$$

(6.4)

Eq. (6.4) assumes that molecules A and B, although having undergone polarization and perhaps changes in geometries, retain their identities after interaction. In order to make the calculation feasible, we designed an approach to partition the overall electronic distribution of the pair after interaction between the two components.

It should be noted that the different definitions of E_{int}^*, E_{int} and ΔE_{stab}. E_{int}^* refers to the molecules with electronic density and geometries as they are after interaction; E_{int} uses ground-state geometries but tries to approximate the effects of polarization; and the stabilization energy ΔE_{stab} corresponds to the complex and its components in their equilibrium ground states. Unlike E_{int}^* and E_{int}, ΔE_{stab} does take account of any changes in the geometries and electronic distributions of A and B that may accompany their interaction. The approach for the calculation of ΔE_{stab} is called the supermolecular method, which poses some practical problems [21]: It requires a high computational level, because ΔE_{stab} is given as a small difference between much larger quantities; thus, any errors in these are likely to be greatly magnified in ΔE_{stab} (except for fortuitous cancellation). There is also the issue of BSSE, the spurious stabilization of the complex because it is described by a larger basis set than its components.

As we already pointed out, the energetic consequence of the conceptual differences between E_{int}^* and E_{int}, ΔE_{stab} are often rather small. It might be

anticipated that this potential problem would be exacerbated in the case of RDX because the molecular conformation changes from chair-AAA in the gas phase [22, 23] to chair-AAE in the crystal [1]. However the MP2/6-31G* and B3LYP/6-311+G** analyses of Rice and Chabalowski show the AAA and AAE conformers to differ in energy by only 0.13 and 0.64 kcal/mol, respectively [22].

The expressions of E_{es}, E_{pol} and E_{int}^{*}, all involve integration over electronic densities. The details of the numerical procedures have been described in previous chapters.

6.3. <u>Procedure</u>

As has been discussed, E_{es}, Eqs (6.1) and (6.2), is normally calculated using the ground-state gas phase geometries of the interacting molecules. In the case of RDX, this would mean the chair-AAA molecular conformation [21, 22]. Since our interest is in interactions within the crystal, however, it is more relevant to use chair-AAE, which is the conformation of the RDX molecule in the lattice [1]. Accordingly, E_{es} was computed from atomic charges, Eq. (6.1), or electronic densities, Eq. (6.2), obtained for individual RDX molecules with the geometries that they are in the crystal [1]. To determine E_{es}, these molecules were placed in the relative positions that they occupy in the lattice; we treated both the interaction within an interlocked pair (Figure 6.3) and that between two molecules in neighboring interlocked pairs (Figure 6.4).

For E_{pol} and E_{int}^*, we calculated the electronic density $\rho_{AB}(\vec{r})$ of the pair of molecules after each mode of interaction (i.e., within and between interlocked pairs), again using the crystal structure. We also looked at how well the point-charge model would approximate E_{int}^*, applying Eq.(6.1) but with the charges obtained for the pairs.

There are several parameters involved in computing E_{es}, E_{pol} and E_{int}^* by numerical integration over electronic densities: the number of e-voxels (which determines the stepsize in the grid), the condensation level n in forming the super e-voxels, and the boundary surface $\rho_{\min}$. In Chapters 3,4 and 5, we have investigated the effects of varying these parameters. We concluded that on the order of 10^6 e-voxels yields satisfactory results, and that n should be small enough so that the number of super e-voxels is greater than 2000. The optimum choice of $\rho_{\min}$ depends on the energy quantity sought; for example, $\rho_{\min}=1.0\times10^{-6}$ au is desirable for E_{es}, $\rho_{\min}=1.0\times10^{-2}$ au for E_{pol} and $\rho_{\min}=1.0\times10^{-4}$ au for E_{int}^*.

All calculations were carried out at both the HF/6-311+G** and B3PW91/6-311+G** levels. Two types of atomic charges were tested: the Mulliken [12] and those derived from electrostatic potentials via the CHelpG technique [24].

6.4. <u>Results and Discussion</u>

The electrostatic and polarization energies, E_{es} and E_{pol}, between individual RDX chair-AAE molecules are given in Table 6.1. In Table 6.2 are the total interaction energies, E_{int}^*, within the pairs of molecules in the crystal lattice.

Looking first at the point-charge results, the E_{es} based on Mulliken charges are quite poor, usually being positive. The CHelpG do predict attractive interactions, but very weak ones; E_{es} and E_{int}^{*} are usually significantly smaller in magnitude than the corresponding values calculated from the electronic density.

Proceeding to the energies obtained from electronic densities, Eqs. (6.2-6.4), the overall interaction is seen to be much stronger within the interlocked pair. This is as anticipated from Figures 6.3 and 6.4, which show more N(nitro)---O electrostatic attractions, over shorter distances, in the interlocked pairs than between pairs.

Interaction	Method	E_{es}, Eq. (6.1)		E_{es},	E_{pol},
		Mulliken	CHelpG	Eq. (6.2)[a]	Eq. (6.3)[b]
Within interlocked pair (Figure 6.3)	HF/6-311+G**	3.4	-2.9	-8.5	-0.4
	B3PW91/6-311+G**	4.3	-2.2	-8.0	-0.3
Between interlocked pairs (Figure 6.4)	HF/6-311+G**	0.5	-1.9	-3.1	-1.4
	B3PW91/6-311+G**	1.2	-1.4	-3.0	-1.2

Table 6.1 Computed electrostatic and polarization interaction energies, E_{es} and E_{pol}, in kcal/mole.

[a] Number of e-voxels $=1.4\times10^{-6}$; stepsize=0.0882 Å; n=5; $\rho_{min}=1.0\times10^{-6}$ au.
[b] Number of e-voxels $=1.4\times10^{-6}$; stepsize=0.1232 Å for Figure 6.2 system, 0.1307 Å for Figure 6.2 system;n=5; $\rho_{min}=1.0\times10^{-2}$ au.

Bukowski *et al* have carried out a symmetry-adapted perturbation theory (SAPT) treatment of dimers of dimethylnitramine (DMNA), $(H_3C)_2N\text{-}NO_2$ [25], which has the same basic structural elements as does RDX. For their most stable dimer, the total interaction energy E_{int} was approximately -11 kcal/mole. This is about 3 kcal/mole more negative that our E_{int}^*; however the two DMNA molecules were considerably closer than our RDX in the crystal lattice. The distance between the centers of mass the former was 3.04 Å, which is comparable to the shortest intermolecular distances in Figures 6.3 and 6.4.

Interaction	Method	Point Charge Model		Eq. (6.4)[a]
		Mulliken	CHelpG	
Within interlocked pair (Figure 6.3)	HF/6-311+G**	0.0	-1.7	-8.8
	B3PW91/6-311+G**	-1.0	-1.1	-7.3
Between interlocked pairs (Figure 6.4)	HF/6-311+G**	2.6	-2.8	-2.8
	B3PW91/6-311+G**	3.6	-2.2	-2.2

Table 6.2 Computed total interaction energies, E_{int}^*, in kcal/mole.

[a] Number of e-voxels $=3.0\times10^{-6}$; stepsize=0.0882 Å; n=5; $\rho_{\text{min}}=1.0\times10^{-4}$ au.

An interesting feature of Tables 6.1 and 6.2 is the marked similarity between the electrostatic and the total interaction energies, E_{es} and E_{int}^*, for both types of interaction, i.e. within and between interlocked pairs, Bukowski *et al* found the

same to be true in the case of dimethylnitramine [25]. For each of the three most stable DMNA dimer structures, E_{es} and E_{int}^{*} differed by $\leq$ 1 kcal/mole. (Bukowski *et al* also list four other contributions to E_{int}, which nearly cancel.) Thus, for molecules such as RDX and DMNA, the electrostatic interaction between the separate components is a good approximation to the total interaction energy, provided that the former is obtained at a sufficient level of accuracy (higher than that afforded by point charges). Table 6.1 shows the polarization energies to be relatively minor.

6.5. <u>Summary</u>

The principal results of this study are the following:

(1). We have obtained reasonable estimates of the energies of two key intermolecular interactions within the RDX crystal lattice; within an interlocked pair, -8 kcal/mole, and between interlocked pairs, -2 to -3 kcal/mole.

(2). These energies can be well approximated by the electrostatic interactions between the individual chair-AAE RDX molecules, using their isolated-state electronic densities.

(3). Mulliken and CHelpG atomic charges are not adequate for modeling these electrostatic interactions.

(4). Polarization of isolated-state molecular electronic densities is a relatively minor factor.

References

[1]. Choi, C.S.; Price, E. *Acta Cryst B*28, **1972**, 2857.

[2]. Politzer, P.; Alper, H. E. in *Computational Chemistry: Reviews of Current Trends,* Vol. 4; Leszczynski, J., Ed.; World Scientific: Singapore, **1999**, ch. 6.

[3]. Politzer, P.; Boyd, S. *Struct. Chem.* 13, **2002**, 105.

[4]. Sorescu, D. C.; Rice, B. M.; Thompson, D. L. in *Energetic Materials. Part 1. Decomposition, Crystal and Molecular Properties*; Politzer, P.; Murray, J.S., Eds.; Elsevier: Amsterdam, 2003, ch. 6.

[5]. Sorescu, D. C.; Rice, B. M.; Thompson, D. L. *J. Phys. Chem. B* 101, **1997**, 798.

[6]. Wallis, E. P.; Thompson, D. L. *J. Chem. Phys.* 99, **1993**, 2661.

[7]. Chambers, C. C.; Thompson, D. L. *J. Phys. Chem.* 99, **1995**, 15881.

[8]. Seminario, J. M.; Concha, M. C.; Politzer, P. *J. Chem. Phys.* 102, **1995**, 8281.

[9]. Szalewicz, K.; Jeziorski, B. *J. Chem. Phys.* 109, **1998**, 1198.

[10]. Karpowicz, R. J.; Brill, T. B. *J. Phys. Chem.* 87, **1983**, 2109.

[11]. Cambridge Crystallographic Data Centre, HTTP://www.ccdc.cam.ac.uk.

[12]. Mulliken, R. S. *J. Chem. Phys.* 23, **1955**, 1833.

[13]. Chirlian, L. E.; Francl, M. M. *J. Comput. Chem.* 8, **1987**, 894.

[14]. Williams, D. E. in *Reviews in Computational Chemistry, Vol. II;* Lipkowitz, K. B.; Boyd, D. B., Eds, VCH: New York, **1991**, ch.6.

[15]. Bachrach, S. M. in *Reviews in Computational Chemistry, Vol. V;* Lipkowitz, K. B.; Boyd, D. B., Eds, VCH: New York, **1994**, ch.3.

[16]. Engkvist, O.; Astrand, P. –O.; Karlstrom, G. *Chem. Rev.* 100, **2000**, 4087.

[17]. Jeziorski, B.; Moszynski, R.; Szalewicz, K. *Chem. Rev.* 94, **1994**, 1887.

[18]. Gavezzotti, A. *J. Phys. Chem. B* 107, **2003**, 2344.

[19]. Gavezzotti, A. *J. Phys. Chem. B* 106, **2002**, 4145.

[20]. Chipot, C.; Dehez, F.; Angyan, J.; Millot, C.; Orozco, M.; Luque, F. J. *J. Phys. Chem. A* 105, **2001**, 11505.

[21]. Rappe, A. K.; Bernstein, E. R. *J. Phys. Chem. A* 104, **2000**, 6117.

[22]. Shishkov, I. F.; Vilkov, L. V.; Kolonits, M.; Rozsondai, B. *Struct. Chem.* 2, **1991**, 57.

[23]. Rice, B.M.; Chabalowski, C.F. *J. Phys. Chem. A* 101, **1997**, 8720.

[24]. Breneman, C. M.; Wiberg, K. B. *J. Comput. Chem.* 11, **1990**, 361.

[25]. Bukowski, R.; Szalewicz, K.; Chabalowski, C. F. *J. Phys. Chem. A* 103, **1999**, 7322.

VITA

Yuguang Ma was born in 1973. In 1991, he began his undergraduate studies at Fudan University, where he got his Bachelors degree. As a graduate student, he attended Shanghai Institute of Organic Chemistry in 1996, where he received a Master of Science degree in 1999. In the spring of 2000 he attended the University of New Orleans and then joined Dr. Peter Politzer's research group for graduate studies. His interest focuses on intermolecular interactions and density functional theory (DFT).